SYNTHESIS AND ANALYSIS OF SILORANES FOR USE AS A BIOMATERIAL

AND EXTENDED TWISTED MOLECULAR RIBBONS

A DISSERTATION IN
Chemistry,
Pharmaceutical Sciences,
And
Oral Biology

Presented to the Faculty of the University
of Missouri – Kansas City in partial fulfillment of
the requirements for the degree

DOCTOR OF PHILOSOPHY

by
BRADLEY DAVID MILLER
B.S. University of Nebraska at Kearney, 2007

Kansas City, Missouri
2013

SYNTHESIS AND ANALYSIS OF SILORANES FOR USE AS A BIOMATERIAL

AND EXTENDED TWISTED MOLECULAR RIBBONS

Bradley David Miller, Candidate for the Doctor of Philosophy Degree

University of Missouri – Kansas City, 2013

ABSTRACT

The development of complex organic molecules with industrial potential requires meticulous synthetic methodologies coupled with detailed investigations surrounding their physical properties. This dissertation encompasses the study of two such projects: (i) the synthesis, optimization, and quality control of siloranes for use as a biomaterial (i.e., bone cements) and (ii) the investigation of the synthesis, physical properties, and barrier to enantiomerization of twisted molecular ribbons.

Optimization of the synthesis of the silorane monomers PHEPSI and CYGEP was completed via metal-catalyzed hydrosilylation. PHEPSI was synthesized utilizing a monomeric version of the rhodium-based Wilkinson's catalyst. The synthesis of CYGEP was accomplished using two versions of the platinum-based Lamoreaux's catalyst (in-house versus commercial). In both cases, formation of CYGEP was accomplished only in those reactions in which acetonitrile was present, otherwise polymerization occurred. A quality control investigation found that for use of these monomers as a potential biomaterial, a high grade of Wilkinson's catalyst must be utilized for the synthesis of PHEPSI, while use of the

commercial catalyst is sufficient for the synthesis of CYGEP. Mixing of the monomers no more than one month post purification prevents the decomposition of PHEPSI.

An exploration into the effect of end caps and substitution of the acene skeleton was completed. The synthesis of the target pentacene and anthracene compounds was focused on the incorporation of isopropyl substituents while extension of the acene skeleton was expanded to the hexacene diol. The targets were synthesized utilizing a series of Diels-Alder and reduction reactions. The incorporation of the isopropyl substituent was accomplished through the use of lithium reagents generated *in situ*. The barrier to enantiomerization was then studied on the aromatized isopropyl acenes utilizing VT-NMR spectroscopy. Coalescence of the methyl peaks in the ^{1}H NMR spectrum was not observed at temperatures up to 408 K. Utilizing this method, the barrier to enantiomerization of these compounds was found to be greater than 24.0 kcal/mol. The stages of the synthesis were determined through mass spectrometry, ^{1}H and ^{13}C NMR spectroscopy, and in some cases X-ray crystallography. Fluorescence of the isopropyl targets was investigated through UV-Vis spectroscopy.

APPROVAL PAGE

The faculty listed below, appointed by the Dean of the School of Graduate Studies have examined a dissertation titled "Synthesis and Analysis of Siloranes for use as a Biomaterial and Extended Twisted Molecular Ribbons," presented by Bradley D. Miller, candidate for the Doctoral of Philosophy degree, and certify that in their opinion is worthy of acceptance.

Supervisory Committee

Kathleen V. Kilway, Ph.D., Committee Chair
Department of Chemistry

Charles J. Wurrey, Ph.D.
Department of Chemistry

Zhonghua Peng, Ph.D.
Department of Chemistry

Simon H. Friedman, Ph.D.
Department of Pharmaceutical Sciences

J. David Eick, Ph.D.
Department of Oral Biology

CONTENTS

ILLUSTRATIONS

Figure Page

TABLES

Table Page

ACKNOWLEDGEMENTS

I would like to express my deepest gratitude to my advisor through this journey, Dr. Kathleen V. Kilway, for her guidance and mentorship. She has been a vital resource in my development as not only a researcher, but more importantly as a lifelong student in the field.

I would also like to thank my committee members, Drs. Charles J. Wurrey, Zhonghua Peng, Simon H. Friedman, and J. David Eick for their support and guidance.

I would like to show my appreciation to my colleagues in the lab group, Robert Clevenger, Dr. Gerardo Marquez, Rachel Weiler, James Bryan, Liz Horn, and Dr. Jenny Melander for all the support over the years, through the good times and the difficult.

The work in this dissertation could not be completed without the help of all others who contributed to the completion of this work: Drs. Linda Bonewald, Thomas Schuman, Delbert Day, Mariano Velez, Lianxiang Bi, and Elisabet Nalvarte for their guidance in the development of the silorane monomers; Drs. Robert Pascal Jr. and Ben King for their assistance with characterization of the twisted aromatics. I want to thank the endless list of fellow graduate students and undergraduate researchers who have assisted in completing the work required to complete this dissertation.

I would also like to extend my sincere gratitude to Dr. Patricia Hovis-French and the Preparing Future Faculty Fellowship for the lessons beyond the normal graduate education.

DEDICATION

I would like to dedicate this dissertation to all of the friends and family who have stood by and supported me in the peaks and valleys. I want to thank my parents, Mark and Carol Miller, for teaching me that I can do whatever I put my mind to. Most importantly, I want to thank my beautiful wife, Dr. Bryna Miller, for her never-ending love and support. Without you this day may never have been possible and for that I am truly grateful.

You guide me with your counsel, and afterward you will receive me to glory.

-Psalm 73:24

CHAPTER 1

DEVELOPMENT OF SILORANES FOR USE IN A BIOMATERIAL

Introduction

Over the last half century, a significant sector of modern healthcare has been devoted to the development and implementation of biomaterials. Clinical applications of biomaterials vary widely, with use in areas from vascular grafts and degradable sutures to orthopedic implants.[1-4] An area that has been of interest to our group has been the use of biomaterials as bone cements. Every year, there are approximately 200,000 hip implant and 300,000 knee implant surgeries in the United States.[5-7] Between the years 2002 and 2006, a majority of primary total knee (~85%) and total hip joint replacements (>70%) were cemented.[8, 9] Since its introduction by Charnley in 1960, polymethyl methacrylate (PMMA, Figure 1) has been the standard in bone cements.[10, 11]

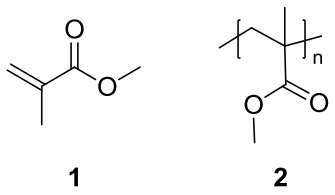

1 **2**

Figure 1: Methyl methacrylate (MMA, **1**) and polymethyl methacrylate (PMMA, **2**).

Comprised of two separate parts (powder and liquid), the composition of PMMA bone cements has not changed substantially over the last half century. The powder portion is composed of pre-polymerized PMMA beads, a methacrylate-styrene-copolymer, benzoyl peroxide initiator, and either barium sulfate or zirconium oxide as a radiopacifier.[12, 13] For the liquid portion, the components are a monomer (methyl methacrylate, MMA), polymerization activator (N,N-dimethyl-*p*-toluidine), and an inhibitor (hydroquinone), which is used to avoid self polymerization of the monomer. In spite of half a century of use, methacrylate-based bone cements suffer from several shortcomings, e.g., high exotherms (potentially >100 ºC, significant increase over body temperature of 37 ºC), toxicity from the leaching of the MMA monomer, and volume change upon polymerization.[5, 9, 14] Over the preceding decades, numerous investigations have focused on developing alternatives to PMMA bone cement, targeting the aforementioned shortcomings.[9, 15-17] Calcium phosphate and bisGMA-TEGDMA (bisphenol A glycidyl methacrylate and triethylene glycol dimethacrylate) based bone cements have recently been developed with improved properties, but both still have their shortcomings as seen in Table 1.

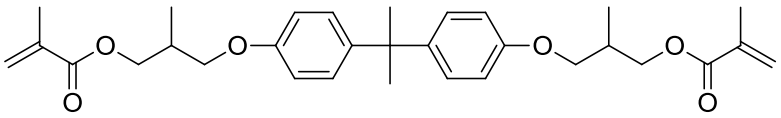

3

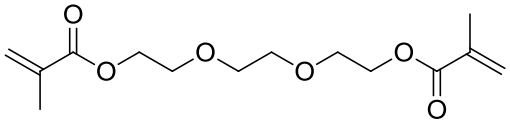

4

Figure 2: Structures of bisGMA (**3**) and TEGDMA (**4**).

Table 1: Advancements of alternative bone cements.[18-26]

Cement Base	Improvement over PMMA	Downfalls
Calcium Phosphate	Good biocompatibility, good handling properties	Can only be used for nonload bearing locations
BisGMA-TEGDMA	Lower exotherm, reduced shrinkage, comparable mechanical properties, improved biocompatibility	Concern over leachables

The development of bisGMA-TEGDMA composites have provided significant improvements in exotherm, shrinkage, biocompatibility, and mechanical properties in comparison to traditional PMMA bone cements. However, there are still concerns regarding the potential of leacheables resulting from the unreacted monomers. Additionally, commercialization of these alternatives has been impacted due to the publication of two independent studies indicating that bisGMA composites provided no additional benefit as compared to no treatment when used for vertebroplasty.[27, 28]

Siloranes

Our group has focused on a relatively new class of ring opening monomers called siloranes. The term silorane was coined as a way to represent monomers, which contain both siloxane and oxirane structural functionalities.[29, 30] Originally developed by 3M-ESPE, siloranes were intended for use in dental composites.[31] These hybrid resins have been shown to have enhanced characteristics compared to bisGMA-TEGDMA composites. The incorporation of a siloxane backbone imparts hydrophobicity, while highly reactive cycloaliphatic oxiranes enable reduced shrinkage in comparison to methacrylates.[31-33] Biocompatibility of the resins has also received excellent ratings; in particular, cytotoxicity and mutagenicity have been reported to be as good as, or better than, that of typical methacrylate monomers.[29, 30, 34-36] Furthermore, siloranes have shown improvements in terms of marginal integrity and microleakage, bond strength, and the ability to bond to bone more effectively than methacrylate resins.[37-39] Combined, these qualities highlight the potential that siloranes present as a viable bone cement alternative.

Bone Cement Formulations

Bone cement composites are comprised of three major components. The first component is the monomer system (methacrylates or siloranes). Second is the initiation system. The type of application determines whether polymerization will be initiated by light, a chemical, or a mixture of the two. The final component is the filler. The filler is added with the intention of improving the other mechanical properties of the composite for its application. The selection of filler will depend on the compatibility (e.g. solubility and reactivity) with the monomer and the desired properties of the biomaterial formed. In cases

where the interface between the filler and resin requires an increase in strength, a modification may be made to the surface of the filler.

SilMix and Composite Formulation

From our previous work with 3M-ESPE and Midwest Research Institute (MRI), two monomers (Figure 3) were selected for utilization in our biomaterial, bis[2-(3{7-oxabicyclo[4.1.0]heptyl})ethyl]methylphenyl silane (PHEPSI, **5**) and 2,4,6,8-tetrakis(2-(7-oxabicyclo[4.1.0]heptan-3-yl)ethyl)-2,4,6,8-tetramethyl-1,3,5,7,2,4,6,8-tetraoxatetrasilocane (CYGEP, **6**).[40]

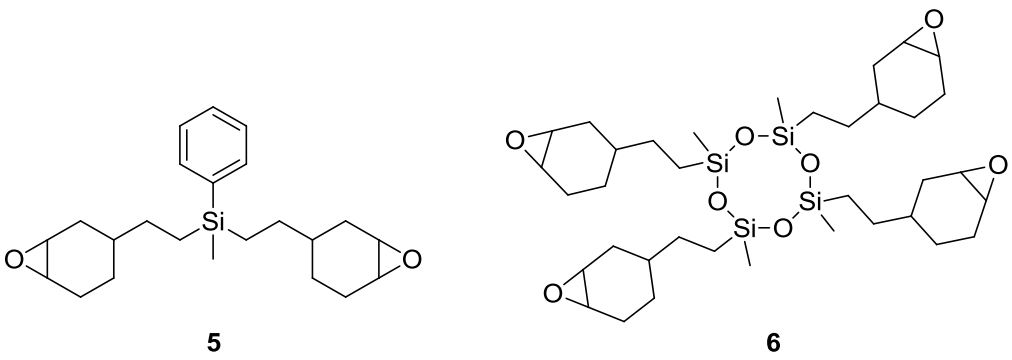

5 **6**

Figure 3: Silorane monomers: PHEPSI (**5**) and CYGEP (**6**).

The base resin (SilMix) was then prepared by mixing PHEPSI and CYGEP in a 1:1 wt/wt mixture. The currently developed dual-cured composite is then prepared through the addition of the other components using a high-speed mixer. The initiation system is comprised of: *p*-(octyloxyphenyl)phenyliodonium hexafluoroantimonate (PIH, ~1.2 wt%),

camphorquinone (CPQ, ~0.4 wt%), and ethyl *p*-dimethylaminobenzoate (EDMAB, ~0.06 wt%) added to SilMix (38 wt%). The filler (60 wt%) is then mixed in, Lamoreaux's catalyst (0.32%) is added and mixed by hand for 30 sec. For extent of polymerization tests, the composite is placed on a glass slide and allowed to polymerize. Polymerization completion was checked at 1 h using a one-pound Gillmore Needle. Passage of the Gillmore Needle Test (GNT) was observed when the sample was able to support the needle for 30 sec, leaving behind no visible marks on the sample.

The current filler compositions utilized by our group are an yttria alumino-silicate glass (DY5) and a barium boroaluminosilicate glass (M12). These glasses were chosen for their ability to provide benefits in mechanical properties, radiopacity, and exothermicity. For both of these glasses, our collaborators have developed surface treatments in order to increase the strength of the composites. The three modifications are (2-(7-oxabicyclo[4.1.0]heptan-3-yl)ethyl)trimethoxysilane (ECHE-TMS, **7**), ((9,9-diethyl-1,5,7,11—tetraoxaspiro[5.5]undecan-3-yl)methyl)trimethoxysilane (1-TOSU, **8**), and (3-(9,9-diethyl-1,5,7,11-tetraoxyaspiro[5.5]undecan-3-yl)propyl)trimethoxysilane (3-TOSU, **9**) as seen in Figure 4.

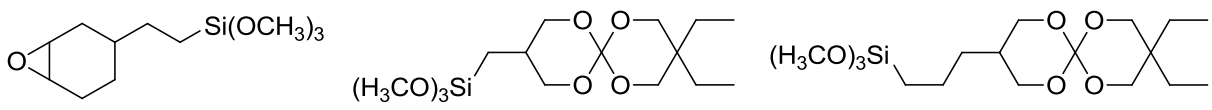

7 **8** **9**

Figure 4: Surface treatment monomers: ECHE-TMS (**7**), 1-TOSU (**8**), and 3-TOSU (**9**).

Investigations are underway to determine the optimal combination of filler and surface modification for use in our biomaterial.

SilMix Availability

Although previously synthesized in the literature, and on an industrial scale, by 3M-ESPE for dental composites, the monomers were not commercially available.[30, 31] Therefore, in the development of our silorane-based biomaterial, several hurdles needed to be investigated and overcome before any further progress could be made. First, the components of the bone cement needed to be acquired in some fashion, either through purchase, donation, or synthesis. Second, the monomers needed to be of a sufficiently high purity so as to surpass the regulatory standards set forth for use as a biomaterial. Finally, in order to fully examine the properties of our biomaterial, a sufficient amount of material needed to be produced using an efficient procedure so as to keep costs at a minimum while maintaining the highest quality achievable. Previous work has been performed on both monomers by Crivello et al. which provided a synthetic starting point.[41, 42]

Hydrosilylation Reaction and Mechanism

In 1947, Sommer reported the reaction between trichlorosilane and 1-octene in the presence of acetyl peroxide (Figure 5), marking the first example of hydrosilylation.[43]

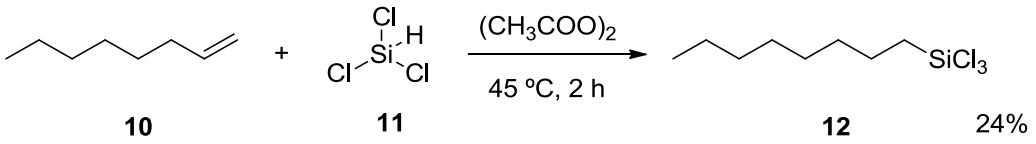

Figure 5: Hydrosilylation of trichlorosilane and 1-octene.

Hydrosilylation has since been defined as the addition of a hydrosilane containing at least one Si-H bond to an unsaturated compound, such as alkenes, alkynes, and carbonyls.[44-46] Since its introduction, hydrosilylation has become one of the most versatile methods in the production of alkylsilanes. The efficiency of this reaction has allowed for improvement of industrial processes in the production of organosilicones used as adhesives, binders, and bioactive compounds.[44, 47] Additionally, this reaction, when, transition metal-catalyzed, has allowed for the development of improved catalytic methodologies important to the field as a whole.[48, 49]

The mechanism of hydrosilylation was proposed by Chalk and Harrod decades ago, and there is a continued search for a more complete understanding of the reaction.[50] The original Chalk-Harrod mechanism was proposed for the hydrosilylation of an alkene with a silane. Since its introduction, this mechanism has been widely accepted for the use of platinum catalysts, but has since been modified for reactions involving Rh, Co, Fe, or Ir catalysts.[51-53] A modified version has been proposed to clarify and address the problems with the original mechanism. It includes a pathway viable for recently developed catalysts as depicted in Figure 6.

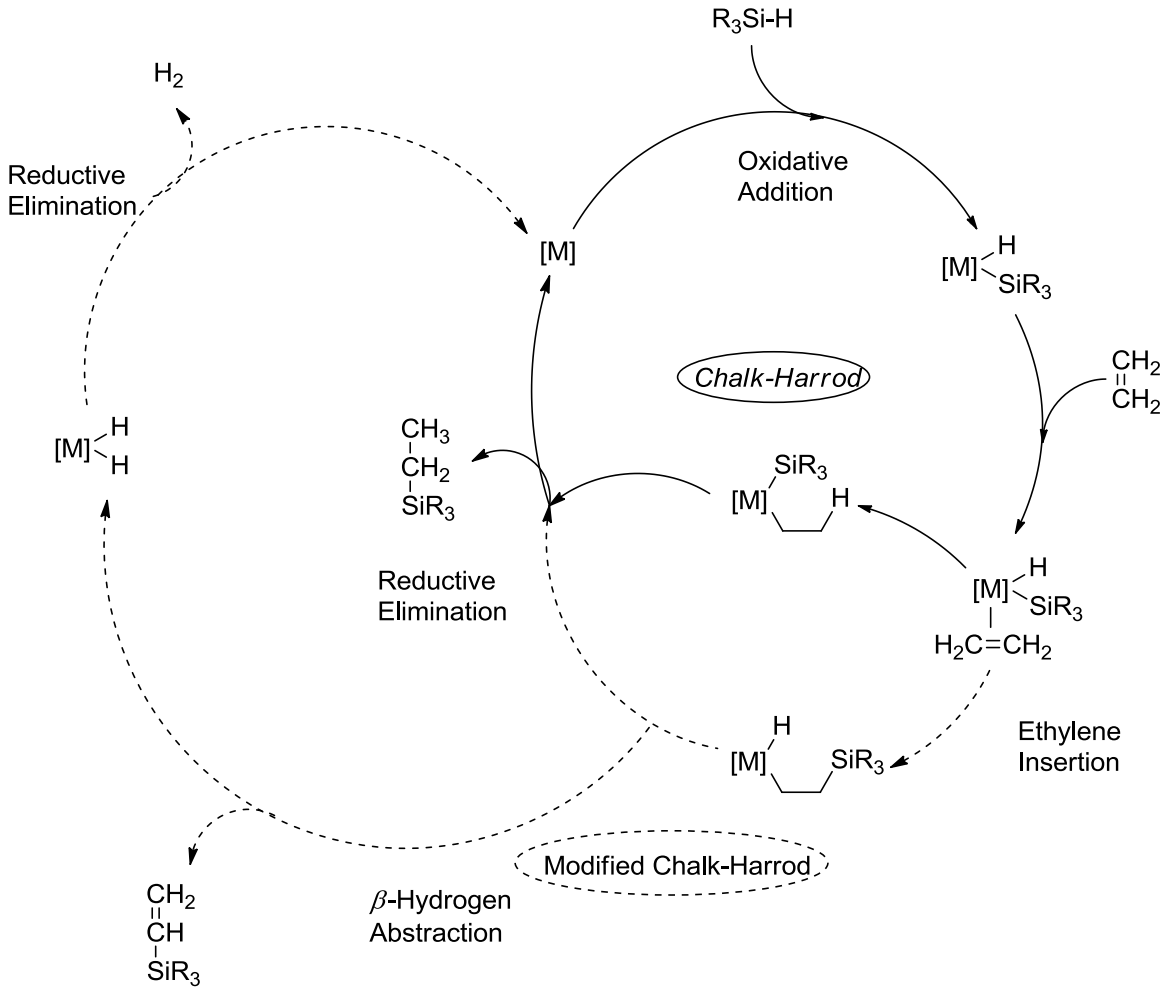

Figure 6: Chalk-Harrod (solid) and modified Chalk-Harrod (dashed) mechanisms for the hydrosilylation of ethylene with a silane.

The original Chalk-Harrod mechanism begins with the oxidative addition of the Si-H bond to the metal center.[46, 51-54] Upon addition of the alkene, insertion occurs into the M-H bond forming a metal(silyl)(alkyl) complex. This complex then undergoes reductive elimination forming an Si-C bond in the silyl product, while regenerating a metal-alkene complex (in the presence of excess alkene).[46, 53] As research became more focused on the reaction, and catalysts became more advanced, a modified pathway was proposed to help

describe the formation of vinyl products.[46, 53, 55, 56] Similar to the original pathway, the modified mechanism begins with oxidative addition and alkene insertion. It is at the insertion step where the pathways diverge. The modified route was found to proceed with insertion into the metal-silyl bond as compared to the metal-hydrogen bond. At that point, the pathway can continue through reductive elimination to produce the desired products or diverge through an alternative route. The alternative pathway proceeds from insertion to β-hydride abstraction, which produces a dehydrogenated vinylsilane. Then, reductive elimination occurs, forming the metal-alkene species. Through the modified route, the dehydrogenated vinylsilane may be produced in addition to the alkyl silane.

To this point, the determination of which pathway a reaction will pass through has mostly been a result of a combination of factors. The type of alkene and silane utilized each plays a role, but most of the research has pinpointed the type of catalyst used to be the major factor. Of the catalysts used, those which have traditionally followed the original Chalk-Harrod mechanism are those based on the Group 10 metals (Pt, Pd, and Ni).[53] Alternatively, reactions following the modified Chalk-Harrod pathway typically utilize catalysts found in Groups 8 (Ir, Ru, and Os) and 9 (Co, Rh, and Ir) of the periodic table. For these reactions, both saturated and unsaturated silyl products have been reported, with Group 8 metals occasionally producing the latter exclusively.[46, 53] A high alkene-to-silane ratio has also been reported to increase the production of the dehydrogenated product compared to the silyl alkane with rhodium catalysts.[52]

The proposal of the modified Chalk-Harrod mechanism has helped to understand several unknown issues, such as the formation of dehydrogenated products, surrounding the hydrosilylation of alkenes. An understanding of the mechanistic pathways for alkenes has

allowed for the development of proposals regarding the hydrosilylation of alkynes and ketones.[48, 54, 57-60] Although valuable information has been collected from several mechanistic explorations, the Chalk-Harrod model still lacks vital information, such as the formation of some side products which include isomerized alkenes. Similarly, recent reports have highlighted the ability of several Ni-, Pd-, and Pt-based catalysts to unexpectedly undergo dehydrogenative hydrosilylation.[61] Thus, while the advancement of the Chalk-Harrod mechanism currently presents a general idea of how to approach a hydrosilylation reaction, there are still several wrinkles which have yet to be ironed out.

Products and Byproducts of Metal-Catalyzed Hydrosilylation

The transition metal-catalyzed hydrosilylation of alkenes has become one of the more important commercial processes. In recent years, several factors have been identified which affect the rate and pathway of the reaction, yield, and composition of the final products.[62] Of the three main components (catalyst, alkene, and hydrosilane) that play a role in the formation of the desired compound, the majority of the focus has been placed on the catalyst. Over the last half century, platinum-based catalysts have been shown to be the most efficient choice for hydrosilylation reactions, even if they have limitations, including regiochemical control. While incredibly useful in the formation of the desired silyl alkane, isomerization and dehydrogenation frequently occur as side reactions, thus forming a series of byproducts.[63-69] This problem is not restricted just to platinum complexes, but it has been observed in other metal-based catalysts (e.g., rhodium, nickel, palladium, cobalt, and iron).[62, 70-72] A generic example of the hydrosilylation of styrene with a trialkylsilane is shown in Figure 7 with the potential products.

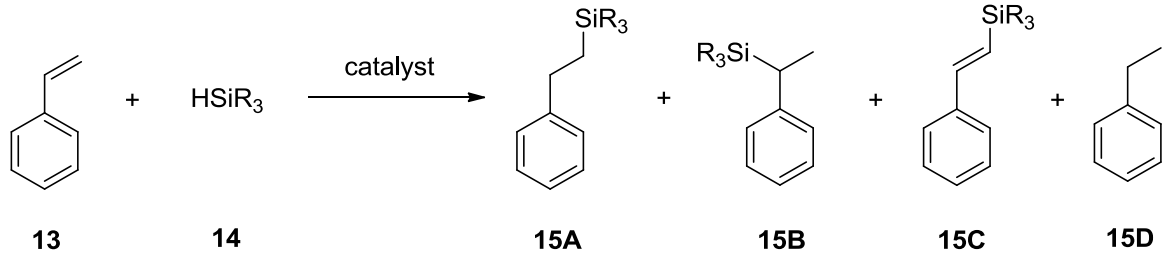

Figure 7: Schematic of the hydrosilylation of styrene with a silane results in the production of the **15A**) anti-Markovnikov β-silyl alkane, **15B**) Markovnikov α-isomerized branched alkane, **15C**) dehydrogenated β-silyl alkene (a vinyl silane), and **15D**) alkane products.

The coupling of a silane with a terminal alkene using a transition metal catalyst predominantly forms the anti-Markovnikov β-silyl alkane **(15A)**. In some cases, poor regiocontrol will lead to the formation of alternative products. Isomerization of the silane during the reaction forms the branched Markovnikov α-adduct **(15B)**, while dehydrogenation produces the β-silyl alkene (vinylsilane) **(15C)**. Additionally, in some cases, hydrogenation of the alkene has been observed to form the alkane product **(15D)**.[68, 70, 71] Use of broad-range generic catalysts (e.g. Speier's, Karstedt's, or Wilkinson's) in hydrosilylation typically provides sufficient reactivity to acquire the anti-Markovnikov product. There is competition with the side reactions due to the lack of regiocontrol (Table 2).

Table 2: Reported products formed using generic hydrosilylation catalysts.[62]

Catalyst	Reported Products of Hydrosilylation
Speier's catalyst (H_2PtCl_6/*i*-PrOH)	β-silyl alkane (A), α-silane (B)
Karstedt's catalyst ($Pt_2(H_2C{=}CSiMe_2OSiMe_2CH{=}CH_2)$)	β-silyl alkane (A), α-silane (B)
Wilkinson's catalyst ($RhCl(Ph_3P)_3$)	β-silyl alkane (A), α-silane (B), β-silyl alkene (C), alkane (D)

Since the hydrosilylation of silanes with alkenes is a vital step in many industrial processes, the lack of specific regiocontrol is a problem with the use of generic standard catalysts. Therefore, alternative catalysts have been developed from these generic precursors, which produce higher regiocontrol to form the desired product. In some cases, the anti-Markovnikov product is the major product, while in other reactions the dehydrogenated product is formed.[62]

Platinum Derivatives

The first step for the synthesis of the monomers is to summarize the different catalysts used in hydrosilylation reactions. Since the discovery of platinum complexes as catalysts in the addition of silanes to alkenes, the two major focal points of research have been on Speier's (H_2PtCl_6/*i*-PrOH) and Karstedt's ($Pt_2(H_2C{=}CSiMe_2OSiMe_2CH{=}CH_2)$) catalysts. Over recent decades, Karstedt's complex has emerged as the more trendy choice for hydrosilylation reactions due to the higher degree of reactivity. Unfortunately, while the desired anti-Markovnikov product can be formed in yields >90%, competing side reactions produce byproducts, such as isomerized alkenes and alkanes. Additionally, there are

numerous reports of formation of a yellow coloration to the solution. The competing reactions and coloration emphasize the need for enhanced catalytic systems.

The competing side products using the general platinum catalysts made it vital for improvements in the reaction and/or conditions and efficient alternative routes. With the already high reactivity and reported yields for Karstedt's complexes, Markó et al. developed a series of N-heterocyclic carbene complexes. These Karstedt derivatives showed very high regioselectivity and chemoselectivity towards the production of the anti-Markovnikov product as shown in Figure 8.[65, 66]

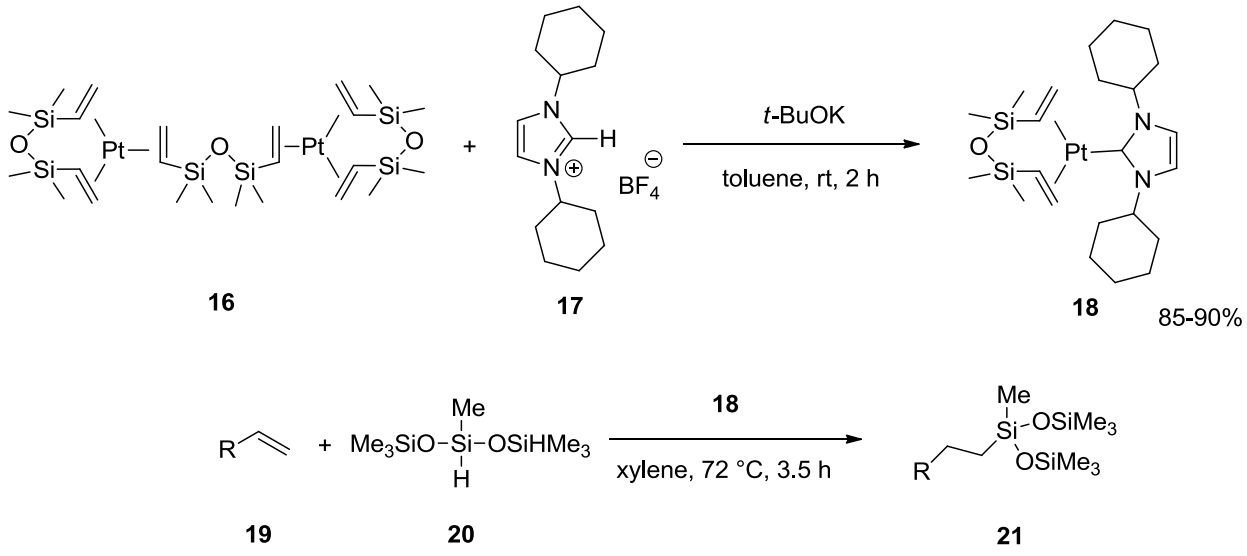

Figure 8: Preparation of Karstedt-derived carbene catalyst and use in hydrosilylation.

Table 3: Hydrosilylation of terminal alkenes using an N-heterocyclic carbene complex.[65]

Entry	R	Product	Yield (%)
1	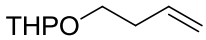	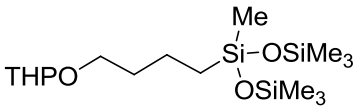	92
2	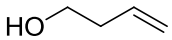	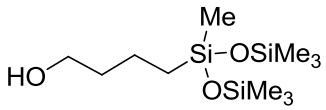	96
3	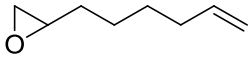	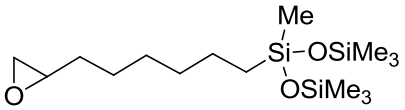	90
4	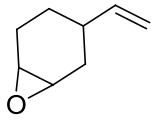	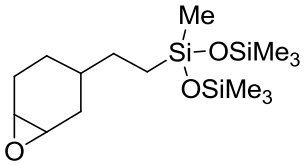	92
5	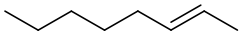	-	-

These carbene complexes were successful over a wide range of functionalized terminal alkenes as shown in Table 3**.** In these reactions, isolated and pure yields were reported, while the same reactions run using Karstedt's catalyst produced a mixture of products and a colloidal platinum species. Interestingly, use of internal alkenes proved to be futile with only quantitative amounts of starting material recovered. Alternatively, Osborn et al. successfully derivatized the Karstedt complex through the replacement of the bridging siloxane with a series of naphthoquinones. One example is seen in Figure 9.[73]

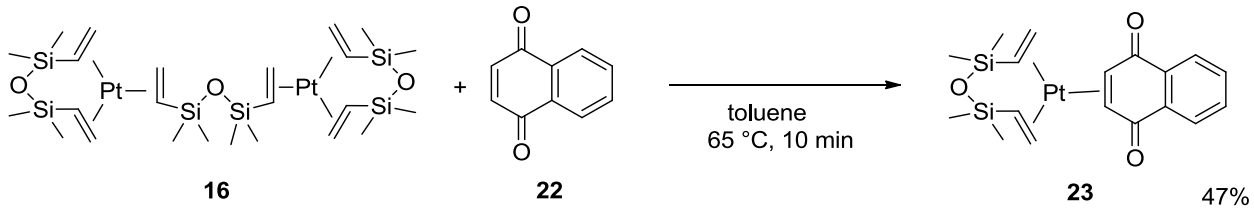

Figure 9: Naphthoquinone-derived Karstedt's catalyst.

Use of these naphthoquinone derivatives in combination with a series of substituted styrenes generally produced the β anti-Markovnikov product as the major product. Unfortunately, in many cases a low yield with minor amounts of the isomerized or dehydrogenated products was observed. In summary, the desire to overcome the lack of regiocontrol exhibited in platinum catalysts has had mixed results, but the development of catalytic derivatives has provided increased control under certain conditions.

A large percentage of the reports on platinum catalysts in the literature mention the formation of colored bodies (typically denoted as a yellow hue) during the reaction.[63, 65] Lewis et al. originally proposed the formation of colloidal platinum complexes, which upon formation became the active species in the reaction and were visible as a colored species. It was proposed that the platinum complex is reduced by the hydrosilane to a colloidal species at which point the alkene adds directly to the hydrosilane to form the products. The proposed mechanism was based on studies using colloidal Pt, Rh, and other metals along with the inhibitory effect of metallic mercury for colloidal metal-catalyzed hydrosilylations.[62] Lack of *in situ* evidence for the formation of colloids during the catalytically active portion of the reaction caused Lewis et al. to further examine their theory. They later published a more

refined study using Karstedt's catalyst and H_2PtCl_6 in which they concluded that mononuclear and soluble platinum complexes are the catalytic species rather than a colloidal complex. In the formation of the colored bodies, yellowing of the reaction was caused by the formation of Pt-Pt and Pt-Si bonded insoluble species at the end of the reaction.[61, 63] The studies by Lewis et al. help to give a better understanding in the still relatively unknown Chalk-Harrod mechanism for hydrosilylation reactions.

A third major, yet less known, catalytic species derived from platinum compounds was developed in 1962 by Lamoreaux.[74] Originally, this catalyst was developed as the next-generation platinum catalyst to revolutionize the formation of silicon-carbon linkages. It was overshadowed by the emergence of Karstedt's catalyst. Similar to Speier's catalyst, Lamoreaux's catalyst is formed from the reaction of chloroplatinic acid hexahydrate in an alcohol (1-octanol) to form the platinum complex. Results show that Lamoreaux's catalyst is a complex mixture of Pt compounds containing aldehyde and ether linkages with both Pt^{IV} and Pt^{II} species present as determined by mechanistic studies utilizing ^{195}Pt NMR spectroscopy.[74, 75] While a highly reactive complex, Lamoreaux's catalyst has failed to gain interest throughout the literature. With very little usage to this point, few details have been reported as to the potential advantages and disadvantages of the complex. Of these, the most notable is the susceptibility of hydrosilylation reactions involving epoxides to gel with the use of Lamoreaux's catalyst.[42, 76]

Rhodium Derivatives

In addition to platinum-based catalysts, rhodium has been widely used for a variety of hydrosilylation reactions. In the majority of cases, the catalyst of choice has been Wilkinson's catalyst, $Rh(PPh_3)_3Cl$ (**24**), as depicted in Figure 10.

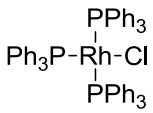

24

Figure 10: Wilkinson's catalyst

In reactions utilizing rhodium catalysts, results indicate that more factors than the catalyst alone affect the resulting products in hydrosilylations. Skrydstrup et al. investigated the coupling of several terminal alkenes with diphenylated silanes using Wilkinson's catalyst.[77] The anti-Markovnikov product was obtained in good yields in reactions using varying solvents as seen in Table 4.

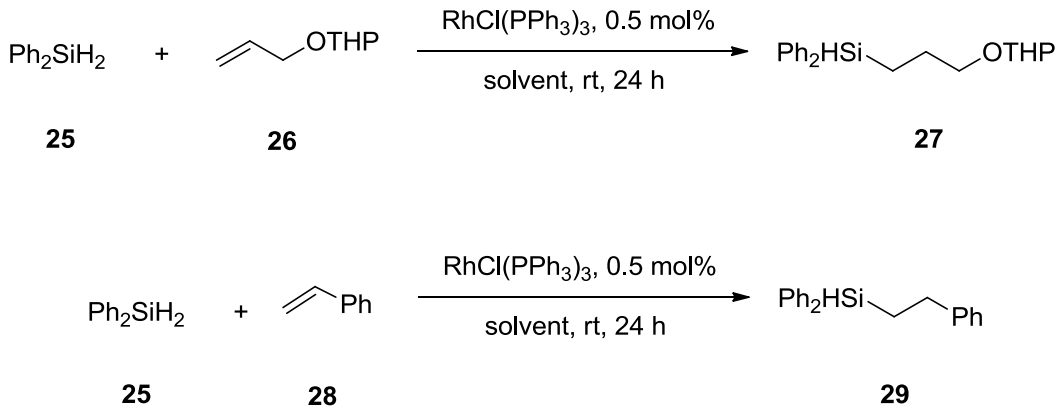

Figure 11: Hydrosilylation of diphenylsilane using Wilkinson's catalyst.

Table 4: The solvent effect in hydrosilylations using Wilkinson's catalyst.[77]

Silane	Alkene	Solvent	Yield (%)
25	26	THF	81
25	26	CH_2Cl_2	71
25	26	Toluene	85
25	26	Acetone	17
25	26	THF + Acetone	50
25	28	THF	38

With the exception of acetone, the effect of solvents for these reactions produced minimal differences in yield. In cases where solvents containing a ketone (C=O) were used, hydrosilylation of the carbonyl group occurs in the presence of Wilkinson's catalyst. Interestingly, in some cases, reproducibility of previously reported reactions proved troublesome. Specifically, there was a problem with recovery of as little as half of the reported yield. In all of the literature reports, the anti-Markovnikov products were obtained

selectively, but it was noted that electronic effects may play a role in the regioselectivity. Similar trials, using compounds, such as *n*-butylacrylate, gave a 46% yield of the Markovnikov product. On the other hand, Li et al. reported only moderate regioselectivity using Wilkinson's catalyst with ethoxysilanes.[70, 71] However, derivitization of the rhodium catalyst with 2-imidazolium phosphines produced higher regioselectivity (up to 99%) of the anti-Markovnikov product as shown in Table 5.

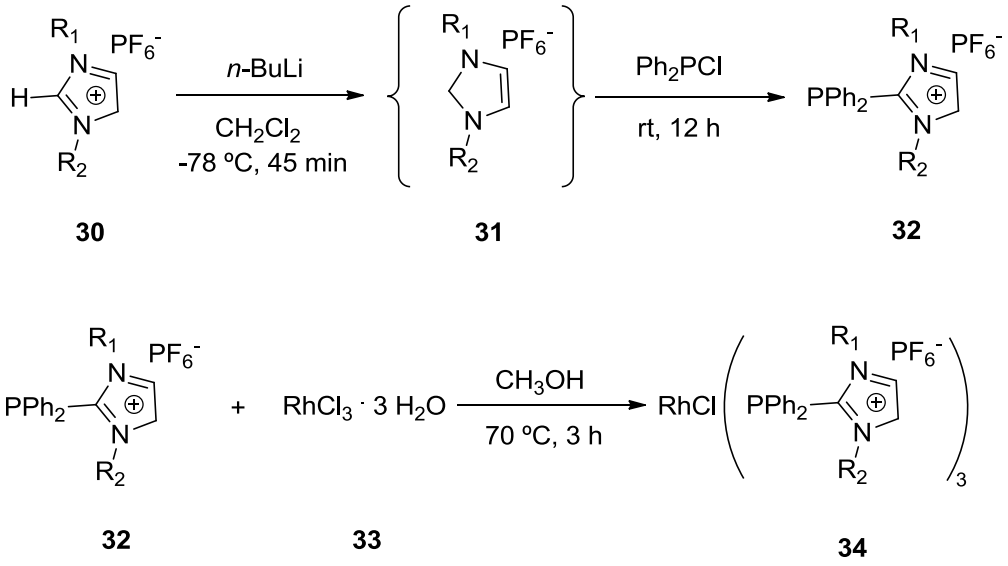

Figure 12: Schematic of imidazolium rhodium complexes. Reaction conditions: alkene 2.5 mmol, triethoxysilane 3.0 mmol, 70º, 5 h. R_1:R_2: **1** (CH_3:C_2H_5), **2** (CH_3:C_4H_9), **3** (CH_3:C_6H_{13}), **4** (C_2H_5:C_4H_9), **5** (C_4H_9:C_4H_9), and **6** (C_4H_9:C_6H_{13}).

Table 5: Effect of rhodium complex on hydrosilylation selectivity.[71]

Catalyst (% substrate mol)	Substrate	Conversion (%)	Selectivity (β:α:alkane)
$RhCl(PPh_3)_3$ 0.1	Styrene	78.1	81.2:16.5:2.3
1 (0.02)	Styrene	100	89.8:4.1:6.1
2 (0.02)	Styrene	99.4	91.6:3.1:5.3
3 (0.02)	Styrene	96.1	94.9:1.6:3.5
4 (0.02)	Styrene	95.7	96.6:1.9:1.5
5 (0.02)	Styrene	94.5	97.3:1.2:1.5
6 (0.02)	Styrene	92.1	99.4:0:0.6
1 (0.005)	1-Hexene	100	99.1:0:0.9
1 (0.005)	1-Heptene	100	98.7:0:1.3
1 (0.005)	1-Octene	100	99.0:0:1.0
1 (0.005)	1-Undene	100	98.8:0:1.2

To this point, the majority of work has been focused on the optimization of the anti-Markovnikov silane. In some cases, the goal may be to produce one of the typical byproducts. The dehydrogenated *β*-silyl alkene or vinylsilane, which may be produced by the modified Chalk-Harrod mechanistic pathway for rhodium catalysts, was reported by Takeuchi et al.[56] They focused on the use of vinylsilanes as an alternative to the hydrosilylation of alkynes. The use of a cationic rhodium complex in an excess of styrene and various silanes produced the dehydrogenated silyl alkene as the major product in several trials as seen in Table 6.

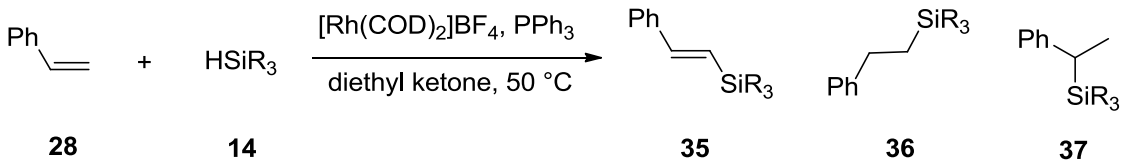

Figure 13: Schematic of hydrosilylation using a cationic rhodium complex.

Table 6: Effect of cationic rhodium complex on hydrosilylation.

Entry	Hydrosilane	Time (h)	Yield (%)	Product Distribution 35:36:37
1	$HSiEt_3$	2	91	78:22:0
2	$HSiEt_2Me$	2	83	51:49:0
3	$HSi(n\text{-}Pr)_3$	2	90	84:16:0
4[a]	$HSi(i\text{-}Pr)_3$	64	81	100:0:0
5[a]	$HSi(t\text{-}Bu)Me_2$	15	85	95:5:0
6	$HSiPhMe_2$	2	88	12:88:0
7[b]	$HSi(OEt)_3$	3	67	26:74:0

[a] Run in 1,2-dichloroethane, [b] refluxed in 1,2-dichloropropane.[56]

Of these trials, only one silane, triisopropylsilane (entry 4), was formed with 100% selectivity of the silyl alkene. The ability to selectively produce the vinylsilane introduces an attractive alternative to the hydrosilylation of alkynes. It also provides useful information as to the selectivity of rhodium catalysts. As with platinum complexes, rhodium-based hydrosilylation catalysts have the potential to selectively produce a certain desired product,

but still have several problems which need to be investigated (e.g., improved efficiency of existing catalysts and recyclability).

Other Transition Metal Catalysts

While the focus of hydrosilylation catalysts has been on the development of platinum and rhodium catalysts, a recent trend has been the development of cheaper, more readily available metals with better selectivity towards certain products (specifically the anti-Markovnikov and dehydrogenated products). Recent advances by Chirik et al. include the use of aryl-substituted bis(imino)pyridine iron complexes (**38**). They have successfully coupled terminal alkenes with hydrosilanes to exclusively produce the anti-Markovnikov product in >95% yield.[64, 69]

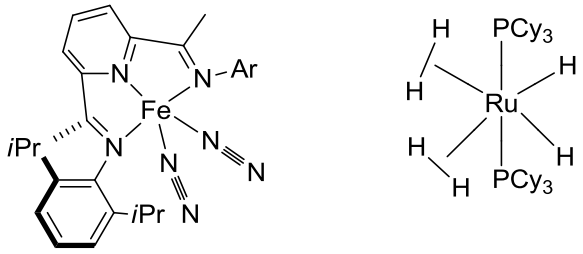

38 **39**

Figure 14: Iron **38** and bis(dihydrogen) ruthenium **39** complexes used as alternative hydrosilylation catalysts.

Christ et al. focused on the goal of predominantly producing the vinylsilane through the use of a bis(dihydrogen) ruthenium complex (**39**) with ethylene and $HSiEt_3$ in yields as high as 97%.[78] These metals, along with palladium and nickel, to name a few, have gained interest as potential alternatives to platinum and rhodium. Each element provides a unique characteristic from affordability and availability to specific regioselective trends in comparison to the aforementioned staples. Current and future research in the field will determine if a superior alternative can be developed.

Mechanism, Products, and Byproducts Wrap Up

The versatility of metal catalysts in the coupling of an alkene with a hydrosilane has made hydrosilylation a very useful synthetic tool. The advancement of mechanistic studies has provided vital information towards the understanding of the original and modified Chalk-Harrod mechanism, specifically for reactions utilizing platinum- and rhodium-based catalysts. The use of platinum and rhodium catalysts has provided highly useful syntheses for the formation of several extended silanes. In determining which metal would be of best use for a reaction, the general belief is that rhodium-based catalysts are better for less polar silanes, while platinum catalysts perform better with more polar silanes.[62] Consequently, in addition to the desired product, many of these reactions produce undesired byproducts. Both the current and historical interests of the field focus on the formation of the anti-Markovnikov β-alkyl silane, but recent advances have included the formation of the dehydrogenated β-silyl alkene or vinylsilane, most notably through Group 8 based catalysts. Improvements in regioselectivity have come through the derivatization of several of the generic catalysts and the advancement of cheaper, greener metal alternatives.

Previous Studies of Crivello

Over the last 30 years, the development of silicon-based monomers and oligomers has become an interesting field due to their excellent polymerization potential and resulting mechanical properties. Crivello et al. extensively investigated the extension of multifunctional silicon-based monomers (siloranes), in particular those containing epoxides, through hydrosilylation reactions.[79-81] The majority of the monomers were prepared starting from silanes, compounds containing an Si-H functionality, or siloxanes, compounds containing an Si-O-Si functionality. Crivello et al. investigated photoinitiated cationically polymerizable silicon-based monomers containing epoxides.[42] They synthesized a series of multifunctional siloxane monomers and oligomers using the condensation of epoxides containing alkenes with siloxanes as seen in Figure 15.

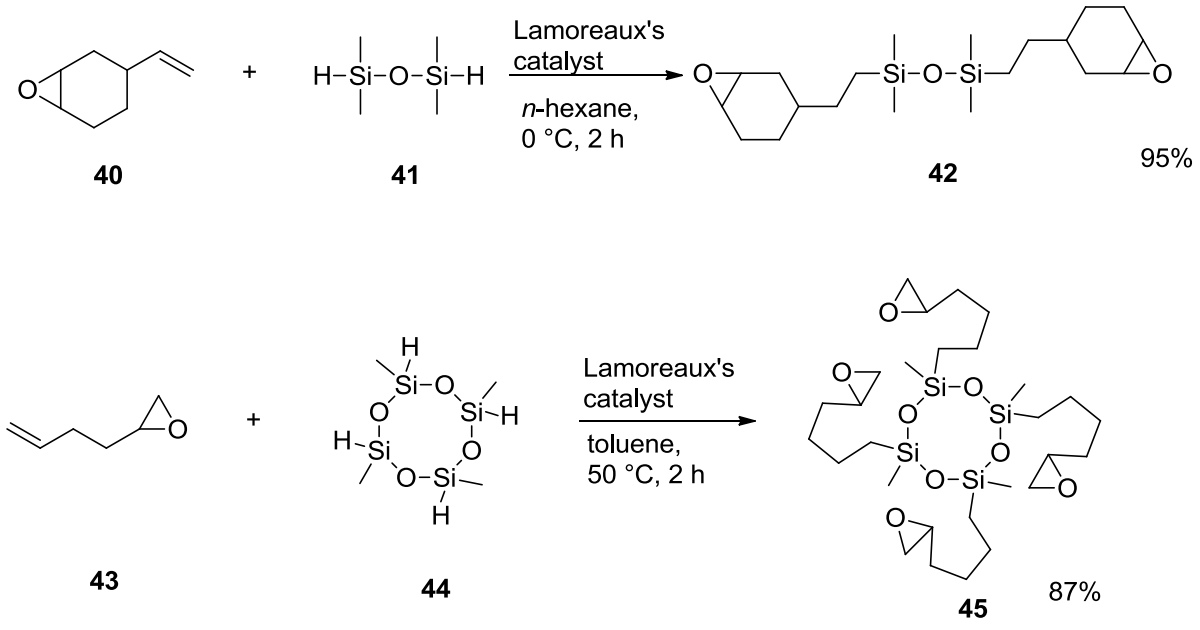

Figure 15: Synthesis of siloxane monomers using Lamoreaux's catalyst.

The use of siloxanes as starting materials required the utilization of a platinum-based catalyst due to its polar Si-O bond. Thus, hydrosilylation of the linear, branched, and cyclic compounds was performed using the platinum-based Lamoreaux's catalyst. Reactions involving the use of platinum catalysts will in general follow the Chalk-Harrod mechanism (Figure 6, solid line) and can be performed between 0-80 ºC using aprotic solvents. While typically run under an inert atmosphere, there are many times when the reaction may proceed under atmospheric conditions. In the case of the cyclic siloxanes, gelation upon addition of the catalyst occurred unless the reaction was performed under nitrogen and extremely dry conditions.[42] It was determined that residual traces of water reacted with the Si-H groups in the presence of the platinum catalyst to form an Si-OH group. These groups would then further condense to give a cross-linked polymer network. To prevent the possibility of polymerization, the reagents were distilled, the condenser was fit with a $CaCl_2$ drying tube, and the reaction mixture was refluxed through a Dean-Stark trap containing CaH_2. The reactions were performed under these conditions and it was possible to successfully synthesize several siloxane monomers using the platinum-based Lamoreaux's catalyst in high yields with no reported byproducts.

In their subsequent work, Crivello et al. investigated the effect of platinum catalysts on reactions containing epoxycyclohexyl groups with compounds containing Si-H moieties.[41] The use of platinum catalysts with these monomers resulted in a high percentage of ring-opening polymerization. To avoid this result, they explored the use of alternative metal-based transition catalysts. It was observed that certain rhodium complexes, in particular Wilkinson's catalyst, were excellent for these particular reactions and were very tolerant to various functional groups. Thus, a series of multifunctional silicon-based epoxides were

synthesized from the corresponding silanes and vinyl epoxides with yields ranging from 86-99% (Figure 16).

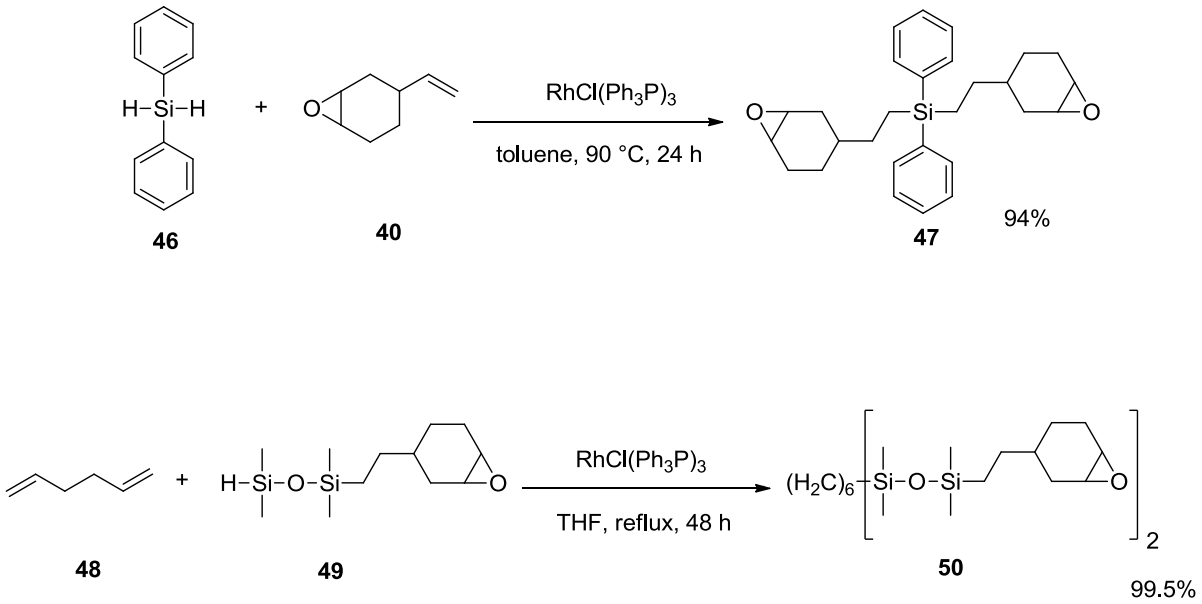

Figure 16: Hydrosilylation of silicon monomers using Wilkinson's catalyst.

In addition to cyclohexyl epoxide monomers, it was found that Wilkinson's catalyst was optimal for the hydrosilylation of dialkyl and diarylsilanes.[41] Furthermore, for the first time in hydrosilylation reactions, Crivello et al. reported the use of a cross-linked polystyrene-bound version of Wilkinson's catalyst. This polymer-bound complex was purchased in the form of insoluble beads as compared to the unbound powder version. They noted that the change in catalyst substrate exhibited equivalent activity and regioselectivity as the more common monomeric powder version. An additional benefit to the polymer-bound catalyst

was the ability of the catalyst to be filtered off after completion of the reaction. Recovery of the catalyst proved to be cost-effective because it could then be used in subsequent reactions without loss of reactivity. In comparison, removal of the powder version is more complicated and is typically performed using chromatography with loss of the material.

The reports by Crivello et al. helped in the advancement of the field of hydrosilylation using epoxy-containing alkenes. Their work highlighted the potential of Lamoreaux's catalyst as a possible catalyst in the presence of epoxides, albeit under extremely dry conditions. Additionally, these results expanded and developed the use of rhodium catalysts, specifically Wilkinson's catalyst, as an excellent alternative for reactions involving epoxides without the detrimental ring-opening side reactions.

Results and Discussion

For the development of our biomaterial, it was essential to acquire the two silorane monomers. Both monomers were unavailable commercially, thus it was essential for the development of synthetic procedures. Therefore, suitable scale up syntheses were developed using work conducted previously by Crivello et al. as a roadmap.[41]

PHEPSI and Polymer-bound Wilkinson's catalyst

A scale-up synthesis of PHEPSI was developed, and the overall reaction is depicted in Figure 17**.**

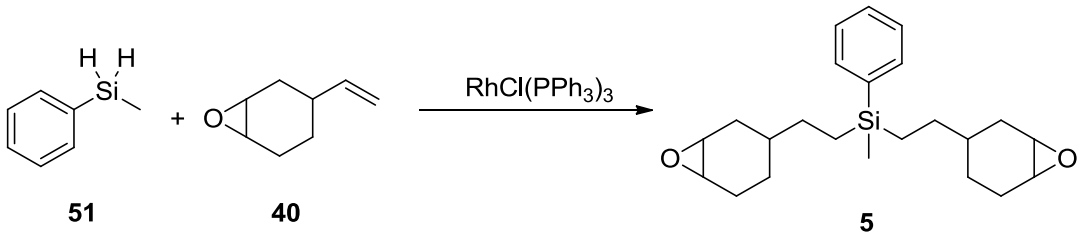

Figure 17: Synthesis of the silorane monomer, PHEPSI.

Attempts at optimizing the hydrosilylation of methylphenylsilane and 4-vinyl-1-cyclohexene-1,2-epoxide are given in Table 7.

Table 7: Attempts to optimize PHEPSI reaction conditions.

Entry	MPS (g)	Wilkinson's Catalyst	Supplier	Temp	Time	% Yield
1	1.2 g	Styrene-divinylbenzene bound	Alfa Aesar	90°	24 h	0
2	1.2 g	Styrene-divinylbenzene bound	Alfa Aesar	90°	48 h	0
3	2.4 g	Powder, 97%	Alfa Aesar	95°	24 h	42
4	9.7 g*	Powder, 97%	Alfa Aesar	95°	24 h	33
5	19.4 g*	Powder, 97%	Alfa Aesar	100°	24 h	67
6	19.4 g*	Powder, 97%	Alfa Aesar	95°	18 h	66
7	19.4 g*	Powder, 99%	Strem	95°	18 h	45
8	9.7 g	Powder, 99%	Strem	100°	24 h	63
9	19.4 g	Powder, 99%	Strem	95°	24 h	46

* indicates side-by-side reactions run and combined after IR spectra were collected.

The initial attempts of the coupling of methylphenylsilane to vinylcyclohexene epoxide utilized a styrene-divinylbenzene polymer-bound Wilkinson's catalyst. These trials used a reaction temperature of 90 ºC for 24 h. The reaction progress was monitored using IR spectroscopy. Since the Si-H peak of methylphenylsilane is found uniquely at 2160 cm^{-1}, it was used to monitor the reaction progress. Disappearance of this peak indicated the starting silane had been consumed. After 24 h, the peak was still present. With subsequent heating for an additional 24 h (trial 2), the peak was still observed. After repeated attempts, no change in the reaction was observed. With these negative results, focus was placed on the use of an alternative catalyst.

Powder Monomeric Wilkinson's Catalyst

Unable to reproduce the published procedure, we switched to the generic crystalline powder form of the catalyst instead of the polymer-bound version.[41] The IR spectrum resulting from heating of the reaction to 95 ºC for 24 h (trial 3) showed the absence of the peak at 2160 cm^{-1} using the powdered Wilkinson's catalyst. This modification resulted in the desired conditions for successful formation of the silorane. With a successful procedure underway, several factors were investigated to find the optimal conditions for the production of PHEPSI.

The factors which were investigated included the temperature, time, and scale of the reaction. Primary trials tested the effect of heat on the reaction versus product formation (Table 7). It was found that heating at 90-100 °C was required for complete conversion, with the optimal conditions from those reactions with temperatures between 95-100 °C resulting in yields of 66 and 67%, respectively. Secondly, reaction time was examined. During the

trials, it was observed that very little visible change occurred in the reaction after ~15-20 h of heating. IR spectra were collected at different time periods and compared to a spectrum collected after 24 h of heating. The absence of the Si-H peak at 2160 cm^{-1} was observed as early as 18 h, thus indicating completion of the reaction. In a comparison of trials 5 (24 h) and 6 (18 h), no significant change in yield was observed. Therefore, these results indicated that the optimal conditions included heating the reaction mixture at 95-100 °C for 18-24 h utilizing the crystalline powder version of Wilkinson's catalyst.

PHEPSI Scale-Up

If these monomers are to be used as a commercial biomaterial, a sizable quantity of resin is required for testing *ex* and *in vivo*; therefore, a reproducible scale-up of the reaction became the next essential task. Preliminary test reactions were run on a small scale (1.2 g of methylphenylsilane) using the polymer-bound catalyst (Table 7). With the use of the powdered Wilkinson's catalyst (Alfa Aesar, 97% purity), the reaction scale was doubled in hopes of producing enough material to fully explore purification routes. PHEPSI was synthesized and isolated in a 42% yield after purification. The scale was again increased to 9.7 g of methylphenylsilane (side-by-side reactions of 4.8 g and combined before purification), but resulted in a lower yield (33%). Again, side-by-side reactions were run, and this time with 9.7 g (19.4 g combined total) resulting in an isolated yield at 67%. In order to investigate the differences in suppliers of the catalyst, a Strem version was run on the same scale. However, this change produced a significant loss of product (or production of byproduct) with a yield of 45%. While the set-up of side-by-side reactions was working, the assembly of two reactions is not conducive to scale-up. A single 19.4 g reaction batch (entry 9) was run and resulted in a 46% yield. This result indicates that the hydrosilylation of

PHEPSI has the potential to be scaled to much larger sizes without significant loss of yield. It is interesting to note that a yield of 63% was obtained utilizing the Strem-manufactured Wilkinson's catalyst on a 9.7 g scale. The large difference in yield between the reaction scales may be due to purification as a principal factor in the loss of product during the process.

The ability to increase the reaction scale in the synthesis of PHEPSI became an essential task as the demands for significant quantities of the monomer rose. While a loss of yield was reported for similarly sized batches using different catalyst suppliers, comparative yields for reactions indicate that this loss of product may be the result of the purification of the product as opposed to catalyst reactivity. At this point, it is believed that further scale-up of the PHEPSI reactions should be successful.

PHEPSI Purification

The previously reported purification of PHEPSI utilized a standard organic chemistry workup (e.g., filtration of the catalyst, followed by the removal of solvents and unreacted starting materials under reduced pressure).[41] In our attempts using this procedure, we were unable to remove either the catalyst or any unreacted starting materials via filtration and concentration under reduced pressure. Additionally, due to the viscosity of the crude material, residual solvents were trapped in the thick liquid as determined by ^{1}H NMR spectroscopy. Thin layer chromatography (TLC) was used to determine the presence of any UV detectable compounds and their potential separability. The presence of two distinct spots (R_f 0.21 and 0.47, solvent: 10% ethyl acetate–hexanes) led to the determination that column chromatography would be a suitable means of purification.

Due to the viscosity of the crude material, the residual solvents were successfully removed via vacuum. Dilution of the crude reaction material in hexanes, which was followed by elution using a solvent gradient that ranged from hexanes to 10% ethyl acetate–hexanes, provided the appropriate separation of the two UV detectable bands on the column. Collection of the bands provided important information about the reaction. It was determined that a combination of unreacted vinylcyclohexene epoxide and an unidentified byproduct were present in the first band at R_f 0.47, and PHEPSI, the product, as a colorless, viscous liquid at R_f 0.21 was the second material. It is of note that fractionation between the bands shows bleeding of the two bands in varying amounts. An increase in the volume of hexanes prior to adjusting the polarity of the mobile phase provided more separation, but only to a small extent. Even through various trials, isolation of pure PHEPSI from the remaining epoxide and byproduct was not achieved. Additionally, further attempts to separate unreacted epoxide from the byproduct were unsuccessful. As expected, Wilkinson's catalyst remained at the top of the column. This successful isolation of the products proved to be an important step in the development of a biomaterial, as it produced PHEPSI in high purity. Through this process it was determined that the ideal purification of PHEPSI is via column chromatography utilizing a solvent-gradient starting with 100% hexanes to 10% ethyl acetate–hexanes.

PHEPSI Byproduct

As discussed previously, rhodium-catalyzed hydrosilylation reactions have been shown to produce several products.[56, 62, 70, 71] The synthesis of PHEPSI followed this trend, as additional products were formed. To gain a better understanding of the reaction, identification of the byproduct was investigated. Purification of the material allowed for the

separation of PHEPSI from the additional products, but the mixture of the byproducts and unreacted monomer could not be further separated. Analysis of the mixture by ^{1}H and ^{13}C NMR spectroscopy allowed for the formulation of what may comprise the mixture. The ^{1}H NMR spectrum contained various peaks which cannot be attributed to methylphenylsilane, 4-vinylcyclohexene-1,2-epoxide, or PHEPSI. Of the peaks, those of interest included the presence of unique peaks between 0.00-0.40, 3.15-3.25, 5.15-5.25, and 7.50-7.60 ppm (Figure 18).

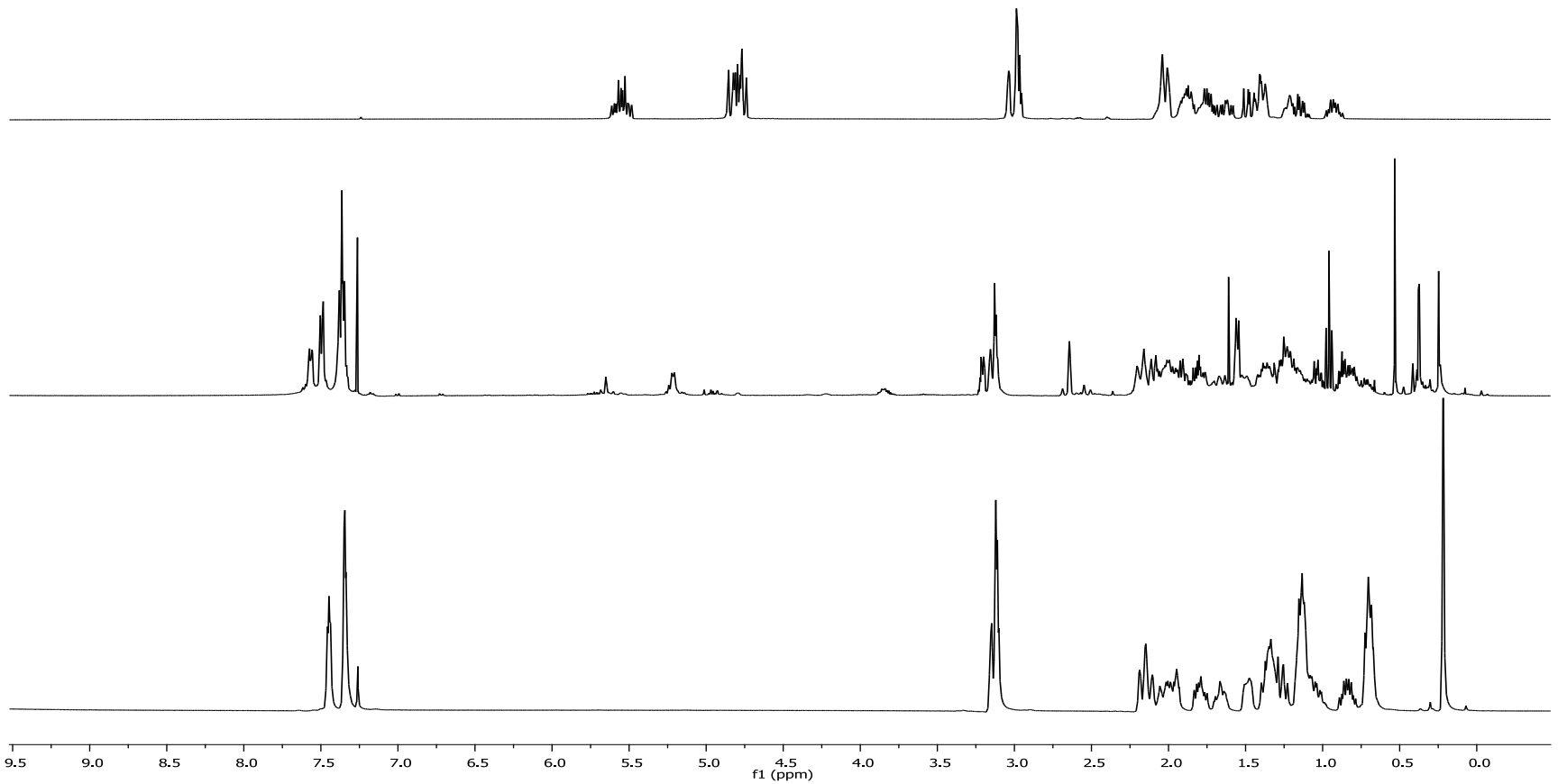

Figure 18: ^{1}H NMR spectra of 4-vinylcyclohexene-1,2-epoxide (top), PHEPSI byproduct (middle), and PHEPSI (bottom).

This combination can be attributed to an additional PHEPSI-like or alternate compound due to the distinct similarities in the spectrum. For the ^{13}C NMR spectrum, the introduction of peaks between 20-40 ppm (up to an additional 10 peaks) and above 100 ppm (up to an additional 8 peaks between 113-133 ppm) further supports the hypothesis of a PHEPSI-like product. Additionally, peaks (vinyl alkene from the cyclohexene epoxide, multiplets at 4.90-5.00 and 5.60-5.75 ppm) appeared in an altered splitting pattern to that of the unreacted form (multiplets 4.85-4.95 and 5.45-5.60 ppm). With the use of the rhodium-based Wilkinson's catalyst, the general thought is that the reaction would proceed through the modified Chalk-Harrod pathway (Figure 6, dashed line). Therefore, it seems likely that a dehydrogenated vinyl silane may be produced. In the case of PHEPSI, where a double hydrosilylation takes place, there is the possibility of two vinyl products being formed as seen in Figure 19.

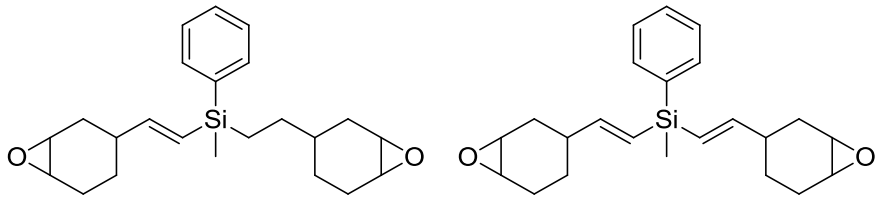

52 **53**

Figure 19: Potential byproducts in the hydrosilylation of PHEPSI include vinyl and divinyl derivatives.

The introduction of peaks in the 5-6 ppm range of the ^{1}H NMR spectrum and above 110 ppm in the ^{13}C NMR spectrums may be attributed to the presence of the alkenes, while the additional aromatic peaks support the presence of a phenyl-bearing compound. Unfortunately, the need to run the reaction using a molar excess of the cyclohexene epoxide ensures the presence of unreacted monomer at the conclusion of the reaction. Optimal reaction conditions have not allowed for full characterization of the byproducts to this point. In addition to formation of the dehydrogenated vinyl silanes, other products may potentially be formed, including α-silane or any combination of α–, β–, or dehydrogenated products.

PHEPSI Optimization Recap

In the development of the first of two silorane monomers for use as a potential biomaterial, PHEPSI was synthesized using the hydrosilylation of methylphenylsilane with 4-vinylcyclohexene-1,2-epoxide using a powdered form of Wilkinson's catalyst. When a polymer-bound catalyst failed to produce the monomer, the crystalline version was employed with improved results. Continued modifications to these procedures led to the determination of the optimal conditions, including heating of the reaction to 95-100 °C for 18-24 h.

Furthermore, the use of a solvent gradient ranging from 100% hexanes to 10% ethyl acetate–hexanes with column chromatography allowed for the best separation of the product from most other components in the crude material. This combination of modifications led to the overall synthesis of PHEPSI in usable yields as high as 67%.

Optimization of CYGEP

During the ongoing optimization of PHEPSI, attempts to identify the ideal route for the synthesis of CYGEP were running concurrently. The first published synthetic procedure of CYGEP by Crivello et al. reported the use of Lamoreaux's catalyst (LMC) under extremely dry conditions in the hydrosilylation of 2,4,6,8-tetramethylcyclotetrasiloxane (TMCTS) and 4-vinyl-1-cyclohexene-1,2-epoxide as depicted in Figure 20.[42]

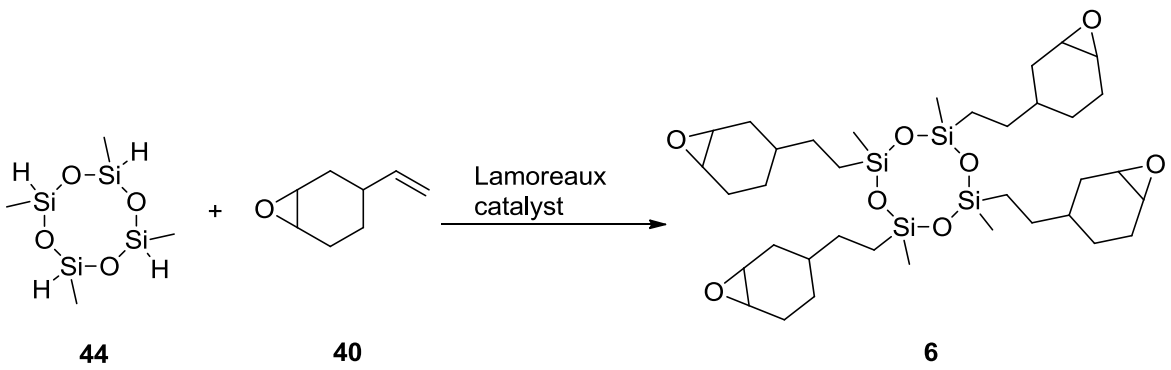

44 **40** **6**

Figure 20: Schematic of the synthesis of the silorane monomer CYGEP.

Therefore, the next step was to review literature for the synthesis of LMC.

Development of Lamoreaux's Catalyst

In the early 1960's, the scope of knowledge concerning the catalysis of hydrosilylation reactions was still in its infancy. At the time, catalysis of such reactions was somewhat limited to organic peroxides and palladium- or platinum-containing materials, each with its own drawbacks. Generally, the most useful reagent was that of chloroplatinic acid in a short-chained alcohol (e.g., Speier's catalyst dissolved in isopropyl alcohol). While Speier's was very versatile in terms of reagent variations, its major drawbacks included potential ineffectiveness at low concentrations, insolubility in many organic materials, and the tendency to become poisoned by external influences.[74]

In an effort to develop a more reliable catalytic option, Lamoreaux introduced a platinum complex derived from the reaction of chloroplatinic acid hexahydrate and octanol in 1962 as seen in Figure 21.[74]

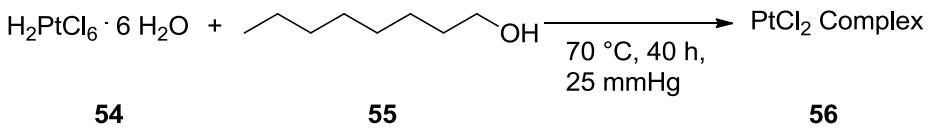

Figure 21: Synthesis of Lamoreaux's catalyst.

A solution of octanol and chloroplatinic acid in a 7:1 mole ratio was heated to 70 °C for 40 h at 25 mmHg and produced a platinum chloride complex with aldehyde and ether linkages

derived from octanol. Lamoreaux reported the use of the platinum complex as a hydrosilylation catalyst for several silicon-containing compounds.[74] Included was the synthesis of ester-containing silanes and saturated cyclic silanes (Figure 22).

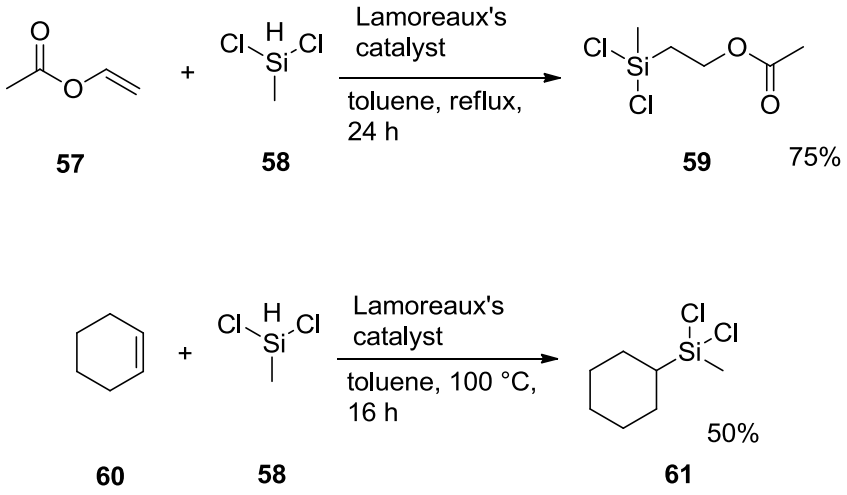

Figure 22: Schematics of Lamoreaux's catalyst catalyzed hydrosilylations.

The resulting complex utilized less rigorous reaction conditions, demonstrated good efficiency at low concentrations, improved degree of solubility in organic solvents, and improved resistance to platinum catalyst poisons. Therefore, the first step in our synthesis of CYGEP was to generate our own version of Lamoreaux's catalyst as we were unable to obtain it commercially. The original procedure by Lamoreaux called for a pressure of 25

mmHg. We used a pressure of 0.01 mmHg, so we lowered the temperature to 50-55 °C and heated the reaction mixture for 42-44 h. The reaction conditions are listed in Table 8.

Table 8: Lamoreaux's catalyst formulations.

Entry	H_2PtCl_6 (g)	Octanol (mL)	Temp (°C)	Time (h)
1	1.01	2.1	50-55	40
2	1.00	2.1	70	40
3	1.00	2.1	50	40
4	1.00	2.1	70	48
5	2.14	4.5	55	42
6	2.14	4.5	50-55	42
7	0.57	1.5	55	42
8	2.15	4.5	55	42
9	2.89	6.0	55	42
10	2.43	5.5	50-55	42.5
11	2.51	5.5	55	42
12	2.49	5.5	55	42
13	2.52	5.5	55	42
14	2.53	5.5	55	43
15	2.50	5.5	55	43
16	2.50	5.5	55 (80 after 30 h)	43
17	2.52	5.5	55	43
18	2.55	5.5	55	43

The resulting complex was a dark black solution with a consistency similar to that of olive oil. IR and ^1H NMR spectra were collected for the starting materials, starting mixture, and final product. The OH peak of octanol (signal variess between 2.5 and 6.0 ppm typically) was used in both spectra to compare the different batches. Subsequent attempts to reproduce the complex were successful, but it was observed that heating to above 70 °C for a fraction of

the reaction time (entry 16) would result in removal of a significant amount of the octanol as determined by ^{1}H NMR spectroscopy. The loss of octanol would result in a solution with less viscosity which was accompanied by a difference in reactivity when the catalyst was used in polymerization tests as determined by the 1-lb Gillmore needle test. Additionally, the use of chloroplatinic acid which had been exposed to air would result in a final product with a granular paste-like texture and lowered reactivity. In an effort to prevent the loss of reactivity, the solution was stored under argon at temperatures <10 °C. It was observed that even with meticulously dry conditions, reproducibility of the reaction was only successful up to 10 days after opening the new chloroplatinic acid.

Repeated trials in the preparation of Lamoreaux's catalyst resulted in optimal reaction conditions with the heating of chloroplatinic acid hexahydrate and octanol to 50-55 °C for 42-44 h at a pressure of 0.01 mmHg. In order to obtain the highest reactivity, storage of chloroplatinic acid under argon between 0 to 10 °C is needed for no more than 10 days post initial opening of the container of chloroplatinic acid.

Reproduction of the Crivello Synthesis

The synthesis of CYGEP originally reported by Crivello et al. required the addition of two drops of Lamoreaux's catalyst to the reaction mixture at room temperature.[42] The solution was then heated to 50-55 ºC for 3 h, followed by standing at room temperature overnight. An IR spectrum was then collected to monitor the completion of the reaction by the disappearance of the Si-H peak at 2100 cm^{-1}. As determined by Crivello et al., this procedure was only successful when the reaction was run under nitrogen and meticulously dry conditions. These conditions could be accomplished by using freshly distilled reagents,

adding a $CaCl_2$ drying tube, and refluxing the solution through a Dean-Stark trap containing CaH_2. In the instances where extreme care was not taken, gelation would occur upon addition of the catalyst to the reaction mixture. This effect was attributed to residual water reacting with the catalyst to form further condensable Si-OH groups resulting in cross-linking of the monomeric materials.[42] Initial attempts to reproduce the results were followed according to a scaled-down version of the reported procedure, but with very different outcomes as shown in Table 9.

Table 9: Formulations in the synthesis of CYGEP.

Trial	2,4,6,8-TMCTS (g)	Temp	Time	Lamoreaux Catalyst	Temp at catalyst addition	CH_3CN	Yield (%)	Polym.
1	6.0 g	reflux	2 h	1 drop	RT	-	0	Yes
2	12.0 g	reflux	2 h	1 drop	0 °C	-	0	No
3	24.0 g	reflux	2 h	2 drops	0 °C	-	0	Yes
4	12.0 g	reflux	2 h	1 drop	0 °C	-	0	Yes
5	12.0 g	reflux	2 h	1 drop	8 °C	-	21	No
6	12.0 g	reflux	2 h	1 drop	16 °C	-	0	Yes
7	24.0 g*	reflux	2 h	1 drop	8 °C	-	56	No
8	12.0 g	reflux	2 h	1 drop	8 °C	-	0	Yes
9	12.0 g	reflux	2 h	0.3 mL (50% solution in toluene)	6 °C	-	0	Yes
10	6.0 g	70 °C	30 min	10 drops (0.50% solution in toluene)	70 °C	0.27 mL	17	No
11	24.0 g*	70 °C	30 min	0.5 mL (0.5% solution in toluene)	70 °C	0.54 mL	49	No
12	24.0 g*	70 °C	30 min	0.5 mL (0.5% solution in toluene)	70 °C	0.54 mL	63	No
13	12.0 g	70 °C	30 min	0.5 mL (0.5% solution in toluene)	70 °C	-	0	Yes

Polym. = polymerization of the solution after the addition of the catalyst, but prior to purification. Yields were recorded as isolated products (* indicates side-by-side reactions were run and combined after IR collected). Reactions were run in anhydrous toluene with minimal outside light.

The addition of Lamoreaux's catalyst (1 drop) to the reaction mixture at room temperature of a 6 g batch (trial 1) resulted in an extremely exothermic reaction that caused immediate polymerization of the materials to a rock-like material. To slow down the rate of reaction and prevent instantaneous polymerization, the system was cooled to 0 ºC prior to the addition of the catalyst. No change was observed upon catalyst addition (trial 2), and the resulting pale yellow solution was then heated to 50 ºC for 3 h before being allowed to stir at room temperature for 16 h. Since the Si-H peak of the starting material (TMCTS) is at 2100 cm^{-1}, it was used to monitor the reaction progress using IR spectroscopy. Purification was attempted using column chromatography (silica gel; solvent: 10% ethyl acetate–hexanes), but no material was recovered from the column. The procedure was repeated with 2 drops of catalyst (trial 3), ultimately resulting in polymerization to a white solid. Trial 2 was repeated, but this time it resulted in gelation occurring 30 min post catalyst addition. Subsequent trials (5 and 6) were concurrently run at 8 and 16 ºC, respectively. After stirring for 16 h at room temperature, an IR spectrum was taken for both reactions. The Si-H peak was absent in the spectrum of trial 5, but still present in the spectrum of trial 6. Trial 6 was then cooled to 8 ºC where an additional drop of catalyst was added, and the solution stirred at room temperature. After 3 h, gelation occurred for trial 6. Trial 5 was then purified by column chromatography (silica gel; solvent: 10% ethyl acetate–hexanes) to obtain CYGEP in a 21% yield. Unfortunately, reproducibility was difficult among the ensuing trials as approximately 75% of attempts resulted in polymerization. Since reproducibility was an issue, an alternative procedure was needed.

Aoki Procedure

A synthesis of organopolysiloxanes or organosilanes bearing an epoxy functionality without undesired polymerization or gelation occuring was reported by Aoki.[82] In his study, he

examined hydrosilylation reactions with alkenyl-group bearing epoxides in the presence of a cyano group-bearing compound, preferably acetonitrile or benzonitrile (Figure 23).

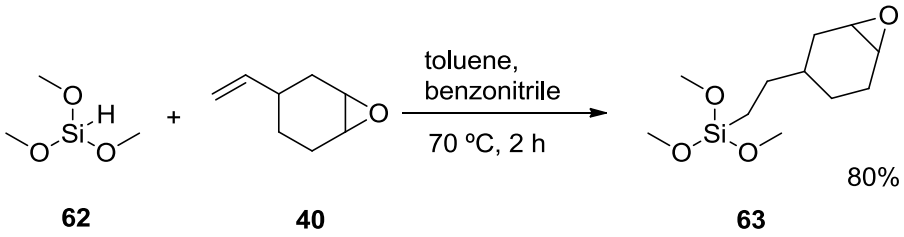

Figure 23: Reaction of trimethoxysilane and 4-vinylcyclohexene-1,2-epoxide in the presence of benzonitrile.

At a minimum of 10 ppm of platinum, an exothermic reaction occurred upon catalyst addition, but proceeded without gelation. Analysis by GPC, and IR and ^{1}H NMR spectroscopies identified the resulting material to be an epoxy-containing organopolysiloxane. The use of volatile nitriles allowed for their removal, along with the reaction solvents under reduced pressure.

Alternative Approach to CYGEP

Unable to routinely prevent polymerization for the synthesis of CYGEP, a modified procedure of Aoki was utilized. The reaction was heated to 70 ºC for 30 min with the inclusion of 0.27 mL of acetonitrile (trial 10). A vigorous exothermic reaction occurred upon the addition of Lamoreaux's catalyst (10 drops of a 0.5% solution in toluene), which raised the temperature to ~130 ºC. After ~3 min, the bubbling subsided, and the solution was allowed to cool back down

to 70 ºC where it was heated for an additional hour. The absence of the Si-H peak at 2100 cm^{-1} in the IR spectrum indicated completion of the reaction. The crude material was purified using column chromatography (silica gel; solvent: 10% ethyl acetate–hexanes) to give CYGEP as a clear, viscous liquid in a 17% yield. Ensuing trials were scaled up resulting in increased yields. The improvement in yield to 63% using 0.5 mL of a 0.5% solution in toluene of the catalyst per reaction is given in Table 9, trial 12.

In summary, any attempts to synthesize CYGEP without acetonitrile resulted in exothermic polymerization of the starting materials to a rock-like material upon the addition of the catalyst. This result indicated the importance of acetonitrile in this procedure and substantiated Aoki's results that the addition of a cyano-group bearing compound allowed for the successful conversion to the silorane without the undesired gelation.

Commercial Lamoreaux's Catalyst (Platinum Octanal/Octanol Complex)

In the optimization of the synthesis of CYGEP, catalysis of the reaction was limited to the use of Lamoreaux's catalyst. During this investigation, a second version of the catalyst became available. A commercially available platinum octanal/octanol complex was found to be available through Gelest. Upon receipt of the octanal/octanol complex, several reactions were run using the commercial complex in place of the synthesized Lamoreaux's catalyst (Table 10). For these reactions, the optimal conditions were used so as to give a comparison between the two catalysts. In all instances, polymerization was not observed upon addition of the commercial catalyst. The vigorous exothermic reaction occurred as was expected, and the temperature increased to ~130 °C. Therefore, the effects of concentration and other conditions were investigated.

Table 10: Optimization of CYGEP with platinum octanal/octanol complex.

Entry	TMCTS (g)	Lamoreaux Catalyst	Acetonitrile	Yield (%)	Polym.
1	24.0 g*	1 mL (1% solution in toluene)	0.54 mL	38	No
2	24.0 g*	1 mL (0.64% solution in toluene)	0.50 mL	17	No
3	12.0 g	1.5 mL (0.50% solution in toluene)	0.50 mL	34	No
4	12.0 g	1 mL (1.5% solution in toluene)	0.50 mL	33	No
5	12.0 g	1 mL (1.75% solution in toluene)	0.65 mL	41	No^
6	23.8 g	1 mL (1.62% solution in toluene)	1.2 mL	27	No^
7	23.8 g	1 mL (3.14% solution in toluene)	1.2 mL	26	No^
8	12.0 g	1 mL (3.14% solution in toluene)	0.6 mL	46	No^
9	12.0 g	1 mL (1.91% solution in toluene)	0.6 mL	40	No^
10	24.0 g*	1 mL (0.79% solution in toluene)	0.54 mL	24	No
11	12.0 g	1 mL (0.79% solution in toluene)	0.54 mL	37	No
12	12.0 g	1 mL (0.79% solution in toluene)	0.54 mL	40	No

All reactions were heated to 70 ºC for 30 min at which point the catalyst was added. Polym. = polymerization of the solution after the addition of the catalyst, ^ indicates the formation of a highly viscous liquid which was insoluble in hexanes.

A difference in reactivity was observed immediately in those reactions using the Gelest complex because it required either larger volumes or higher concentrations of solutions for the reaction to occur. Use of a 1% solution of the Gelest catalyst required the addition of 1 mL of the catalyst (entry 1) as compared to the use of only 0.5 mL of a 0.5% (Table 10, entry 12) solution with the synthesized catalyst. Upon purification of the crude material, this formulation proved to show other differences as well. In entry 1 of Table 10, 1-mL of the 1% Gelest complex resulted in a 38% yield of CYGEP. In addition to a decreased yield, an additional peak was observed in the ^{1}H NMR spectrum at 4.6 ppm. In trials where the peak at 4.6 ppm was present, additional shoulders or side bands emerged out of the Si-CH_3 peak at 0.0 ppm. As seen in Table 10, subsequent reactions were performed using varying concentrations of the catalyst in

hopes of finding the most favorable range in which no polymerization occurred while producing the highest yield.

In an effort to compare the reactivity of the catalysts using similar concentrations, a trial was run using the Gelest catalyst at a 0.50% weight percent solution in toluene. At the same weight percent, the reaction involving the Gelest catalyst required 1.5 mL to produce the vigorous exothermic reaction, which is observed in the formation of CYGEP. Under the same conditions, the synthesized version of Lamoreaux's catalyst required only 0.5 mL for completion. Additionally, upon purification, the ^{1}H NMR spectrum of the Gelest batch (entry 3) had the additional peak at 4.6 ppm, whereas the peak was absent in the trials using the synthesized catalyst. A comparison of the yields also favored the use of the synthesized catalyst with yields $\leq$63% as compared to the 34% yield obtained using the Gelest catalyst. The weight percent of the Gelest complex was then increased in hopes of increasing monomer production. The amount of catalyst was held constant at 1-mL while the solution concentrations were increased. Trials 4 through 9 were run with weight percents from 1.50 to 3.14%, resulting in yields of 41% (trial 5, 1.75% catalyst) and 46% (trial 8, 3.14% catalyst). The increase in catalyst concentration required for production of product seemed to correlate with the appearance of the peak at 4.6 ppm (Table 11).

Table 11: Comparison of catalyst concentration and volume to peak intensities in CYGEP using the Gelest catalyst.

Concentration (%)	Volume (mL)	Peak Intensity (a:b:c)
0.50	1.5	1:12.6:4.9
0.65	1.0	1:33.4:17.1
1.62	1.0	1:75.5:40.3
1.75	1.0	0:151:78.5
1.91	1.0	1:60.4:36.6
3.14	1.0	1:302:164

Newly observed peak (a, 4.6 ppm) compared to known investigated signals for CH-O of epoxides (b, 3.1 ppm) and Si-CH_3 (c, 0.0 ppm).

At higher catalyst concentrations, the peak was either faintly visible or absent. However, at lower concentrations, the peak was present. Secondly, use of the Gelest catalyst resulted in byproducts as determined by TLC (solvent: 10% ethyl acetate–hexanes) of the crude material. Finally, at catalyst concentrations greater than 1.50%, a small fraction (~15-20%) of the resulting crude material had a higher viscosity than is observed at lower concentrations. In preparation for column chromatography, the crude material was dissolved in hexanes, but the higher viscosity liquid was observed because it was insoluble in hexanes. On the other hand, the residue was readily soluble in more polar solvents, such as ethyl acetate and acetone. This residue was collected and the solvents were removed under vacuum. Spectra (^{1}H and ^{13}C NMR) were collected for the crude residue. In a comparison with the corresponding spectra for the purified material from the reaction, those peaks associated with pure CYGEP correlated with the crude material. In the ^{1}H spectrum of the residue, several extra signals were also present, which included peaks at 0.2 and 4.6 ppm (included in the catalyst investigation), at ~5.0 and 5.7 ppm (potentially unreacted vinyl epoxide), 0.9 ppm (multiplet arising out of the multiplet at 0.8 ppm),

and 1.0 ppm (doublet). Of these, the latter two signals were unique to any previously observed spectral abnormalities. Interestingly, it was noted that as time elapsed (several days), the ratio of these unique peaks decreased in comparison to other signals in the spectrum. After more than a week, a spectrum was collected and the absence of the unique peaks was noted. A minimal amount of hexanes was added to the sample, and the presence of the unique peaks returned. A third spectrum was collected after a second addition of hexanes with the peaks overpowering those peaks representative of CYGEP. Thus, the latter unique peaks in the residue were determined to be residual hexanes, which were not removed via the vacuum pump. Comparison of the ^{13}C NMR spectrum of the purified and crude residue resulted in two new peaks (-0.4 and 1.5 ppm). However, with the exception of 25.3 ppm, all the peaks typical of CYGEP were doubled and split. The shifts of the signals in the same order as CYGEP allows for the determination that the residue has very close structural similarities to that of CYGEP. However, additional investigations needed to be undertaken to obtain a better understanding of the residue.

Analysis of the NMR Signal at 4.6 ppm

The substitution of the synthesized catalyst for the commercially available Gelest catalyst in the synthesis of CYGEP resulted in the presence of a new peak in the ^{1}H NMR spectrum. The broad peak appeared at 4.6 ppm and varied in intensity from trial to trial. It was noted that the peak intensity generally correlated with the concentration of Lamoreaux's catalyst used in the reaction. In comparison to the starting materials, a similar observation was noted with the Si-H peak at 4.65 ppm in the spectrum of 2,4,6,8-tetramethylcyclotetrasiloxane. As mentioned previously, visible shoulders or side bands emerged (at ~0.1 ppm) from the Si-CH_3 peak at 0.0 ppm in those trials in which the peak at 4.6 ppm was present. A comparison was then made of the ^{13}C NMR spectra for CYGEP with and without the peak at 4.6 ppm. This sample included

all signals for pure CYGEP, but with additional daughter-type peaks. The peaks were present at -1.2 and 0.9 (-0.8), 13.6 (13.9), 29.1 (29.2), and 29.6 (29.8) ppm in a low proportion to those peaks in parentheses. These additional peaks in both the ^{1}H and ^{13}C NMR spectra display similarities to both CYGEP and unreacted TMCTS. Additionally, the presence of a small peak at 2100 cm^{-1} in the IR spectrum is observed in these reactions. The observations seemed to correlate with the effect of catalyst concentration, possibly leading to incomplete conversion of all four Si-H bonds of the epoxy substituent (Figure 24).

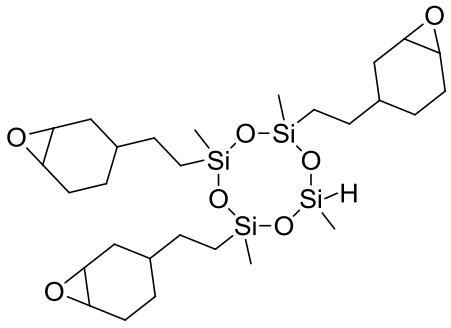

64

Figure 24: Trifunctional monomer potentially formed due to incomplete conversion of all four Si-H bonds in the hydrosilylation of CYGEP.

CYGEP Scale Up

As in the case of PHEPSI, the ability to produce CYGEP in large quantities was important if this co-monomer mixture would be used as a biomaterial. After the successful

synthesis of CYGEP was accomplished, side-by-side reactions were run on 12.0 g reactions. Upon reaction completion, these batches were combined and purified together resulting in yields of up to 63%. With the continued success of the procedure, no further scale-up trials were attempted using the prepared catalyst.

With the acquisition of the catalyst from Gelest, reactions were run using similar conditions and scale as used for the prepared catalyst. Unable to achieve comparable yields, the procedures were modified to improve upon the results. In lieu of side-by-side reactions, a single 23.8 g reaction was run resulting in recovery of only 27% of the desired product. Repeated trials resulted in no improvement of the yield, and attempts at any further scale-up were abandoned. On the other hand, a general improvement was observed in the instances where the reactions were not combined for purification. Rather, they were purified individually on 12.0 g scales obtaining yields in the 40-46% range. Even though increased reaction size generally resulted in decreased yields, the scalability of the reaction has been accomplished in reactions up to 23.8 g.

CYGEP Purification

Purification of CYGEP according to previously reported procedures was achieved first by the removal of solvents and excess epoxide under vacuum.[42] In our attempts using this procedure, we were unable to remove the catalyst and unreacted starting materials. In addition, the residual solvents remained due to the viscosity of the crude material, which included unidentified byproducts. The ability to purify PHEPSI by column chromatography drove the decision to utilize the process in the purification of CYGEP.

The use of TLC as a means of tracking elution of the material became a difficult task. Visualization of TLC plates was not a viable option as none of the reaction components were

observed using a UV lamp, which is due to the lack of aromatic or π-conjugated functional groups. However, after testing several visualization methods, the iodine method was determined to be useful for the co-monomer. For the reactions involving the catalyst synthesized in-house, two spots were visible at R_f 0.07 and R_f 0.44 in a 10% ethyl acetate–hexanes mobile phase. After purification of the material using column chromatography, the two spots were separated. After concentration under reduced pressure and removal of residual solvents under vacuum, the spot at R_f 0.07 was identified as CYGEP using ^{1}H NMR spectroscopy, while the band at R_f 0.44 was identified as a mixture of unreacted vinyl epoxide plus other potential side products. While separation of the two bands was possible, bleeding of the two bands was observed regardless of the size and solvent gradient used, which resulted in a decrease in the obtainable yields.

When the commercial Lamoreaux's catalyst was used, the same two bands at R_f 0.07 and 0.44, as well as two additional bands were present. These bands at R_f 0.21 and 0.28 had not been previously detected in the synthesis of CYGEP. Elution of the crude material allowed for the isolation of fractions of the unreacted vinyl epoxide/unidentified products and CYGEP bands which were previously isolated, but similar bleeding made isolation of the middle two bands unobtainable. Collection of a mixture of the bands at R_f 0.21 and 0.28 with a small amount of CYGEP present was obtained. The ^{1}H NMR spectrum was very similar to that of CYGEP, but with the peak at 4.6 ppm in higher proportion than previously seen.

The purification of CYGEP was achieved through the use of column chromatography using a 10% ethyl acetate–hexanes mobile phase. While effective, this procedure did present complications in terms of the bleeding of bands together regardless of column size and length. In the use of both catalysts, isolation of both major bands was accomplished, but complete isolation of the two unique bands in the Gelest reactions was unsuccessful.

CYGEP Byproducts

Similar to PHEPSI, the synthesis of CYGEP produced more than one product. In our investigation, two versions of Lamoreaux's catalyst were utilized. Both provided products at R_f 0.07 and 0.44 when run on TLC (10% ethyl acetate–hexanes mobile phase). In addition to the two products, the Gelest catalyst also included products at R_f 0.21 and 0.28. After purification, the TLC spot at 0.07 was determined to be CYGEP through ^{1}H and ^{13}C NMR spectroscopy. The product with R_f 0.44 was able to be isolated, but the ^{1}H NMR spectra collected varied from batch to batch. Since the reaction was run in an excess of the vinyl epoxide, unreacted starting materials were identified to be in the band. However, as in the case of PHEPSI, the band often contained a multiplet between 5.0-5.3 ppm in the ^{1}H NMR spectrum. Other discernible irregularities included the presence of several singlets between 2.4-2.8 ppm. Due to the variance of the peaks from reaction to reaction, identification of the additional products in the band has not been completed. The presence of peaks in the vinylic region of the ^{1}H NMR spectrum raises the possibility of the presence of a minor amount of the dehydrogenated product. Mechanistically, this result would not be expected, as platinum-based hydrosilylations are generally known to proceed through the Chalk-Harrod pathway. However, recent reports of some platinum or palladium catalysts producing the dehydrogenated vinylsilane introduce the possibility of this byproduct.[61]

Bleeding of the bands together prevented the isolation of the products at R_f 0.21 and 0.28. Instead, the bands were collected containing minimal amounts of CYGEP. ^{1}H NMR spectra of these samples showed an increased intensity of the peaks at 0.1 and 4.6 ppm, while ^{13}C spectra showed differences at -1.2 and 0.9 ppm. Taking these results in combination with the presence of a band at 2100 cm^{-1} in the IR spectrum, it is believed that complete conversion of all four Si-H

bonds did not occur. The resulting structures are believed to be a combination of a di-functionalized monomer or the tri-functionalized monomer seen in Figure 24.

CYGEP Optimization Recap

The synthesis of the second silorane monomer, CYGEP, was achieved after an investigation which spanned differing procedures and the use of two versions of Lamoreaux's catalyst. The hydrosilylation of 4-vinylcyclohexene-1,2-epoxide with 2,4,6,8-tetramethylcyclotetrasiloxane and a synthesized version of Lamoreaux's catalyst was achieved in moderate yields (63%) utilizing an adapted procedure of Aoki. Under similar conditions, the utilization of a platinum octanal/octanol complex produced the silorane, albeit in decreased yields (46%). Both reactions formed a minor amount of unidentified byproducts. It is hypothesized that those reactions using the Gelest complex exhibited a dependence between the concentration of the catalyst and substitution of all four Si-H bands. Lower concentrations of catalyst resulted in an increasing ratio of unreacted Si-H moieties consequently producing the mono-, di-, and trisubstituted monomers along with the desired tetrafunctional CYGEP. For synthetic purposes, optimal conditions for the production of CYGEP require the addition of 0.5 mL of a 0.50% in-house prepared Lamoreaux's catalyst solution diluted in toluene to be added to a solution of the starting reagents previously heated to 70 °C for 30 min. However, for purposes of using CYGEP as a co-monomer in a chemically cured biomaterial, the addition of 1.0 mL of a 0.79% solution of Lamoreaux's catalyst (Gelest) in toluene is the optimal catalyst condition.

Monomer Storage and Stability

Once isolated, both monomers were stored until a sufficient quantity of each was produced to make a batch of SilMix (typically between 40-60 g of each monomer). Prior to

mixing, both monomers were stored inside amber bottles under argon at 8-10 ºC. Unfortunately, the length of storage time varied depending on the efficiency at which the monomers were produced. During prolonged storage, new peaks were observed in the NMR spectra of PHEPSI. After two weeks, noticeable peaks formed in the vinylic region for both ^{1}H (Figure 25, 4.5-6.0 ppm) and ^{13}C NMR (Figure 26, 110-150 ppm), which were not present in the spectrum of the initially purified sample.

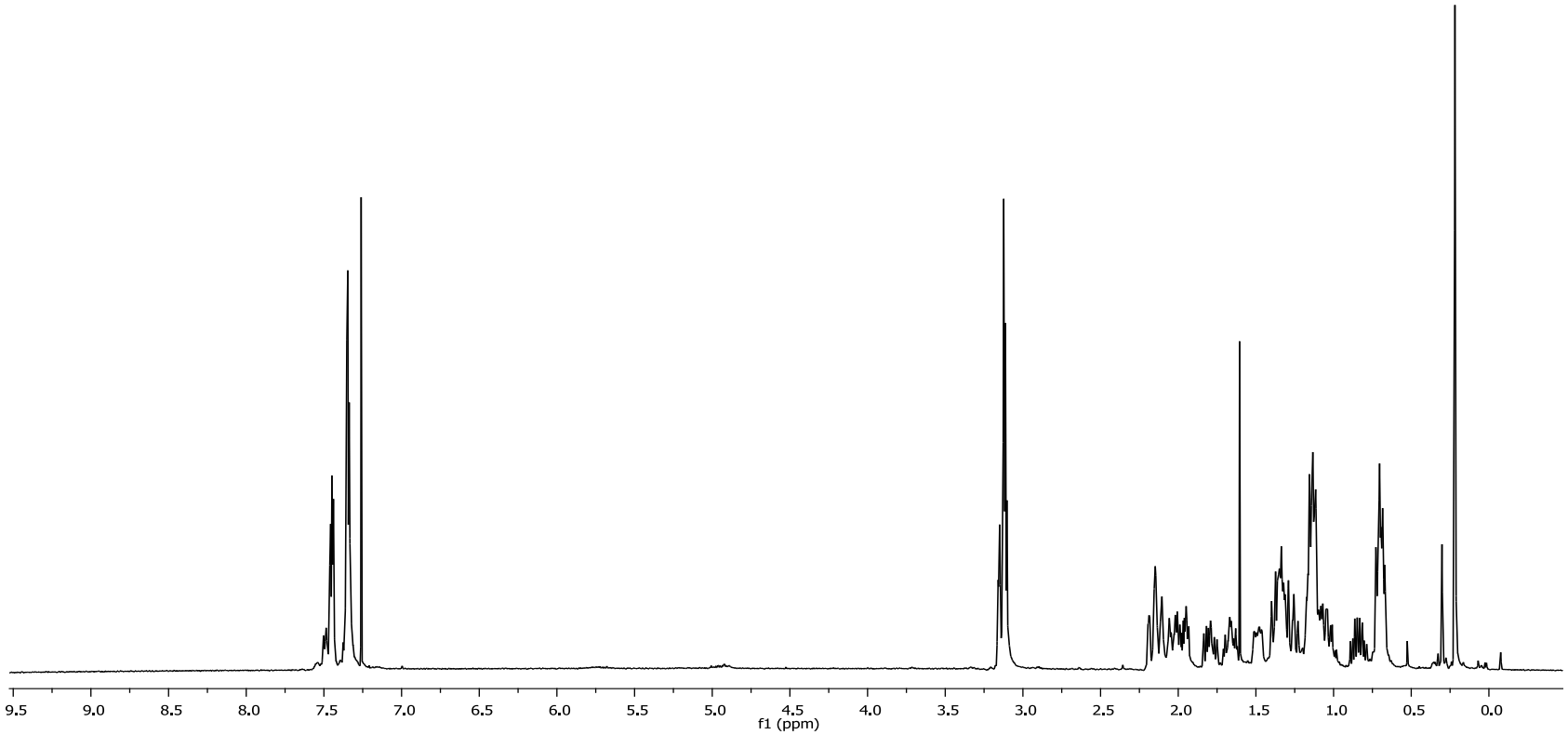

Figure 25: ^{1}H NMR spectrum of PHEPSI decomposition.

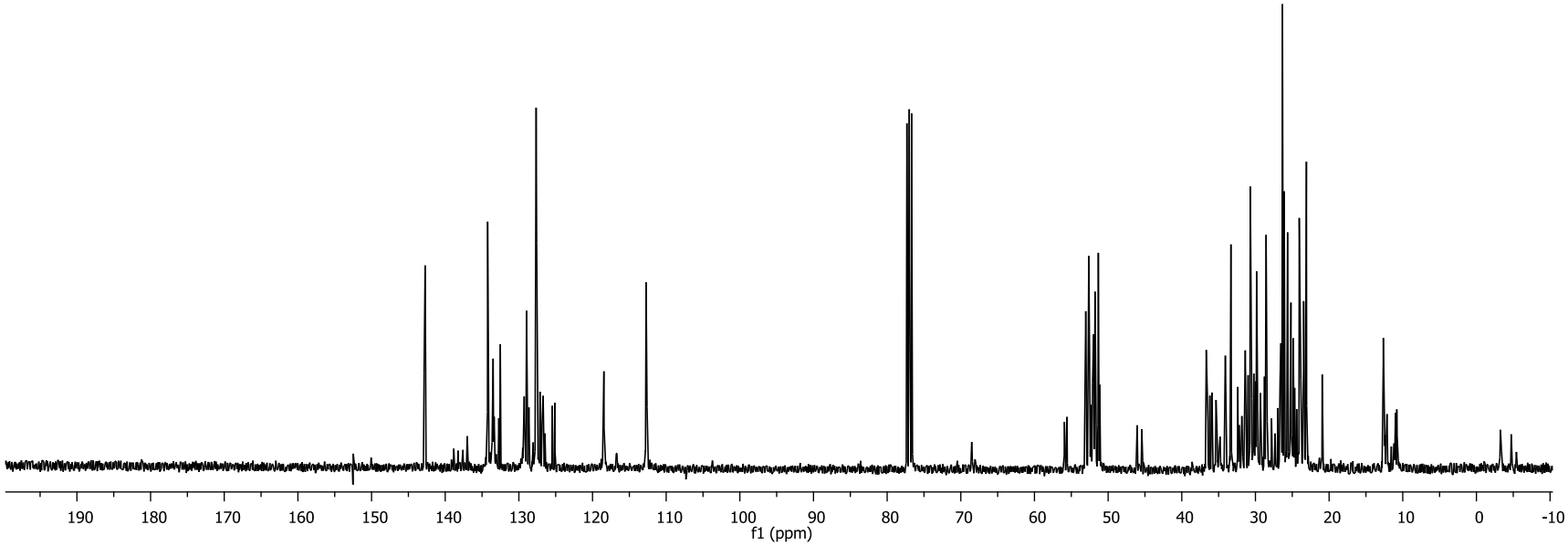

Figure 26: ^{13}C NMR spectrum of PHEPSI decomposition.

Further analysis indicated these peaks were associated with slight decomposition/polymerization of PHEPSI and not through the addition of an outside contaminant. For use as a co-monomer of a biomaterial, the storage stability of PHEPSI needed to be improved. A comparative investigation of CYGEP revealed no such decomposition after a period of six months (Table 12). With the observed stability of CYGEP and plans for its use as a co-monomer system, we investigated the effect on its stability when combined to form SilMix. After two years, no degradation was observed as determined by ^{1}H NMR. When combined, the higher viscosity silorane CYGEP provides a stabilizing effect on PHEPSI.

Table 12: Stability of SilMix components.

System	Stability
PHEPSI	1 month
CYGEP	>6 months
SilMix	>2 years

Once we became aware of the decomposition issue, special attention was paid to the storage and handling procedures which increased the stability of PHEPSI to approximately one month (Table 12). Once purified, monomers were stored in oven-dried amber glass vials or sterilized plastic cups in the refrigerator. A protocol was established for the mixing of monomers no more than one month post isolation of PHEPSI in order to prevent the possibility of monomer decomposition.

Quality Control Exploration

The use of a biomaterial as a novel bone cement from bench top to bedside requires the need to problem-solve any potential complications which could detract from the use of this material. During the development of the dually cured bone cement, a freshly mixed batch of SilMix failed to polymerize upon addition of Lamoreaux's catalyst. Several additional samples were evaluated from the same batch, all resulting in failure of the 1-lb Gilmore needle test for polymerization. In an effort to discover the cause for the failure, an investigation of quality control of the resin production was commenced (Tables 13 and 14).

Table 13: Quality control steps for CYGEP.

Batch	Location	2,4,6,8-TMCTS	Vinyl Epoxide	Lamoreaux's Catalyst	Hexanes	Silica Gel	Polym
CYGEP 48	FH 524	Gelest, >95%	Gelest, >97%	In house (bm207)	Aluminum can	Lot #: 020427	No
CYGEP 49	FH 524	Alfa, 99%	Gelest, >97%	In house (bm207)	Aluminum can	Lot #: 020427	No
CYGEP 50	FH 524	Alfa, 99%	Gelest, >97%	In house (5bm015)	Aluminum can	Lot #: 020427	No
CYGEP 51	FH 524	Alfa, 99%	Gelest, >97%	In house (5bm015)	Aluminum can	Lot #: 011014I	No
CYGEP 52	FH 528	Alfa, 99%	Gelest, >97%	In house (5bm015)	Aluminum can	Lot #: 020427	No
CYGEP 53	FH 528	Alfa, 99%	Gelest, >97%	In house (5bm015)	Aluminum can	Lot #: 051113J	No
CYGEP 55	FH 528	Alfa, 99%	Gelest, >97%	In house (5bm015)	Aluminum can	Lot #: 051113J	No
CYGEP 57	FH 528	Alfa, 99%	Gelest, >97%	In house (5bm015)	Glass bottle	Lot #: 051113J	No
CYGEP 58	FH 528	Alfa, 99%	Gelest, >97%	Gelest, <10% complex	Glass bottle	Lot #: 051113J	Yes
CYGEP 59	FH 528	Alfa, 99%	Aldrich, 98%	In house (5bm015)	Glass bottle	Lot #: 051113J	Yes
CYGEP 60	FH 528	Alfa, 99%	Aldrich, 98%	Gelest, <10% complex	Glass bottle	Lot #: 051113J	Yes
CYGEP 61	FH 528	Alfa, 99%	Aldrich, 98%	Gelest, <10% complex	Glass bottle	Lot #: 051113J	Yes

Polym. = passing of the 1-lb Gilmore needle test at 1 hr.

Table 14: Quality control steps for PHEPSI.

Batch	Location	MPS	Vinyl Epoxide	Wilkinson's Catalyst	Hexanes	Silica Gel	Polym
PHEPSI 79	FH 524	Gelest, >95%	Gelest, >97%	Alfa, 97%	Aluminum can	Lot #: 020427L	No
PHEPSI 80	FH 524	Gelest, >95%	Gelest, >97%	Alfa, 97%	Aluminum can	Lot #: 020427L	No
PHEPSI 81	FH 524	Gelest, >95%	Gelest, >97%	Alfa, 97%	Aluminum can	Lot #: 020427L	No
PHEPSI 82	FH 524	Gelest, >95%	Gelest, >97%	Alfa, 97%	Aluminum can	Lot #: 020427L	No
PHEPSI 83	FH 524	Gelest, >95%	Gelest, >97%	Alfa, 97%	Aluminum can	Lot #: 011014I	No
PHEPSI 84	FH 528	Gelest, >95%	Gelest, >97%	Alfa, 97%	Aluminum can	Lot #: 020427L	No
PHEPSI 85	FH 528	Gelest, >95%	Gelest, >97%	Alfa, 97%	Aluminum can	Lot #: 051113J	No
PHEPSI 87	FH 528	Gelest, >95%	Gelest, >97%	Alfa, 97%	Glass bottle	Lot #: 051113J	No
PHEPSI 88	FH 528	Gelest, >95%	Gelest, >97%	Alfa, 97%	Glass bottle	Lot #: 051113J	No
PHEPSI 89	FH 528	Gelest, >95%	Aldrich, 98%	Strem, 99%	Glass bottle	Lot #: 051113J	Yes
PHEPSI 90	FH 528	Gelest, >95%	Aldrich, 98%	Strem, 99%	Glass bottle	Lot #: 051113J	Yes
PHEPSI 91	FH 528	Gelest, >95%	Aldrich, 98%	Strem, 99%	Glass bottle	Lot #: 051113J	Yes
PHEPSI 92	FH 528	Gelest, >95%	Aldrich, 98%	Strem, 99%	Glass bottle	Lot #: 051113J	Yes
PHEPSI 93	FH 528	Gelest, >95%	Aldrich, 98%	Strem, 99%	Glass bottle	Lot #: 051113J	Yes

Polym. = passing of the 1-lb Gilmore needle test at 1 hr.

Shelf Life

This unreactivity occurred between differing batches of SilMix. Therefore, the shelf life of the failed materials was examined. Once a batch was purified, an ^{1}H NMR spectrum was collected. The batches were combined in an amber jar and kept in the refrigerator at 6 ºC until a sufficient amount of both monomers was available for mixing. Storage of the individual monomers was typically no more than three weeks after purification. In the case of SilMix 41, the first batch of each monomer placed in the stock had been purified more than eight weeks prior to mixing. From this information, it was determined to investigate whether the shelf life of the individual monomers was the overriding factor in the failure of the system to polymerize.

To test this, PHEPSI 79 and CYGEP 48 were synthesized using the same reagents that were used to prepare the materials for SilMix 41. Once the pure monomers were isolated, they were mixed within hours of the collected NMR spectrum. The resulting resin again failed to harden during the expected time period as determined by the GNT. PHEPSI 80 was also purified and combined with CYGEP 48 yielding similar results. Further variables were then explored as the cause of the problem.

Reagents

The next variable examined was the starting reagents involved in the synthesis of the monomers. The possibility that an unknown contaminant may have affected the monomers resulted in the acquisition of new starting materials. For the synthesis of CYGEP, the original procedure utilized 2,4,6,8-tetramethylcyclotetrasiloxane purchased from Alfa Aesar (99% purity), but in the previous year the suppliers were switched to Gelest (>95% purity)

for budgetary reasons. During the change, no change in yields or reaction conditions had been observed. It was decided to return to the materials from Alfa in order to use the highest purity reagents available, and were ones known not to have any prior issues for our system. ^{1}H NMR spectra were taken of the newly acquired starting materials and compared with the previously used starting materials. There was no decomposition or added impurities in any of the samples of the starting materials. PHEPSI 81 and CYGEP 49 were then prepared using the new materials. Again, the sample failed the Gilmore needle test after 1 h. With similar results to the previous trials, alternative variables were examined.

Platinum Catalyst Poisons

While the use of a platinum catalyst in the synthesis and polymerization of a biomaterial has shown tremendous potential, however, loss of reactivity of platinum catalysts due to poisoning of the system by outside factors has been reported in the literature.[83] Depending on the type and formulation of the reaction, the extent of the effect may range from slightly slowed reaction time to complete reaction inhibition. Platinum catalysts have a long list of potential poisons, including sulfur compounds, amines, phosphines, silver salts, and tin salts, to name a few. The presence of these types of compounds in the working environment could potentially lead to loss of polymerization of the biomaterial. Those compounds in the laboratory, which may contain any of these poisons, were moved to an adjoining room in an effort to eliminate potential inhibition.

Cleaning of Glassware and Laboratory

With the synthesis of the monomers taking place in a multi-project laboratory, the laboratory was cleaned to remove any potential impurities that may have been lingering and

undetected. The continued production of additional monomers, which failed to polymerize called for further action. The synthesis of SilMix was then moved to an unoccupied laboratory in which no other chemical syntheses were being performed at the time. Prior to this transfer, all supplies and equipment were either purchased new or thoroughly cleaned. A protocol was developed to clean all glassware using NOCHROMIX.

The laboratory transfer began by initially taking a step backwards. The first few batches produced (PHEPSI 84 and CYGEP 52) introduced additional complications. In the ^{1}H NMR spectrum, unanticipated peaks were found at 4.26 (quartet) and 8.11 (singlet). With a new glassware-cleaning protocol, newly used equipment, and a new environment, several variables were incorporated. Detection of the unique peaks was not observed until after the crude monomer was run through a column and concentrated under reduced pressure. The first step taken was to collect NMR spectra of all the solvents (hexanes, ethyl acetate, acetone, and toluene) used in purification of the monomers. All spectra were absent of the unique peaks. With the solvents ruled out, focus was shifted to the equipment. A different rotary evaporator due to the location change was examined. The apparatus was disassembled, thoroughly cleaned, and reassembled numerous times. After each cleaning, a sample was concentrated and an ^{1}H NMR spectrum collected. Each sample produced a spectrum in which the unique peaks were still present in varying intensities. With no correlation between the rotary evaporator and the intensity of the peaks, alternative sources of these peaks were investigated.

Conscious of the fact that the monomers are higher viscosity liquids, the issue of solvent purity was re-evaluated. An experiment was conducted in which 10-mL samples of hexanes, ethyl acetate, acetone, and a 10% ethyl acetate–hexanes solution were placed into

vials and concentrated to dryness. An ^{1}H NMR spectrum was collected, and the unique signals due to the contaminant were observed in both the hexanes and 10% ethyl acetate–hexanes solution. A fresh container of hexanes was opened, and the above experiments rerun. The disappearance of those signals led to the determination that an impurity was present at minimal levels in the previous supply of hexanes. This conclusion led to the decision to purchase solvents in glass bottles rather than large quantities in aluminum cans to prevent possible contamination from the aluminum containers.

Change in Wilkinson's Catalyst and Reaction Procedure

Returning to the issue of polymerization, GNT tests were run using the individual monomers. Experiments of the individual monomers revealed substantial information because CYGEP samples would pass the polymerization tests while PHEPSI samples would not. Therefore, the synthesis of PHEPSI became the primary focus of this investigation. With no recent change in the synthetic procedure, it left Wilkinson's catalyst as the potential problem. A comparison of the certificates of analysis in the varying lots revealed a difference of trace metals present. Due to the variability of trace metals from lot to lot for Wilkinson's catalyst supplied by Alfa (97%), an alternative supplier was sought. It was found that Wilkinson's catalyst could be purchased through Strem Chemicals at 99% purity.

Meanwhile, a closer look at the mechanism of hydrosilylation reactions and previous examples from the literature indicated that the order of addition of reagents may have an effect on the product distribution. Mechanistically, the addition of the silane to the catalyst allows for the oxidative addition in Chalk-Harrod pathway to begin prior to the addition of the alkene. Thus, the addition of the alkene to the metal intermediate may drive the pathway

directly to reductive elimination and minimize the quantity of material that passes through the β-hydrogen abstraction route. Therefore, the procedure for the synthesis of PHEPSI was altered such that methylphenylsilane was added to the catalyst stirring in toluene and the vinyl epoxide was added afterwards, a minimum of 10 min later to allow for the metal-silyl intermediate to begin formation.

After the changes in catalyst and modification of the procedure were implemented, the polymerization tests were again performed with much improved results (Table 15).

Table 15: Modifications for the synthesis of PHEPSI.

Procedure	Wilkinson's Catalyst	Solvents	Reagent Addition
Original	Alfa (97%)	Large quantity (aluminum cans)	No specific order
Revised	Strem (99%)	Smaller quantity (glass bottles)	MPS added to catalyst followed by vinyl epoxide (after at least 10 min)

A positive test for polymerization of the new co-monomers was indicated by passing of the 1-lb GNT at 1 h. From these results, it was concluded that the major contributors to polymerization inhibition in this case were the variability in trace metals present from the lower-purity Wilkinson's catalyst and the order of reagent addition in the synthetic procedure

for PHEPSI. Therefore, the former was accomplished by the purchase of a higher-grade (99% purity) Wilkinson's catalyst, while the latter was a result of procedural changes. Additionally, a protocol was established for the purchase of solvents in glass bottles as compared to aluminum cans, as well as transfer of solvents from larger containers, which may introduce a contaminant from the linings.

CYGEP Polymerization Complications

Shortly after overcoming the loss of polymerization due to the obstacles surrounding the synthesis of PHEPSI, complications arose with CYGEP. Due to the loss in polymerization previously, subsequent batches of both monomers were tested individually to check for changes in reaction time. Upon testing this procedure, several batches of CYGEP failed to pass the 1-lb GNT at 1 h. Examination of several batches of CYGEP indicated a link between failure of the test and the percent and type of catalyst used (Table 16).

Table 16: Comparison of catalyst type and concentration in the polymerization of CYGEP.

Batch	Catalyst	Cat %	IR Si-H	NMR ~4.6 ppm	Polym.
CYGEP 58	Gelest	0.65	No	Yes	Pass
CYGEP 59	5bm015	0.55	No	Yes	**FAIL**
CYGEP 60	Gelest	0.66	Yes	Yes	Pass
CYGEP 61	Gelest	0.64	Yes	Yes	Pass
CYGEP 62	Gelest	0.70	Yes	Yes	Pass
CYGEP 63	Gelest	0.50	Yes	Yes	Pass
CYGEP 64	Gelest	0.72	Yes	Yes	Pass
CYGEP 65	Gelest	1.5	Yes	Yes	Pass
CYGEP 66	Gelest	1.75	No	No	**FAIL**
CYGEP 67	5bm042	0.50	No	Yes	**FAIL**
CYGEP 68	Gelest	1.75	No	No	**FAIL**
CYGEP 69	Gelest	1.62	Yes	Yes	Pass
CYGEP 70	Gelest	3.14	Yes	Yes	**FAIL**
CYGEP 71	Gelest	1.91	Yes	Yes	Pass
CYGEP 72	Gelest	3.14	Yes	Yes	**FAIL**
CYGEP 73	5bm078	0.59	Yes	No	**FAIL**
CYGEP 75	Gelest	0.79	Yes	Yes	Pass
CYGEP 76	Gelest	0.79	Yes	Yes	Pass
CYGEP 77	Gelest	0.79	Yes	Yes	Pass
CYGEP 78	Gelest	0.79	Yes	Yes	Pass
CYGEP 79	Gelest	0.79	Yes	Yes	Pass
CYGEP 80	Gelest	0.79	Yes	Yes	Pass

Polym: Pass = passage of the 1-lb Gilmore needle test at 1 h.

The results indicate an interesting correlation between batches of CYGEP made using the in-house developed catalyst and failure of polymerization. Those batches which were synthesized using the in-house catalyst failed to pass the polymerization test after 1 h. The type of catalyst used is not the only predictor for test failure, though. With one exception, trials which used a weight percent over 1.75% of catalyst:toluene failed to pass the 1-lb test at 1 h. Upon closer examination, it was determined that use of a 0.79% solution of the

octanal/octanol complex provided the best conditions at which polymerization was consistently observed. Examination of the spectra from these batches presented interesting clues to the complications. The batches which showed no indication of the signal at 4.6 ppm in the ^{1}H NMR spectrum failed to polymerize. Additionally, those batches with the signal at 4.6 ppm visible, but at a low ratio failed to pass the test as well. However, batches which indicated a strong peak at 4.6 ppm followed in line with previous work and passed the 1-lb test at 1 h. Using the preceding data, the procedure for ensuing reactions of CYGEP was determined to require the use of the platinum octanal/octanol complex at 0.79% by weight for reproducible polymerization results.

Quality Control Recap

From the conception of an idea to a commercial entity, several factors play into the time frame in which the development proceeds. One such factor of high importance for any innovation is the generation of a set of quality control and analysis guidelines. These guidelines enable the product to be commercialized safely and reproducibly. In the development of a biomaterial with the specific target as a bone cement, numerous synthetic barriers were encountered and overcome. The successful completion of synthetic procedures for the silorane monomers PHEPSI and CYGEP marked the beginning of the journey to a viable biomaterial. Careful examination of the variables indicated that the procedures of both monomers required modifications. In the synthesis of PHEPSI, due to the variability of trace metals a higher quality grade of Wilkinson's catalyst (99% purity) was required. Additionally, the order of addition of the reagents was determined to potentially reduce the quantity and type of byproducts from the reaction. For CYGEP, the use of the Gelest

Lamoreaux's catalyst at 0.79% provided the appropriate conditions for a material to polymerize as needed.

Conclusion

Adapted procedures for the synthesis of PHEPSI and CYGEP and quality control guidelines were developed and optimized for the production of silorane monomers for use as a biomaterial. The optimal procedure for PHEPSI entailed the utilization of a crystalline powder version of Wilkinson's catalyst (>99% purity) and heating the reaction mixture to 95-100 °C for 18-24 h. The addition of 4-vinylcyclohexene-1,2-epoxide as the final component of the starting materials reduced the production of byproducts. Development of a reproducible synthetic procedure for CYGEP was accomplished only after the inclusion of acetonitirile in the reaction mixture. Attempts to synthesize the monomer without acetonitrile led to polymerization upon addition of Lamoreaux's catalyst. The use of two different catalysts produced differing results. Lamoreaux's catalyst as supplied by Gelest (1.0 mL of a 0.79% solution) produced CYGEP with an additional signal at 4.6 ppm in the ^{1}H NMR spectrum while the signal was absent in reactions utilizing the in-house LMC (0.5 mL of a 0.5% solution). Optimal reaction conditions for CYGEP, regardless of the Lamoreaux's catalyst utilized, required heating to 70 ºC for 30 min.

A quality control analysis for our bone cement formulations was investigated. A loss of polymerization occurred in formulations where PHEPSI had been synthesized using a lower grade of Wilkinson's catalyst (97%). The variation of the trace metals was found to contribute to the loss of polymerization and thus a higher grade catalyst (>99%) was designated for use in this preparation. PHEPSI was found to begin to decompose

approximately one month after purification. However, it was discovered that decomposition can be prevented by the mixing of PHEPSI with CYGEP in a 1:1 ratio by weight. Thus, for monomers designed for the biomaterial, use of the Gelest Lamoreaux's catalyst was found to be optimal.

Experimental section

General procedures. Proton NMR spectra were recorded on a Varian AC 400 MHz spectrometer. Carbon NMR spectra were recorded on a Varian AC 400 spectrometer operating at 100 MHz. All commercial chemicals and solvents were used as supplied unless otherwise stated. Anhydrous toluene (>99.8%), 4-vinylcyclohexene-1,2-epoxide (98%), and octanol (>99%) were purchased from Aldrich. 2,4,6,8-Tetramethylcyclotetrasiloxane (99%) was purchased from Alfa Aesar. Methylphenylsilane (>95%) and platinum octanal/octanol complex (2.0-2.5% Pt in octanol) were purchased from Gelest. The chloroplatinic acid hexahydrate (99.9% Pt) and Wilkinson's catalyst (>99%) were purchased from Strem Chemicals.

bis[2-(3{7-oxabicyclo[4.1.0]heptyl})ethyl]methylphenyl silane (PHEPSI, 5). PHEPSI was synthesized from an adapted procedure by Crivello.[41] Wilkinson's catalyst (40 mg) and methylphenylsilane (11.0 mL, 9.79 g, 80.1 mmol) were added to toluene (80 mL) and stirred for 10 min under argon. 4-Vinyl-1-cyclohexene-1,2-epoxide (25.2 mL, 24.0 g, 193.0 mmol) was added, and the solution was heated to 95 °C for 18-24 h. The reaction was monitored for the disappearance of the Si-H peak from methylphenylsilane at 2160 cm^{-1} by IR spectroscopy. The solvent was removed via vacuum. The resulting dark orange liquid was purified using column chromatography (silica gel; solvent: solvent gradient hexanes, 2% ethyl acetate–hexanes, 4% ethyl acetate–hexanes, 6% ethyl acetate–hexanes, 8% ethyl acetate–hexanes, and 10% ethyl acetate–hexanes). Residual ethyl acetate and hexanes were removed via vacuum to obtain PHEPSI (19.8 g, 53.4 mmol, 66.7%) as a colorless viscous liquid. ^{1}H NMR ($CDCl_3$, 399.8 MHz) δ0.22 (s, 3H), 0.67-0.73 (m, 4H), 0.79–2.19 (m, 18H), 3.10–3.16 (m, 4H), 7.34–7.35 (m, 3H), 7.44–7.46 (m 2H) ppm; ^{13}C NMR ($CDCl_3$, 100

MHz) δ -5.4, 10.6, 10.8, 23.6, 23.9, 25.3, 26.7, 30.1, 30.3, 30.6, 31.5, 32.5, 35.5, 51.9, 52.0, 52.7, 53.3, 127.7, 128.8, 133.7, 138.2 ppm.

2,4,6,8-tetrakis(2-(7-oxabicyclo[4.1.0]heptan-3-yl)ethyl)-2,4,6,8-tetramethyl-1,3,5,7,2,4,6,8-tetraoxatetrasilocane (CYGEP, 6). CYGEP was synthesized from an adapted procedure by Aoki.[82] 2,4,6,8-Tetramethylcyclotetrasiloxane (12.1 mL, 12.0 g, 49.9 mmol), 4-vinyl-1-cyclohexene-1,2-epoxide (31.3 mL, 29.8 g, 240.0 mmol), acetonitrile (0.5 mL, 0.4 g, 10 mmol), and toluene (21 mL) were heated at 70 °C for 30 min. Lamoreaux catalyst (0.5 mL of 0.5% solution in toluene, prepared in-house) was slowly added. Upon addition, the temperature increased to ~130 °C for 10 min before slowly cooling to rt while stirring. The reaction was monitored for the disappearance of the Si-H peak from 2,4,6,8-tetramethylcyclotetrasiloxane at 2100 cm^{-1} by IR spectroscopy. The solvent was removed via vacuum. The clear liquid was purified using column chromatography (silica gel; solvent: solvent gradient hexanes, 2% ethyl acetate–hexanes, 4% ethyl acetate–hexanes, 6% ethyl acetate–hexanes, 8% ethyl acetate–hexanes, and 10% ethyl acetate–hexanes). Residual ethyl acetate and hexanes were removed via vacuum to obtain pure CYGEP (23.1 g, 31.3 mmol, 62.8%) as a colorless viscous liquid. ^{1}H NMR ($CDCl_3$, 399.8 MHz) δ 0.03 (s, 12H), 0.46 (t, J = 8 Hz, 8H), 0.81–2.19 (m, 36H), 3.14–3.17 (m, 8H) ppm; ^{13}C NMR ($CDCl_3$, 100 MHz) δ -0.8, 13.9, 14.0, 14.1, 23.6, 24.0, 24.1, 25.3, 26.8, 29.3, 29.8, 30.4, 31.5, 31.6, 32.0, 32.1, 35.1, 35.2, 51.9, 52.0, 52.7, 53.2 ppm

Lamoreaux's catalyst (56) was synthesized from an adapted procedure by Lamoreaux.[74] Chloroplatinic acid hexahydrate (2.89 g, 7.05 mmol) and octanol (6 mL) were heated to 55 °C for 42 h under vacuum. The black solution was vacuum filtered and washed with hexanes (15 mL). The filtrate was placed under vacuum for 8 h to remove solvents. The remaining

black liquid (~2 mL) was placed in the refrigerator under argon and used without any further purification.

CHAPTER 2

SYNTHESIS AND ANALYSIS OF EXTENDED TWISTED MOLECULAR RIBBONS

Introduction

Over the last few decades, there has been an increased interest in the synthesis and applications of polycyclic aromatic hydrocarbons (PAH), especially in the area of acenes.[84-88] Acenes, linearly fused benzenes, are a series of compounds that have been used for a wide range of purposes, including moth repellents, artificial dyes, and more recently in the materials field due to their semiconducting potential which arises from the extensive conjugated π system with lower energy bandgaps.[86, 89-91] As a result, acenes have been targeted and used in technological applications, such as organic light-emitting diodes (OLEDs), organic field-effect transistors (OFET's), organic photovoltaics, and even solar cells.[87, 92-96] This potential has increased interest in the field and thus allowed for the development and study of this class of compounds to be pushed to remarkable lengths.

The shortest and most abundant acenes are those of benzene (**65**), naphthalene (**66**), and anthracene (**67**) with one-, two-, and three-fused benzene units, respectively (Figure 27).[90, 97]

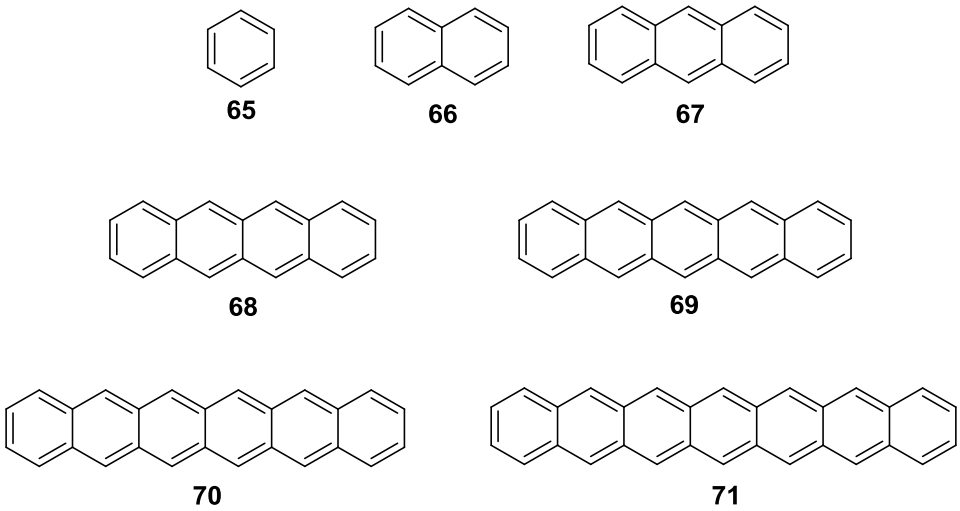

Figure 27: Structure of acenes from benzene (**65**) through heptacene (**71**).

The intermediate acenes, which include tetracene (4 units, **68**) and pentacene (5 units, **69**), have garnered a great deal of attention over the last few decades in part due to their high charge-carrier mobilities and decreasing HOMO-LUMO gaps.[84] More recently, the attempted syntheses of higher-order acenes, hexacene (6 units, **70**) and heptacene (7 units, **71**), have been of investigated for this same reason, but have faced several challenges along the way.

Synthetic Challenges

The extension of the higher-order acenes produces compounds with increasingly interesting electronic properties, including higher charge-carrier mobilities and smaller band gaps. However, this increase comes at the cost of solubility and stability.[89, 92, 98] An added challenge comes from the limited amount of publications for the synthesis of higher-order acenes, especially with the numerous accounts of withdrawn or retracted reports.[99-101]

Regardless, several procedures have been developed for the formation of the higher-order molecules. Pentacene (**69**) has been synthesized through the aldol condensation of phthalaldehyde (**72**) and 1,4-cyclohexanedione (**73**) to give quinone **74** which was then reduced to the acene (Figure 28).[102]

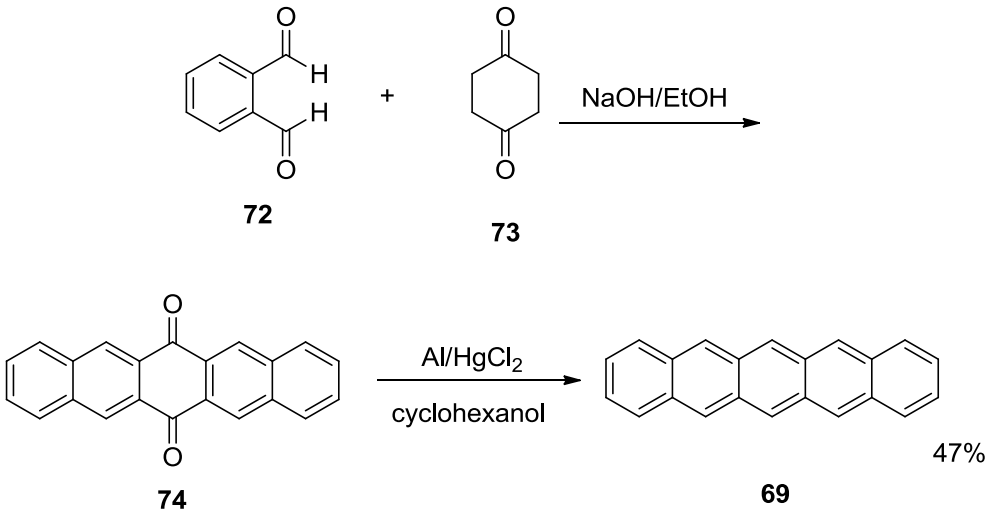

Figure 28: Synthesis of pentacene **69**.

Unfortunately, even in dilute solutions of 1,2-dichlorobenzene, **69** will begin to oxidize to quinone **74** and/or dimerize to the "butterfly dimer" (**75**, Figure 29) within five minutes unless it is carefully isolated from air and light.[71, 91, 103]

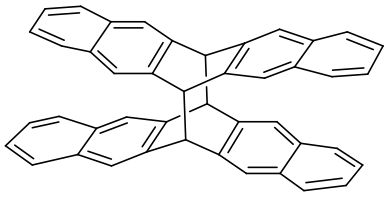

75

Figure 29: Butterfly pentacene dimer.

Successful syntheses of both hexacene (**70**) and heptacene (**71**) have been reported in the literature, but the extremely low solubility and stability of these molecules have made advanced studies on these compounds very difficult.[84, 91] Recently, Watanabe et al. reported a solid-state procedure for the synthesis of hexacene (**70**), which when prepared and stored in the dark was stable for more than one month (Figure 30).[104]

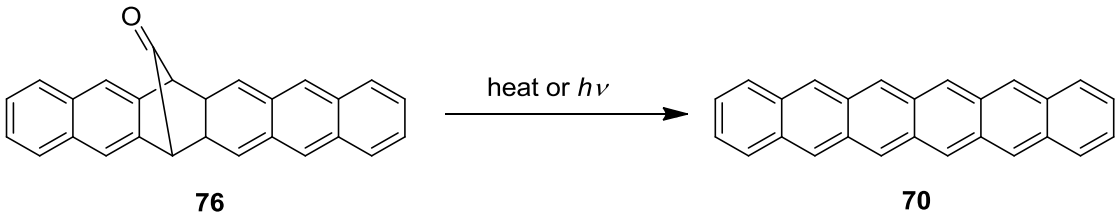

76 **70**

Figure 30: Formation of hexacene (**70**) from the monoketone precursor **76**.

However though, similar to pentacene, both **70** and 71 are susceptible to decomposition and/or dimerization.

The susceptibility of acenes to decompose or dimerize is caused by a nonequivalency of bonds in the aromatic system due to partial bond fixation. In the case of naphthalene, the C1–C2 bond is more apt to be attacked because of the higher double bond character observed in resonance forms.

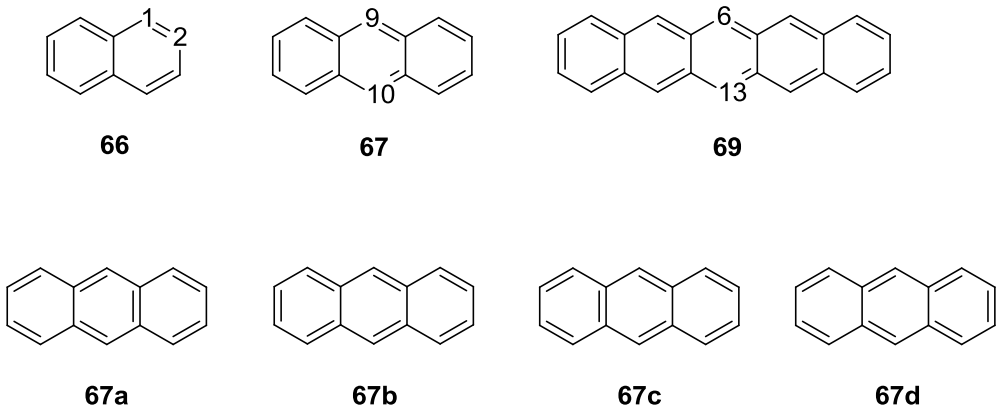

Figure 31: Higher reactivity sites for naphthalene (**66**), anthracene (**67**), and pentacene (**69**) and the resonance structures of anthracene (**67a-67d**).

In the case of anthracene, the 9,10-positions are the reactive hotspot, especially for Diels-Alder reactions, such as the addition of maleic anhydride.[105] This is due to the bond order from the possible resonance structures. In addition to the double bond character, formation of two isolated benzene rings factors into the increased reactivity at the 9,10-

positions of anthracene.[106, 107] Finally, following the trend to pentacene, reactions such as decomposition to the quinone or dimerization at the 6,13-positions would divide the skeleton into two separate naphthalene systems within the molecule.[108, 109] The understanding of this process has allowed for the development of strategies to reduce reactivity at these positions and thus increase the versatility of the compounds.

The Effect of Substitution on Acenes

Due to the high reactivity and low solubility of acenes, most notably pentacenes, research has been directed towards syntheses and studies entailing the effects resulting from the addition of functional groups to the acene skeleton.[87, 110, 111] One such strategy has been the addition of bulky substituents through the reduction of a quinone. The use of lithium reagents for the reduction of a carbonyl group to an alcohol have been used previously in the synthesis of substituted acenes (Figure 32) .[85, 91, 112, 113]

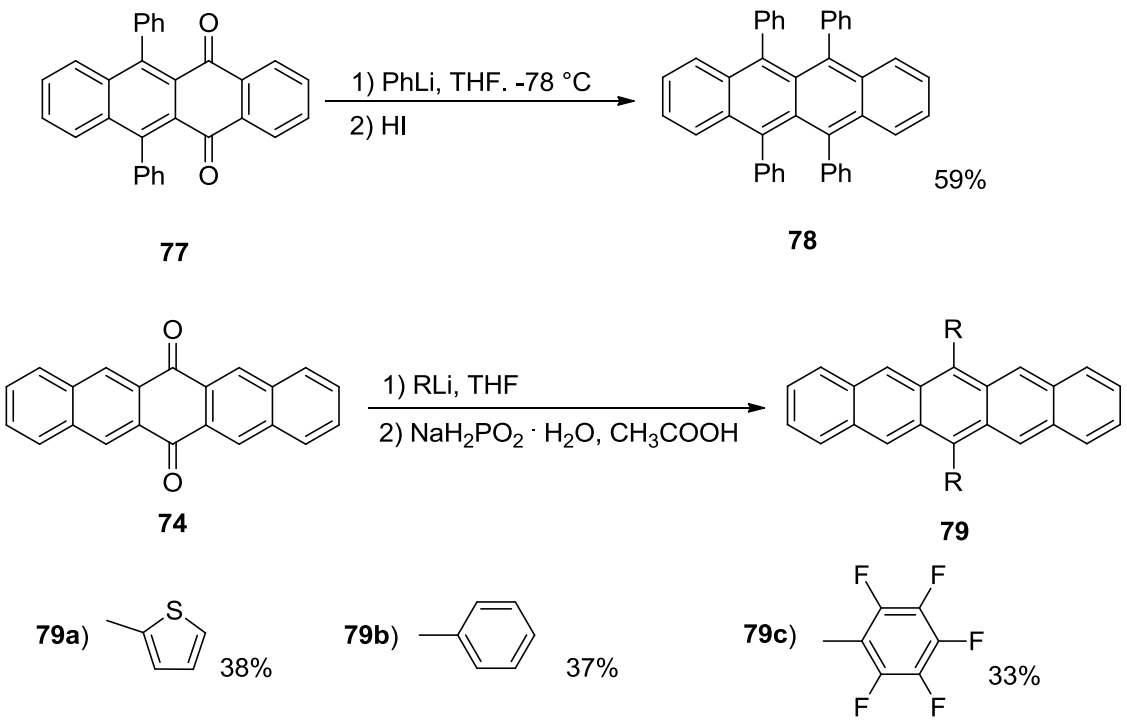

Figure 32: Reduction of acene quinones using organolithium adducts (two equivalents).

Reduction of the quinone with an organolithium reagent results in a diol which can then be aromatized to the acene by a subsequent reduction using one of several reducing agents (i.e., HI, NaH_2PO_4, or $SnCl_2$). One of the first reported functionalizations of both anthracene and pentacene was the addition of phenyl and phenylethynyl groups to the acene skeleton at the reactive positions of the acenes (C9–C10 and C6–C13, respectively) by Maulding and Roberts.[114] Substitution was accomplished by reduction of the respective quinone with the corresponding organolithium adduct, followed by aromatization with tin chloride to give the derivatives of **79** (Figure 33).[114]

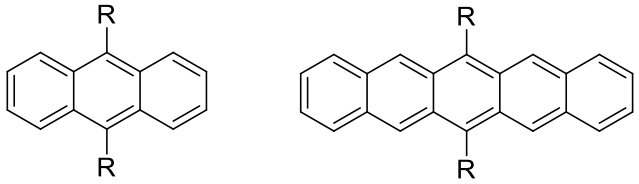

80a: -H
b: -CCC_6H_5
c: -C_6H_5
d: -$CHCHC_6H_5$

81a: -H
b: -CCC_6H_5

Figure 33: Structures of substituted anthracene (R = H, **80a**; -$C{\equiv}CC_6H_5$, **80b**; -C_6H_5, **80c**; and –$CH{=}CHC_6H_5$, **80d**) and pentacene (R = H, **81a** and -$C{\equiv}CC_6H_5$, **81b**).

The resulting molecules had an increased fluorescence efficiency and large red shifts to longer wavelengths of emission and absorption spectra in comparison to the unsubstituted acenes (Table 17).[111]

Table 17: UV-Vis absorption and fluorescence of substituted and unsubstituted acenes.[111]

Compound	Absorption (nm)	Fluorescence (nm)
Anthrancene (**67**)	382	388
Phenylethynyl anthracene (**80b**)	455	486
Pentacene (**69**)	576	578
Phenylethynyl pentacene (**81b**)	655	680

As a result of this successful approach, numerous additional 6,13-pentacene derivatives have been synthesized utilizing organolithium reagents.[85, 91] In general, the 6,13-disubstituted pentacenes have increased stability and solubility as compared to the unsubstituted molecule. An investigation by Ono et al (Figure 32) found pentacenes **79a-c** to be soluble in common organic solvents while pentacene is not.[113] Additionally, pentacene **79c** was stable in solution for up to 2 h. However, functionalization of the acene skeleton has also been expanded to sites other than the most reactive positions in an effort to increase stability.[89, 115-117]

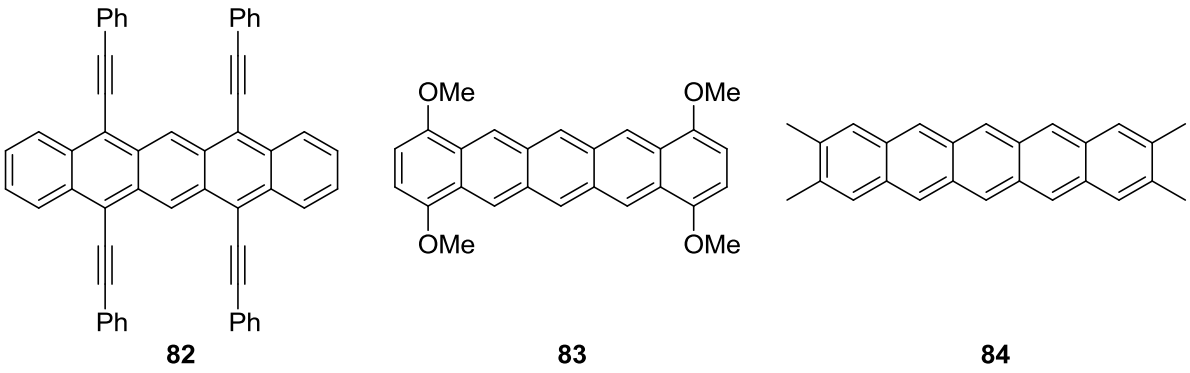

82 **83** **84**

Figure 34: Additional substituted pentacenes **82-84** at other positions.

Interestingly, incremental substitution to the acene skeleton introduces a deformation to the structure.[118]

Acene Twist

The idea that acenes are flat molecules is a common misconception. In fact, the energy required to deform many polycyclic aromatic compounds from planarity is quite modest (e.g., only 3.2 kcal/mol is needed to twist naphthalene by 20º).[118] The simple acenes have a small bend to their structure while more substituted compounds have a twist and will bend out of plane due to sterics. This "twisting" along the central unit is calculated from the torsion of angles ABCD (Figure 35) and typically becomes more prominent in molecules that contain a higher degree of substitution (steric crowding) or benzannulated molecules.

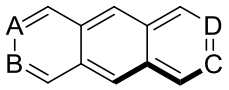

Figure 35: Torsion angles used in the determination of molecule twist, ABCD or BADC.

The extent of twist as a result of substitution may most simply be described by the sterics of the substituents. In the simpler cases, persubstitution of naphthalene with bromine, chlorine, and methyl groups highlights the effect bulkiness has on degree of twist (Figure 36).[119, 120]

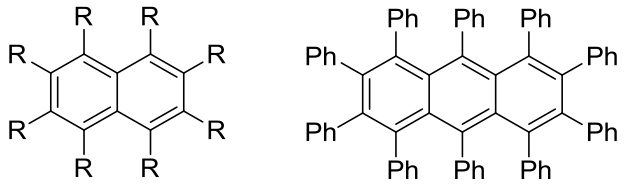

85a: Br
b: Cl
c: Me
d: Ph

86

Figure 36: Structures of persubstituted twisted naphthalenes **85a-d** and anthracene **86**.

Octabromonaphthalene (**85a**) exhibits a 31º end-to-end twist while the octachloro- (**85b**) and octamethylnaphthalene (**85c**) are slightly less twisted at 24º and 26º, respectively. When overcrowding is caused by phenyls as in compound **85d**, the naphthalene core remains essentially untwisted, while the phenylated anthracene **86** becomes highly twisted at 63º due to the severe *peri* interactions.[118] *Peri* interactions are the steric effects rising from bumping of atoms along the acene framework.[121] In naphthalene, the 1- and 8-positions are closer than substituents in the *ortho* position. The substitution of the anthracene framework with phenyl groups incorporates an overall increase in steric hindrance. Therefore, to prevent such bumping of substituents, the phenyls are forced into a propeller-like orientation, which tilts the phenyls out of plane.[118]

In addition to substitution, another way of inducing twist into the acene skeleton is through benzannulation.[118] The fusion of benzo groups to the ends of the acene skeleton provides molecules with entirely different absorbance spectra due to the inclusion of additional conjugation. One route to these structures has been the fusion of stable aromatics

(e.g., phenanthrene (**87**), pyrene (**88**), acenaphthene (**89**), and corannulene (**90**)) to the ends of acenes, as seen in Figure 37.

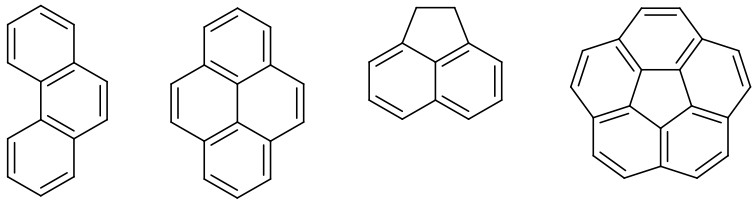

87 **88** **89** **90**

Figure 37: Common acene end caps.

The development of both single- and double-terminated unsubstituted acenes (**91** and **92**, respectively as depicted in Figure 38) has received some interest in hopes of offering protection from dimerization and oxidation, but has to this point has not solved the issue of stability.[122, 123]

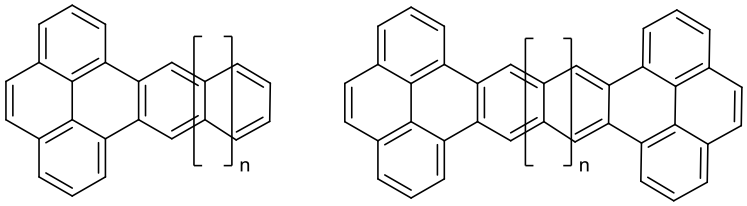

91 **92**

Figure 38: Single- and double-terminated unsubstituted acene structures **91-92**, respectively.

Thus, this work has been overshadowed. Used individually, substitution of acenes with bulky functional groups or benzannulation provides significant distortions to the acene skeleton. However, the largest distortion has been observed on those compounds utilizing both ideas.[118] Several compounds of varying length and structure have been synthesized and their deviation from planarity as defined by the ABCD torsion angle has been reported in the solid state (Figure 39 and Table 18).[124-127]

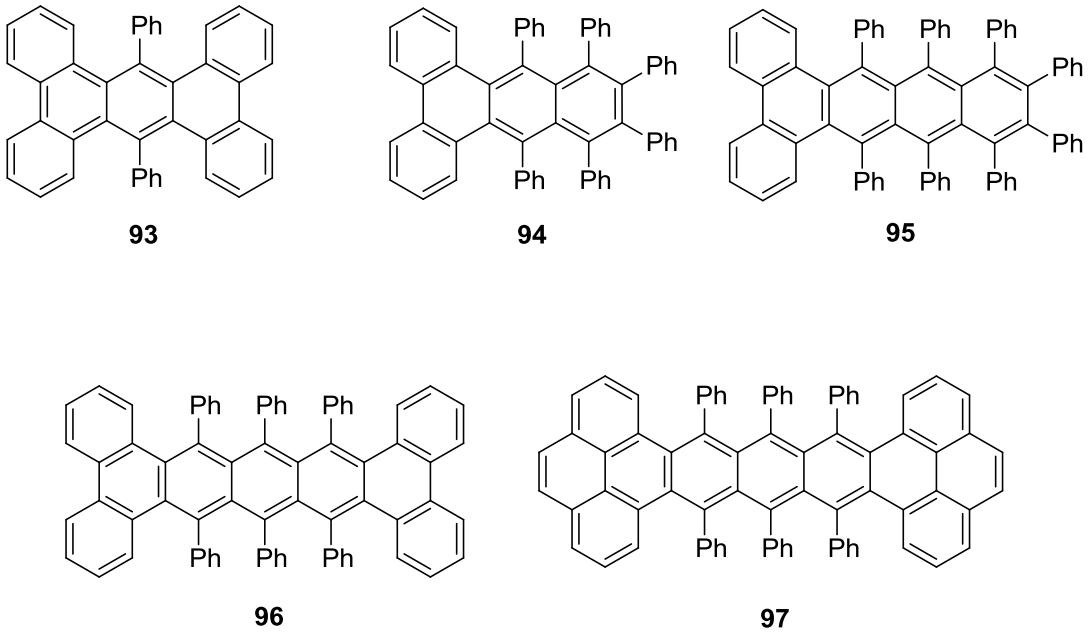

Figure 39: Structures of crowded acenes.[124, 126]

Table 18: Twist of crowded acenes from solid state structures.[124,126]

Compound	Twist
93	66º
94	60º
95	105º
96	144º
97	138º

The largest end-to-end twists are attributed to clashing of the phenyls with the hydrogens of the benzo end groups.[118, 122] Crystallographic analysis of 9,18-diphenyltribenzo [f,k,m]tetraphene (**93**) was found to have a twist of 66º, while the single terminated anthracene **94** was slightly smaller at 60º.[126, 128] The addition of another benzene unit as in compound **95** increased the twist to 105º.[118] The extension to longer acenes increases the twist to higher degrees. Pentacenes **96** and **97** have end-to-end twists of 144º and 138º, respectively, with **96** currently being the most highly twisted PAH reported to date.[125] All of the structures (Figure 12) are fluorescent compounds with increased stability in both air and light. It is believed that even further extended acenes may be developed, but no synthetic pathways are currently reported in the literature.

Barrier to Enantiomerization

As discussed previously, the overall twist of acene skeletons have been attributed to substituent effects along the length of the acene.[118] As a result of the twist, compounds, such as those given in Table 18 are chiral and exist in the solid. Compounds with higher degree twists exhibit a stereochemistry similar to that observed in helicenes, molecules comprised of *ortho*-fused aromatic rings.[129] The corkscrew conformation results from the repulsion of the faces of the rings as well as the steric-bulk of the groups required to interconvert from one enantiomeric conformation through the transition state to the other one.[126] The minimum amount of energy required for this process is the barrier to enantiomerization. Helicenes exhibit chirality without the presence of a stereogenic center.[130] A "plus-minus" naming system was proposed by Cahn et al. by which helicenes are labeled according to their left- ("minus", *M*) and right- ("plus", *P*) handedness, as seen in Figure 40.[131]

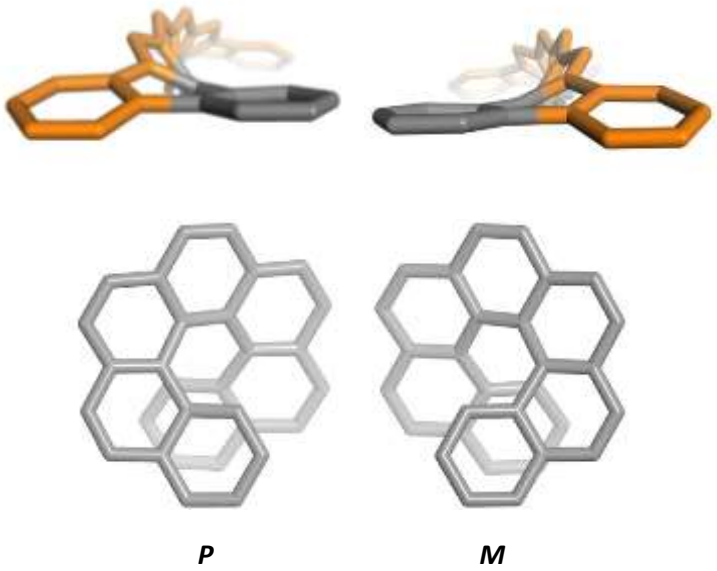

Figure 40: Handedness of [7] heptahelicene, “plus” (*P*) on left and “minus” (*M*) on right.

In these molecules, the racemization process occurred quite easily as determined experimentally by H/D exchange which were placed on the ends of the molecule.[132] It was determined that the interconversion was enabled by the twisting of the aromatic bonds of the molecule. For helicenes, it was noted that conformational stability of individual racemates and the energy for the process as determined experimentally and computationally from [5] pentahelicene through [9] nonahelicene (~22.9 to 41.7 kcal/mol) (Table 19).[124, 132]

Table 19: Barrier to enantiomerization of helicenes. (Values listed in kcal/mol)[132]

Compound	Experimental	AM1	B3LYP/3-21G
[5] Pentahelicene	22.9	22.9	28.02
[6] Hexahelicene	35.0	31.4	40.50
[7] Heptahelicene	40.5	34.7	44.31
[8] Octahelicene	41.0	34.9	43.38
[9] Nonahelicene	41.7	34.0	40.80

In the study, the calculated AM1 and B3LYP/3-21G values are useful in approximating the barrier to enantiomerization of helicenes in comparison to their experimental values. A similar investigation of barriers to racemization has been utilized in acenes as well. The helical twist of acenes has been thoroughly investigated through the use of X-ray crystallography and computational analysis. Unfortunately, it is not possible to synthesize only one conformer because synthetic procedures yield racemates.[133] Due to this inability to produce a single enantiomer the research focus has shifted towards the study and determination of the barrier through alternative means. One such method has been the incorporation of a substituent which may act as a "handle" and able to monitor this conversion using Dynamic NMR Spectroscopy.[134-138] It is well known that isopropyl groups are enantiotopic and can be utilized in an achiral environment to investigate the barriers using variable temperature NMR spectroscopy. One such study by Pascal et al. reported that the racemic anthracene **93** has a twist of 66º.[126] He and his co-workers prepared anthracene **98**

which incorporated isopropyl groups at positions 9 and 10 of the anthracene skeleton (Figure 41).

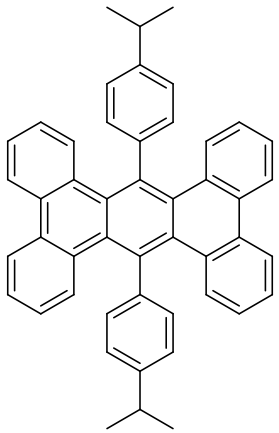

98

Figure 41: Isopropyl substituted anthracene (**98**).

Using Variable Temperature ^{1}H NMR spectroscopy, the coalescence of the methyl groups was observed at 300 K. Using the Gutowsky-Holm approximation (Eq. 1) and a standard propagation or error analysis (Eq. 2), the barrier was determined to be 16.7 kcal/mol. The $\Delta\nu$ is the difference in frequency of the signals at the coalescence temperature, T_c and the coupling constant, J_{ab}.[126, 139] While the barrier is slow on the NMR timescale, it is much too low for the separation and isolation of the two enantiomers.

$$\Delta G = 4.576T_c(10.319 + \log (T_c/k_c)) \quad \text{Eq. 1}$$

$$k_c = \pi/2 \, (\Delta \nu_{ab}^2 + 6J_{ab}^2)^{1/2} \quad \text{Eq. 2}$$

Two additional methods have been used to determine the barrier of enantiomerization are to measure the half-life of a resolved compound by specific rotation or enantiomeric excess.[124] Pascal et al. used both procedures to determine the barrier pentacene **96**. Pentacene **96** was resolved by preparative HPLC with the specific rotation measured within minutes of peak elution. The half-life for the decay of optical rotation was then recorded and determined to be 9.3 h at 25 ºC. Additionally, the half-life for the loss of enantiomeric excess was determined to be 6.2 h at 27 ºC by HPLC analysis. Both measurements resulted in a barrier of 23.8 kcal/mol. Using all of these results, it was proposed that acenes, such as hexacene **99** (Figure 42) would be configurationally stable after separation at rt.[124]

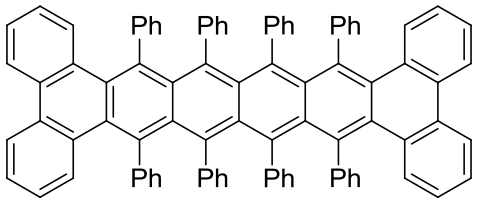

99

Figure 42: Phenanthrene terminated hexacene **99**.

Objectives and Synthetic Approaches

The focus of the work by our group has been on the development of synthetic schemes for the extension of the acene backbone. We have been able to prepare pentacene **96** via an alternative synthesis from that of Pascal et al.[140] They reported a five-step procedure with an overall yield of 2% (Figure 43, pathway a).[124] In this procedure, diepoxide **102** was formed by reacting compound **101** with furan **100** in the presence of *n*-butyllithium in a 26% yield. Deoxygenation was then accomplished using *n*-butyllithium and $TiCl_3$ to give **96** as a bright red solid in a 27% yield (0.2% overall synthetic yield).

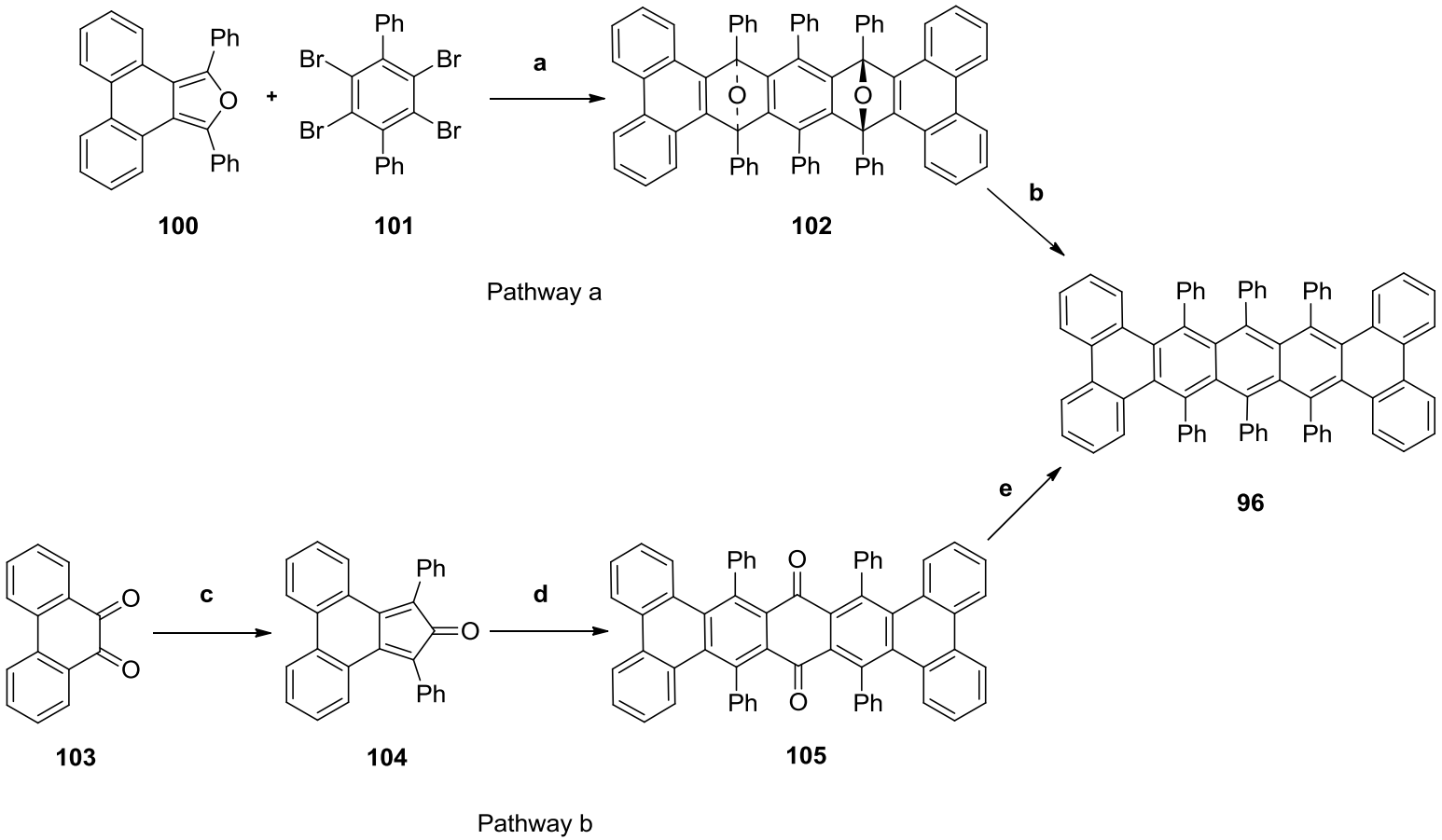

Figure 43: Synthetic routes for **96**, pathway a 0.2% overall yield, pathway b 36.7% overall yield. Conditions: a) *n*-BuLi, hexanes, toluene, 26%; b) *n*-BuLi, $TiCl_3$, ether, hexanes, 27%; c) 1,3-diphenylacetone, ethanol, NaOH, 85%; d) *p*-benzoquinone, nitrobenzene, 51% and e) (i) PhLi, THF, 91% (ii) $TiCl_2$, THF, HCl, 72%.

Our alternative synthesis of **96** (Figure 43, pathway b) required four steps and resulted in an overall yield of 36.7%. In this pathway, two equivalents of cyclone **104** were reacted with *p*-benzoquinone in a Diels-Alder reaction to give quinone **105** in a yield of 51%. Reduction of **105** to the diol was then accomplished by the addition of two equivalents of phenyllithium in a 91% yield. The aromatized product was then formed by reduction using $TiCl_2$ to give pentacene **96** in 72% yield. Therefore, the use of a simple Diels-Alder reaction followed by lithium reductions provided an efficient synthetic route to a highly crowded pentacene. Using this methodology, our group was able to develop the symmetric double pyrene terminated pentacene **97**, along with the asymmetric phenanthrene-pyrene terminated pentacene **97** as seen in Figure 44.

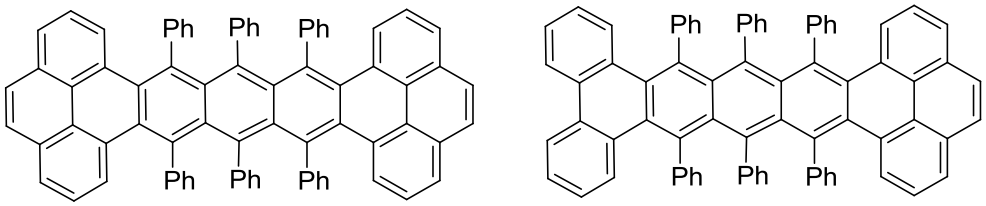

97 **106**

Figure 44: Pyrene terminal pentacene **97** and phen-pyrene pentacene **106**.

For the cases in which a pyrene endcap was utilized, oxidation of pyrene (**88**) to the 4,5-dione (**107**) was required (Figure 45).[141] Once the dione was obtained, pathway b (Figure 43) was followed according to the same procedures used for phenanthrene endcaps.

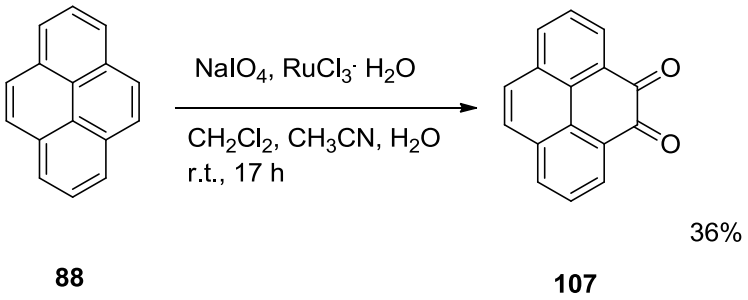

Figure 45: Oxidation of pyrene.

This pathway provides a roadmap in the synthesis of acenes with alternative end groups and substituents.

The goal of this study was to synthesize novel acenes derived from pentacene **96** using the synthetic pathway previously developed by our group (pathway b, Figure 43). Derivatization of pentacene **96** was focused on three specific areas: 1) the addition of alternative end groups to the acene skeleton, 2) the functionalization of the acenes with isopropyl groups, a possible Variable-Temperature NMR spectroscopic probe for the determination of the barrier to enantiomerization, and 3) the extension of the acene skeleton.

Results and Discussion

The development of the reducibility of acene quinones using phenyllithium allowed for the pursuit of a variety of synthetic strategies.

Corannulene

In this investigation of endcaps the first choice was corannulene (**90**). Functionalization of corannulene was centered on its use for larger structures including carbon nanotubes.[142-145] However, as far as we know corannulene has not been used as an endcap in the development of extended acenes. In order to follow our established methodology, oxidation of corannulene to the dione was the first necessary step in this synthetic pathway (Figure 46).[146]

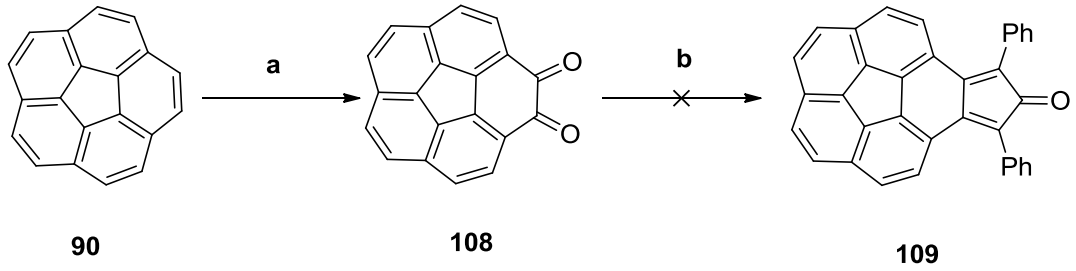

Figure 46: Development of corannulene endcap. Conditions: a) CH_3CN, ammonium cerium sulfate, H_2SO_4, 35%; b) EtOH, NaOH, rt, 15 min, 0%.

Thus, corannulene dione **108** was synthesized through the oxidation of **90** using ammonium cerium sulfate and H_2SO_4 (35% yield).[146] From there, numerous trials to form cyclone **109** via the aldol condensation using 1,3-diphenylacetone were unsuccessful using an array of bases, including NaOH, KOH, and Triton B (benzyltrimethylammonium hydroxide). Reactions were run varying the temperature (rt to 100 °C for 1 h) with no formation of the

desired product as determined by ^{1}H NMR. After numerous attempts, no feasible route to cyclone **109** was discovered, and the development of a corannulene endcap was discontinued.

Use of Pyrene as a Central Unit

As discussed previously, pyrene has been utilized as endcaps for acenes. The first step in the synthesis is the oxidation of pyrene **88** to the 4,5-dione **107** (Figure 45).[141] Having already successfully developed a synthetic route of pyrene as an endcap, the oxidation of the C4, C5, C9, and C10 positions to the tetraone was proposed. Disubstitution would allow for expansion on both sides of pyrene rather than just at the C4 and C5 positions. However, there are solubility issues with planar structures. In our previous work, we added *tert*-butyl groups to increase solubility and enable solvent chemistry. Using this approach *tert*-butyl groups were first added to the C2 and C7 positions of pyrene (Figure 47).[147]

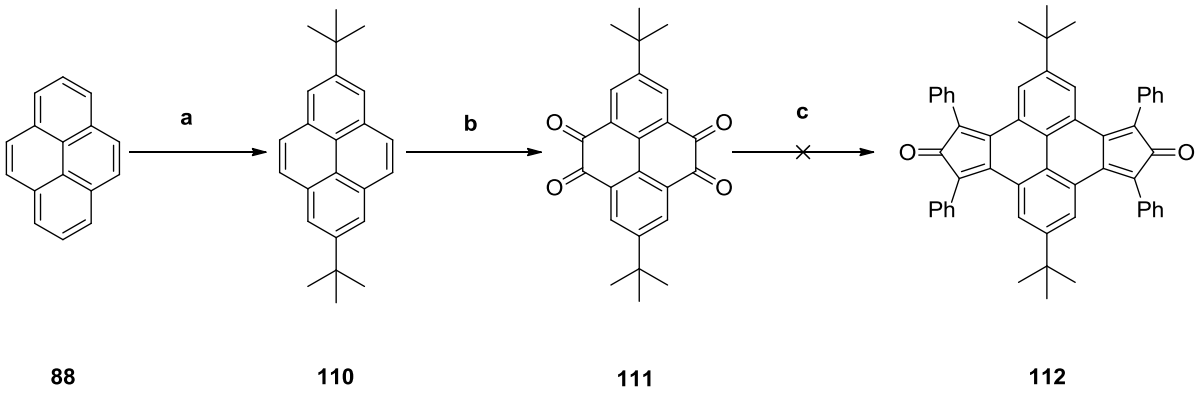

Figure 47: Attempted synthesis of central pyrene acene. Conditions: a) $AlCl_3$, *t*-butylchloride, 79%; b) CH_2Cl_2, CH_3CN, H_2O, $NaIO_4$, $RuCl_3 \cdot H_2O$, 17%; c) 1,3-diphenylacetone, NaOH, 0%.

Di-*t*-butyl pyrene **110** was then oxidized to quinone **111** using the same procedure as for the 2,7-dione, but with two equivs. of ruthenium chloride while heating to 60 ºC.[141] From there, the synthesis of dicyclone **112** was attempted through the aldol condensation with 1,3-diphenylacetone. In the case of the corannulene endcap, reactions to make the cyclone equivalent were unsuccessful. As with corannulene, the reaction attempts to form cyclone **112** were unsuccessful. This approach included a variety of bases (e.g., NaOH, KOH, and Triton B), temperatures (rt to 100 °C), and reaction times (15 min to 3 h). Further attempts to synthesize a central pyrene unit were discontinued.

Isopropyl Derivatives

The investigation into the barrier of enantiomerization of our acenes was focused on the incorporation of a substituent capable of studies by Variable-Temperature NMR spectroscopy. The probe selected for the investigation was that of an isopropyl group as in the case of anthracene **98** previously synthesized by Pascal.[126] For this investigation, target compounds of pentacene **113** and anthracene **115** were selected (Figure 48). It was proposed that the barrier to enantiomerization would be between 23-24 kcal/mol for **113** and 16-18 kcal/mol for **115**. These proposals were based upon the calculated values for corresponding compounds **96** (23.8 kcal/mol) and **97** (16.7 kcal/mol), respectively.[118]

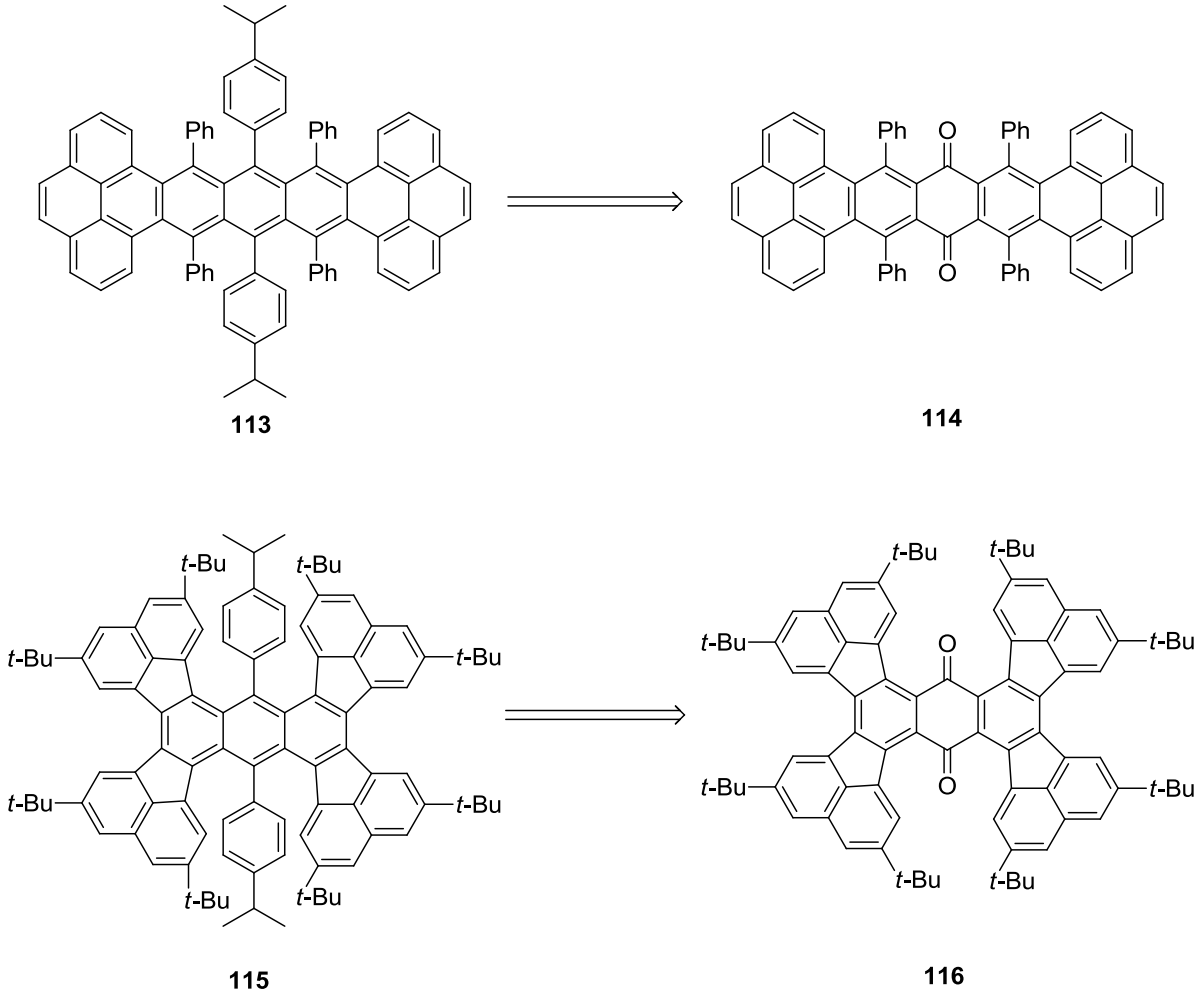

Figure 48: Retrosynthetic analysis of isopropyl acenes.

In both cases, the fully aromatized compounds were synthesized from the quinone precursor (**114** and **116**, respectively).

Pyrene Isopropyl Pentacene

Synthesis of pentacene **113** was performed mirroring the methodology used for pathway b in Figure 17. Quinone **114** was obtained in a four-step process beginning with the oxidation of pyrene to dione **107** in 36% yield (Figure 49).

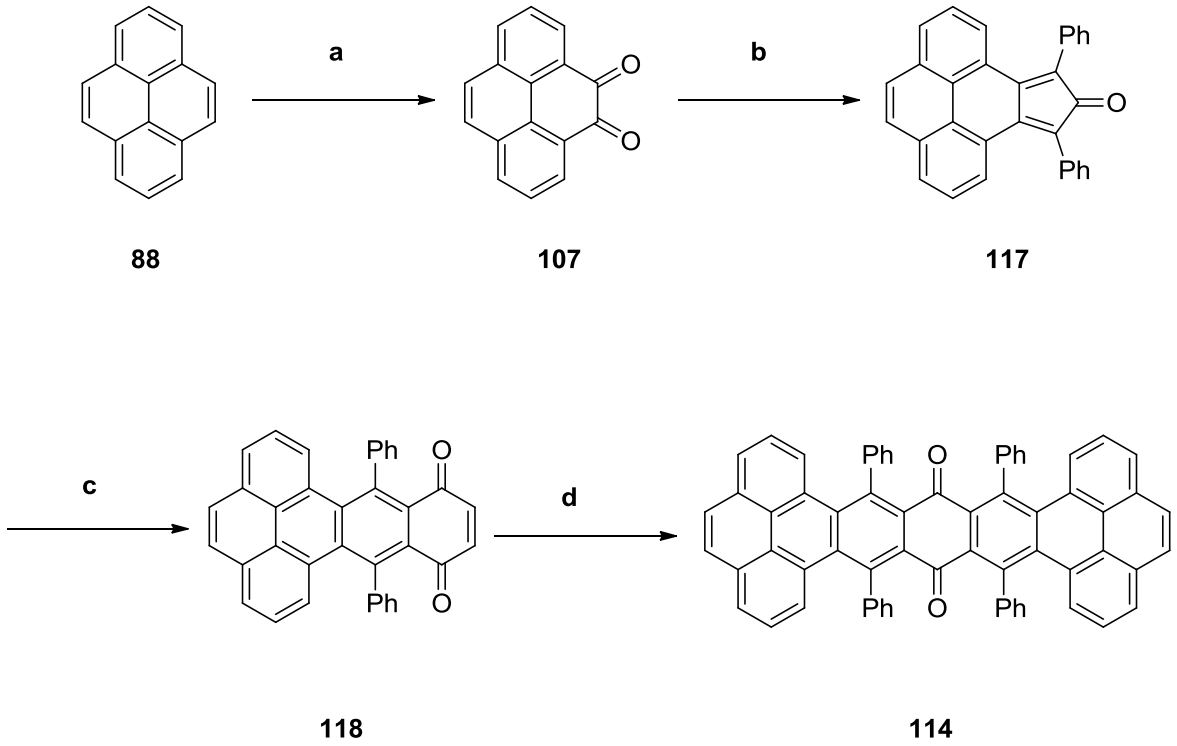

Figure 49: Synthesis of pyrene pentacene quinone. Conditions: a) CH_2Cl_2, CH_3CN, H_2O, $NaIO_4$, $RuCl_3 \cdot H_2O$, 36%; b) 1,3-diphenylacetone, NaOH, EtOH, 59%; c) *p*-benzoquinone, nitrobenzene, 58%; d) cyclone **117**, nitrobenzene, 59%.

Cyclone **117** was then obtained through the aldol condensation of dione **107** with 1,3-diphenylacetone (59% yield). A solution of cyclone **117** and benzoquinone was refluxed 1 h in nitrobenzene which afforded quinone **118** as a red-orange solid in 58% yield. Then pentacene quinone **114** was obtained through an additional Diels-Alder reaction which entailed refluxing quinone **118** and cyclone **117** in nitrobenzene for 24 h. The resulting green solid (59% yield, 7.2% overall yield) was highly insoluble in organic solvents and required no further purification.

The ability to reduce quinone **114** to the diol using phenyllithium, followed by reduction to the aromatized acene, enabled exploration into the possibility of further substituted materials. One way to measure the barrier to enantiomerization as previously described by Pascal is to incorporate isopropyl handles at some point during the synthesis.[126] Therefore, an isopropyl organolithium reagent was utilized in the reduction of quinone **114** in lieu of phenyl lithium using a procedure adapted from Miller et al.[92] The isopropyl adduct was produced by the slow addition of *n*-butyllithium to a solution of 1-bromo-4-isopropylbenzene and THF at -78 °C (Figure 50).

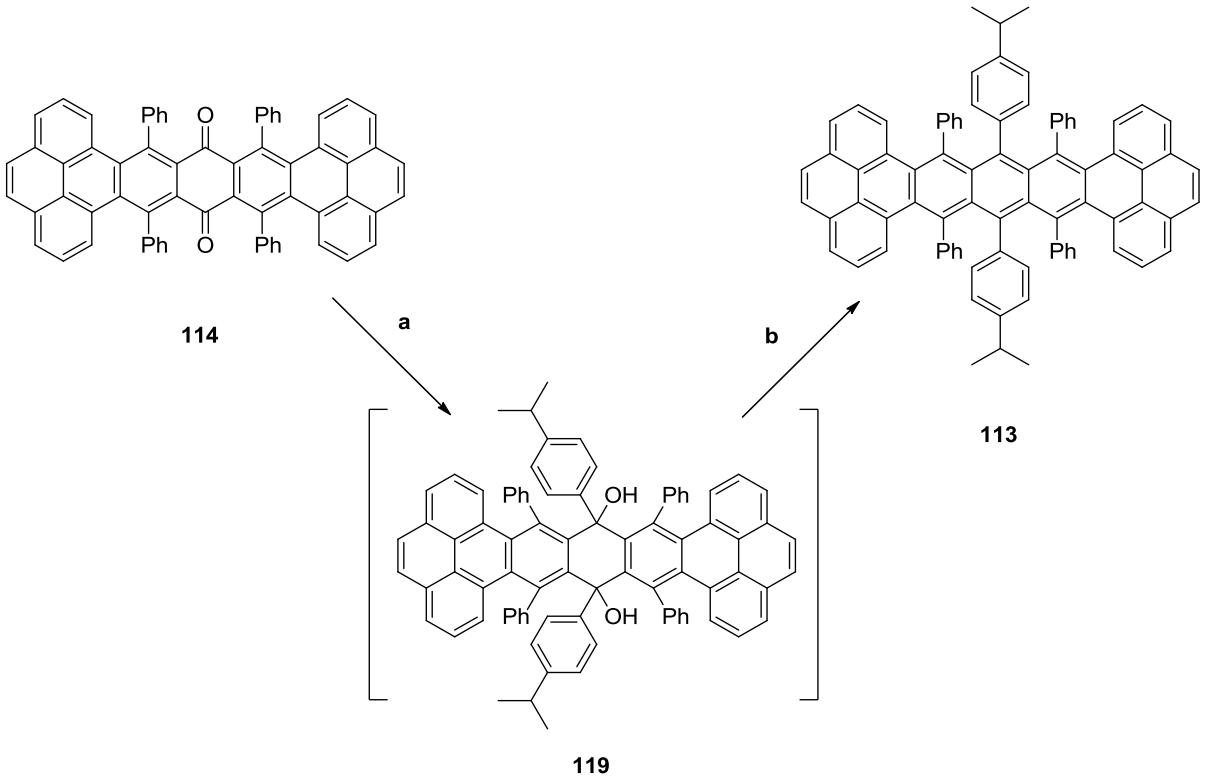

Figure 50: Synthesis of pyrene isopropyl pentacene **113**. Conditions: a) *n*-BuLi, THF, 1-bromo-4-isopropylbenzene, 46%; b) THF, $SnCl_2$•2 H_2O, HCl, 40%.

After stirring at -78 °C for a minimum of 20 min, the cloudy solution was warmed until it became clear. Then, the isopropyl lithium adduct was added to a stirring suspension of quinone **114** in THF. Upon addition, the green suspension turned a deep red color and was stirred at rt for 24 h. The reaction solution was quenched with an acid water and yielded diol **119** as a yellow solid in 46% yield. Aromatization was then achieved by the reduction of diol **119** to pentacene **113** using tin (II) chloride and HCl in THF. The red-orange solid was collected by filtration after recrystallization from $CHCl_3$–MeOH in a 40% yield (1.3% overall yield). The pentacene was characterized by mass spectrometry, ^{1}H and ^{13}C NMR

spectroscopy, and X-ray crystallography of crystals grown in $CHCl_3$–MeOH. Analysis of the crystal structure revealed the end-to-end twist of the molecule to be 126º (Figure 51 and Table 20). In comparison to compound **97** (138º) there was a decrease in the overall twist of the compound upon the addition of isopropyl substituents.

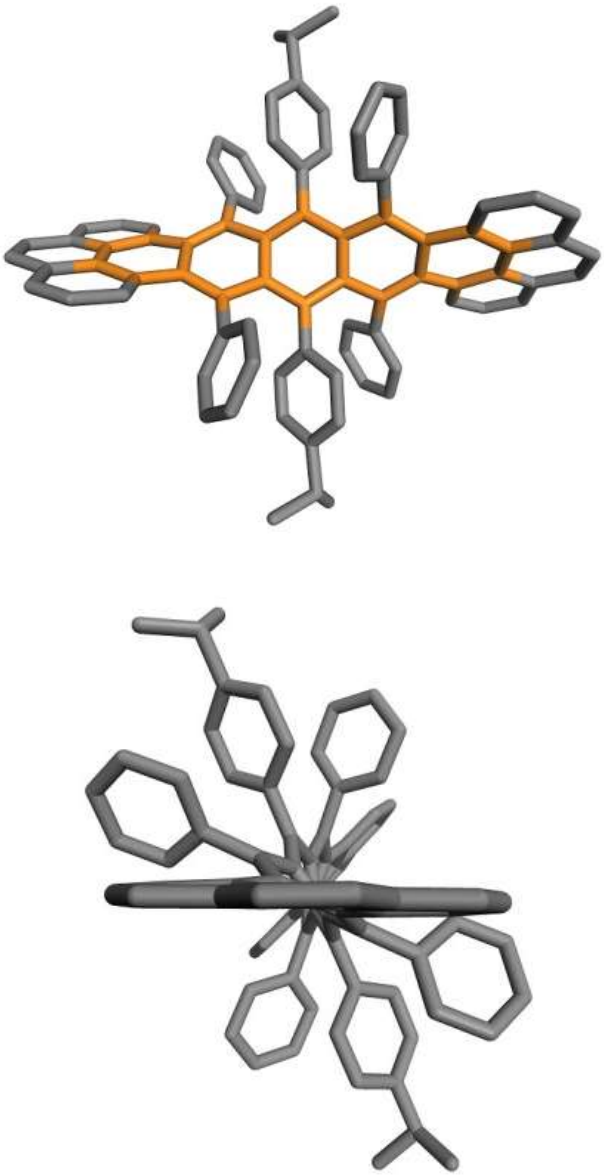

Figure 51: X-ray crystal structures of pyrene isopropyl pentacene **113** displaying the end-to-end twist (126º) of the acene skeleton.

Table 20: Crystal data for Compound **113**, $C_{86}H_{56}$ (2), CCl_4O_2

Compound	$C_{86}H_{56}$ (2), CCl_4O_2
Chemical Formula	$C_{169}H_{112}Cl_4O_2$
Formula weight	2316.39
Crystal system	Tetragonal
Space group	*P* 4/*n*
a, Å	19.8596(16)
b, Å	19.8596(16)
c, Å	15.1473(13)
α, deg.	90
β, deg	90
γ, deg	90
V, Å^3	5972.5(11)
Z	2
ρ (calcd.), g cm^{-3}	1.288
crystal size	0.26 x 0.08 x 0.07
μ, mm^{-1}	0.160
T, K	100(2)
F(000)	2420.0
θ_{max}, deg	22.500
Reflections	
Total	73056
Unique	3915
observed [I > 2s(l)]	2404
R_{int}	0.1701
Parameters	398
R(*F*) (obs data)[a]	0.0941
wR(F^2) (obs data)[a]	0.2940
R(F) (all data)[a]	0.0941
wR(F^2) (all data)[a]	0.2940
S (all data)[a]	1.025

[a] $R(F) = \Sigma||F_o| - |F_c||/\Sigma|F_o|$; $wR(F^2) = [\Sigma w(F_o^2 - F_c^2)^2/\Sigma w(F_o^2)^2]^{1/2}$; *S* = goodness of fit on F^2 = $[\Sigma w(F_o^2 - F_c^2)^2/(n-p)]^{1/2}$, where *n* is the number of reflections and *p* is the number of parameters refined.

Table 21: Atomic coordinates and equivalent isotropic displacement parameters for **113**.

Atom	*x*	*y*	*z*	U_{eq}
C1	0.2200(3)	1.0084(3)	0.4180(4)	0.0439(15)
C2	0.2097(3)	1.0709(3)	0.4571(4)	0.0478(16)
C3	0.1777(3)	1.1211(3)	0.4121(4)	0.0477(16)
C4	0.1200(3)	1.1625(3)	0.2786(5)	0.0520(18)
C5	0.0969(3)	1.1515(3)	0.1969(5)	0.0559(18)
C6	0.0732(3)	1.0744(3)	0.0738(4)	0.0536(17)
C7	0.0776(3)	1.0114(3)	0.0377(4)	0.0515(17)
C8	0.1045(3)	0.9577(3)	0.0845(4)	0.0414(15)
C9	0.1500(3)	0.8421(3)	0.2052(4)	0.0336(13)
C10	0.3168(3)	0.7759(2)	0.2563(3)	0.0343(14)
C11	0.2623(3)	0.8862(2)	0.3046(4)	0.0353(14)
C12	0.1523(3)	1.1095(3)	0.3281(4)	0.0383(14)
C13	0.0993(3)	1.0857(3)	0.1578(4)	0.0469(16)
C14	0.1300(3)	1.0317(3)	0.2051(4)	0.0361(14)
C15	0.1299(3)	0.9655(3)	0.1694(4)	0.0334(14)
C16	0.1609(3)	0.9107(3)	0.2196(4)	0.0338(14)
C17	0.1959(3)	0.7931(2)	0.2442(3)	0.0326(13)
C18	0.2601(3)	0.8181(2)	0.2685(4)	0.0340(14)
C19	0.2098(3)	0.9295(2)	0.2879(4)	0.0340(13)
C20	0.1984(3)	0.9946(3)	0.3333(4)	0.0353(14)
C21	0.1599(3)	1.0450(2)	0.2888(4)	0.0353(14)
C22	0.1011(3)	0.8145(2)	0.1399(4)	0.0339(14)
C23	0.0319(3)	0.8189(3)	0.1506(4)	0.0411(15)
C24	-0.0110(3)	0.7925(3)	0.0873(4)	0.0480(16)
C25	0.0142(3)	0.7631(3)	0.0133(4)	0.0503(17)
C26	0.0835(3)	0.7589(3)	-0.0003(4)	0.0408(15)
C27	0.1257(3)	0.7835(2)	0.0636(4)	0.0349(14)
C28	0.3856(3)	0.8038(2)	0.2556(4)	0.0349(14)
C29	0.4028(3)	0.8568(3)	0.1981(4)	0.0441(15)
C30	0.4659(3)	0.8840(3)	0.2000(4)	0.0555(18)
C31	0.5144(3)	0.8616(3)	0.2568(4)	0.0544(18)
C32	0.4984(3)	0.8084(3)	0.3128(4)	0.0489(16)
C33	0.4349(3)	0.7804(3)	0.3127(4)	0.0384(14)
C34	0.3166(3)	0.9003(3)	0.3708(4)	0.0355(14)
C35	0.3193(3)	0.8606(3)	0.4469(4)	0.0412(15)
C36	0.3650(3)	0.8738(3)	0.5118(4)	0.0511(17)
C37	0.4098(3)	0.9262(4)	0.5026(5)	0.061(2)

Table continued

Table 21 continued

Atom	*x*	*y*	*z*	U_{eq}
C38	0.4081(3)	0.9657(3)	0.4288(5)	0.061(2)
C39	0.3617(3)	0.9532(3)	0.3623(4)	0.0458(16)
C40	0.5837(4)	0.8957(4)	0.2570(5)	0.072(2)
C41	0.6038(11)	0.9253(12)	0.3450(10)	0.080(6)
C42	0.6422(9)	0.8438(9)	0.2686(18)	0.095(7)
C51	0.6344(13)	0.8470(12)	0.221(3)	0.097(9)
C52	0.5799(11)	0.9492(11)	0.3349(11)	0.046(6)

Isopropyl Anthracene

The second isopropyl derivative studied was anthracene **115**. Addition of a phenyl isopropyl substituent was made possible by the availability of anthraquinone **116,** which had previously been developed by Kilway et al. through the Diels-Alder reaction of thiophene **111** and benzoquinone **112** (Figure 52).[127]

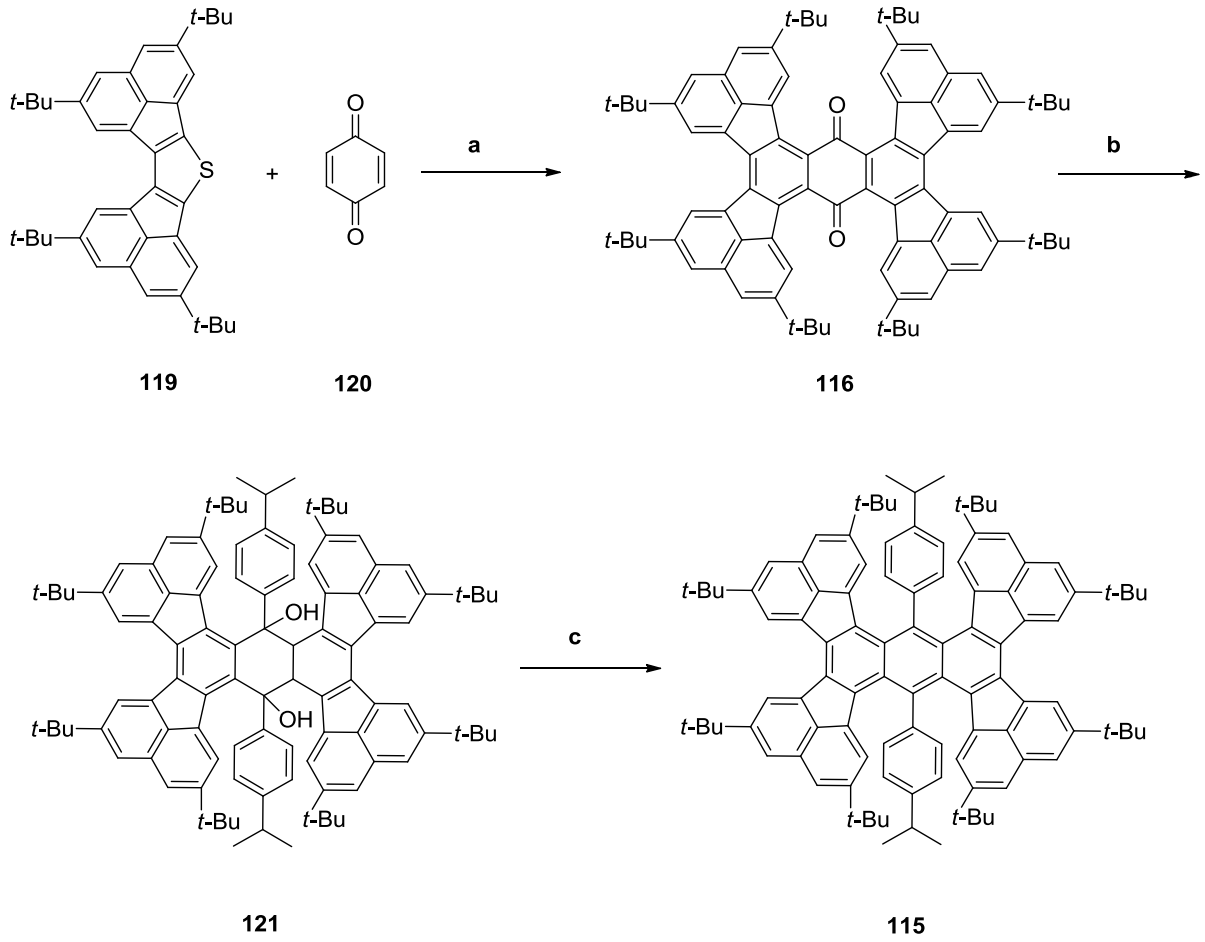

Figure 52: Synthetic scheme for isopropyl anthracene **115**. Conditions: a) nitrobenzene, reflux, 12%; b) *n*-BuLi,1-bromo-4-isopropylbenzene, THF, benzene, 35.6% crude; c) THF, $SnCl_2$•2 H_2O, HCl, 2.3%.

Reduction of the quinone was again achieved by *in situ* formation of the lithium isopropyl phenyl adduct at -78 ºC in THF and *n*-butyllithium. Once formed, the lithium adduct was then added to a refluxing solution of anthraquinone **116** in benzene. The resulting dark green solution was refluxed for an additional 1 h followed by stirring for 24 h at rt. Acid workup of the solution resulted in diol **121** as a brown solid. A final reduction to anthracene **115** was achieved by the addition of tin chloride and HCl to a stirring solution of the diol and THF at

a gentle reflux. Within minutes of addition, the solution became a dark green color and was heated for an additional 20 min. Filtration and purification resulted in isopropyl anthracene **115** as a green solid, which was verified by ^{1}H and ^{13}C NMR spectroscopy (2.3% yield, 0.9% overall yield).

UV Studies

Pentacene **113** is soluble in polar solvents, such as chloroform and methylene chloride, and exhibits a dark orange hue when dissolved in chloroform (Figure 53 light). Under UV irradiation (wavelength: 365 nm), the solution emits a bright orange fluorescence (Figure 53 dark). Anthracene **115** is soluble in polar solvents as well but, becomes a dark green solution when dissolved in chloroform (Figure 53). Under UV irradiation at 365 nm, the solution exhibits no fluorescence.

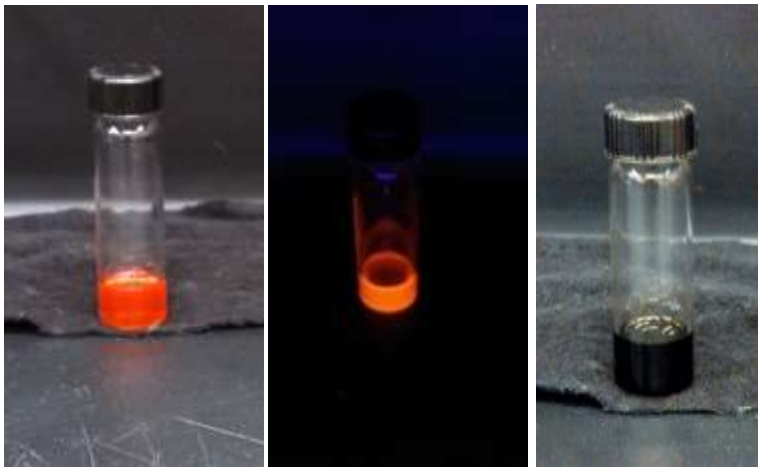

Figure 53: Pyrene isopropyl pentacene **113** (3.5×10^{-5} M left and middle) in $CDCl_3$ in light and under UV Isopropyl and anthracene **115 (**1.7×10^{-5} M, right) under regular light.

113 was studied using UV-Vis spectroscopy resulting in absorbances at 422, 491, 515, and 551 nm. The longest λ_{max} was determined to be 551 nm, which was similar to the parent compound **97** (λ_{max} of 553 nm). The extinction coefficient was determined to be 50772 for λ_{max} of 422 nm using dilution studies (from 2.27×10^{-5} to 1.45×10^{-6} M, see Figure 54).

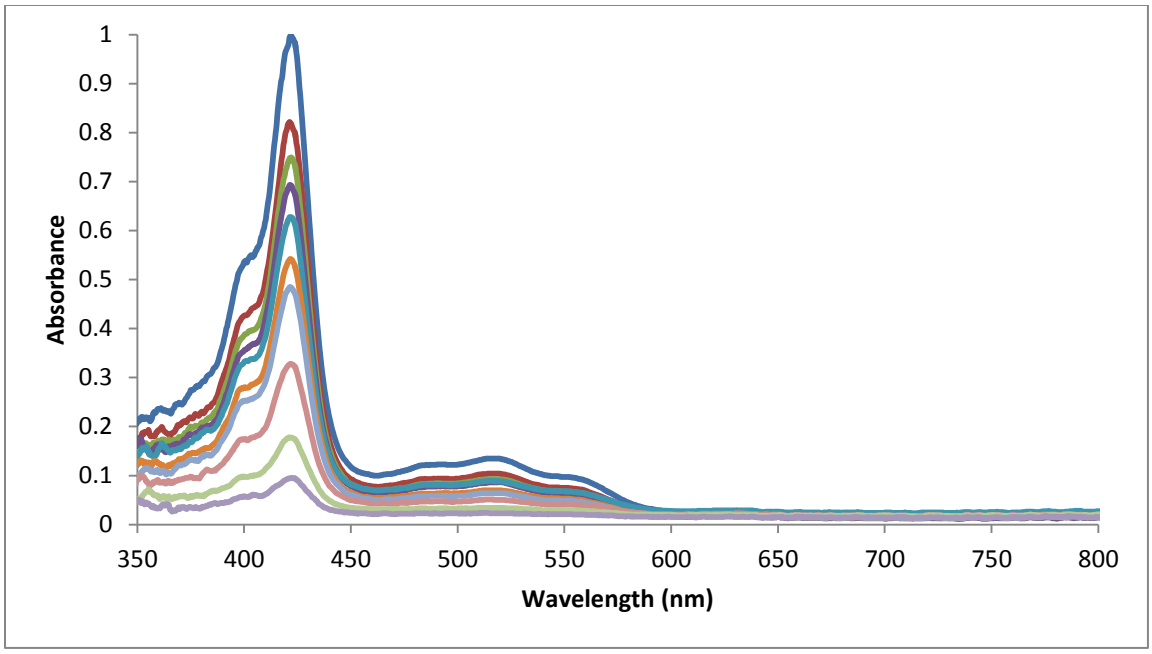

Figure 54: UV-Vis spectral dilution studies for pyrene isopropyl pentacene **104**.

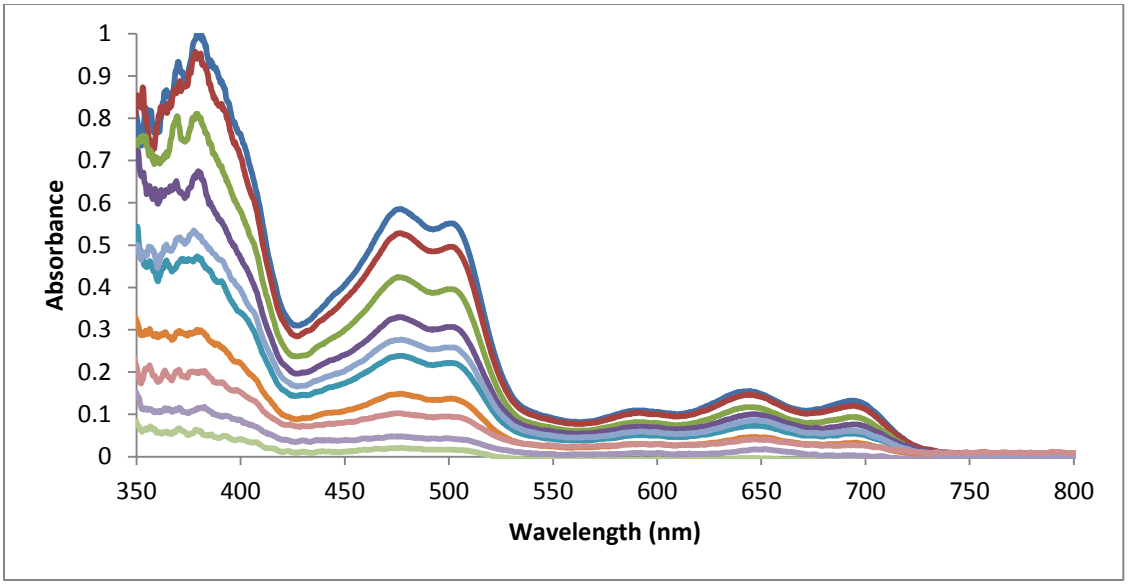

Figure 55: UV-Vis spectral dilution studies for isopropyl anthracene **115** in $CHCl_3$.

Anthracene **115** was studied in $CHCl_3$ using UV-Vis spectroscopy resulting in λ_{max} of 380, 477, 501, 644, and 693 nm. The longest λ_{max} was determined to be 693 nm which was similar to the parent compound **122** (λ_{max} of 690 nm, Figure 55).

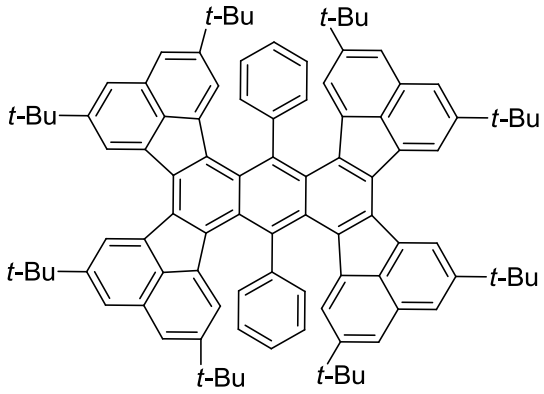

122

Figure 56: Phenylated anthracene **122**.

The extinction coefficient was determined to be 69295 for λ_{max} of 379 nm using dilution studies (from 1.32×10^{-5} to 6.39×10^{-7} M, see Figure 55). In comparison, the extinction coefficient of parent compound **122** was determined to be 82045.

In comparing the spectral properties of the newly synthesized isopropyl compounds in relation to the parent phenylated compounds, a hypsochromic shift of 2 nm was observed

for the pyrene derivatives, while a bathochromic shift of 3 nm was observed for the anthracene compounds (Table 21).

Table 22: Comparison of isopropyl to parent compounds.

Compound	λ_{max} (nm)	Exctinction coefficient
113, isopropyl	551	50772
97	553	Not determined
115, isopropyl	693	69295
122	690	82045

The extinction coefficient for **97** was not collected in the experiment, but a decrease of nearly 13000 was observed by the addition of an isopropyl substituent to **115** in comparison to **122**. A more detailed study comparing a larger series of phenylisopropyl derivatives to the parent phenyl compounds would allow for a closer determination of the effect of the added functionalization.

Variable-Temperature NMR Studies

As previously mentioned, Pascal et al. used the enantiotopic isopropyl groups and the Gutowsky-Holm approximation to estimate the barriers of racemization in his twisted sterically bulky acenes.[126] For a typical Ph-$CH(CH_3)_2$ group, the ^{1}H NMR spectrum would

exhibit a splitting pattern of a doublet for the methyl groups which are split by the methine proton and a septet for the methine proton due to the six protons of the methyl groups. These signals can be decoupled and would thus be observed as two singlets. Since the two isopropyl groups are enantiotopic, they would be split into two pairs of doublets in the event of slow exchange (e.g., slow interconversion between two chiral environments) because they are now diastereotopic. Two doublets would be observed in the decoupled ^{1}H NMR spectrum. For rapid interconversion, the signals would be a doublet for the two the averaged diastereotopic methyl groups. Compounds **113** and **115** were purified as determined by ^{1}H and ^{13}C NMR spectra and submitted to Variable-Temperature ^{1}H NMR experiments. In order to approximate the barrier, it is necessary to observe coalescence (rapid exchange on the NMR timescale) and baseline separation of the signals at the low and high temperatures

At 294 K in $CDCl_3$, the two sets of decoupled doublets are resolved, indicating the fast interconversion between the helical conformations. With an increase in temperature to 328 K, which was the upper limit for this experiment due to the boiling point for chloroform, coalescence of the two signals was not observed. In fact, the two sets of signals were still separated and resolved. Therefore, it was necessary to switch to a deuterated solvent with a higher boiling point but with signals, which do not interfere with isopropyl signals. Thus, 1,1,2,2-tetrachloroethane-d_2 ($C_2Cl_4D_2$; b.p. 418K) was chosen as a suitable next solvent. ^{1}H NMR spectra were collected at temperatures from 293 K – 408 K (Figure 57)

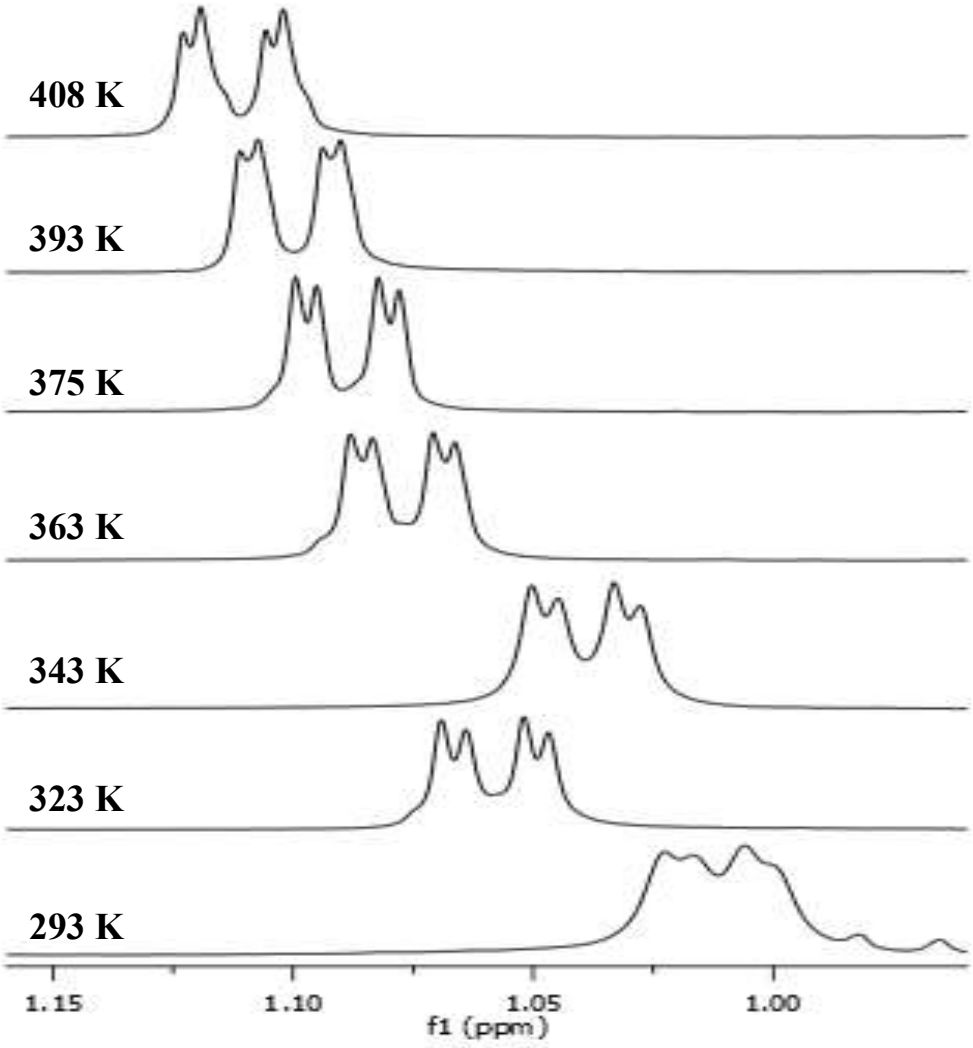

Figure 57: ^{1}H Variable-Temperature NMR spectra of pyrene isopropyl pentacene **113**.

As in the case with $CDCl_3$ as the solvent, no coalescence of the isopropyl signals was observed. There were small shifts for the resonances due to temperature and solvent effects. When the actual coupling for the splitting of the signals was compared over the temperature

range, there was a small decrease (0.8 Hz) starting with 2.4 Hz to 1.6 Hz for 293 K and 408 K, respectively. Unfortunately, since there was no rapid exchange observed, it indicates that higher temperatures are required to determine the barrier for this exchange.

In the case of compound **115**, the same investigation was carried out using Variable-Temperature NMR spectroscopy (Figure 58).

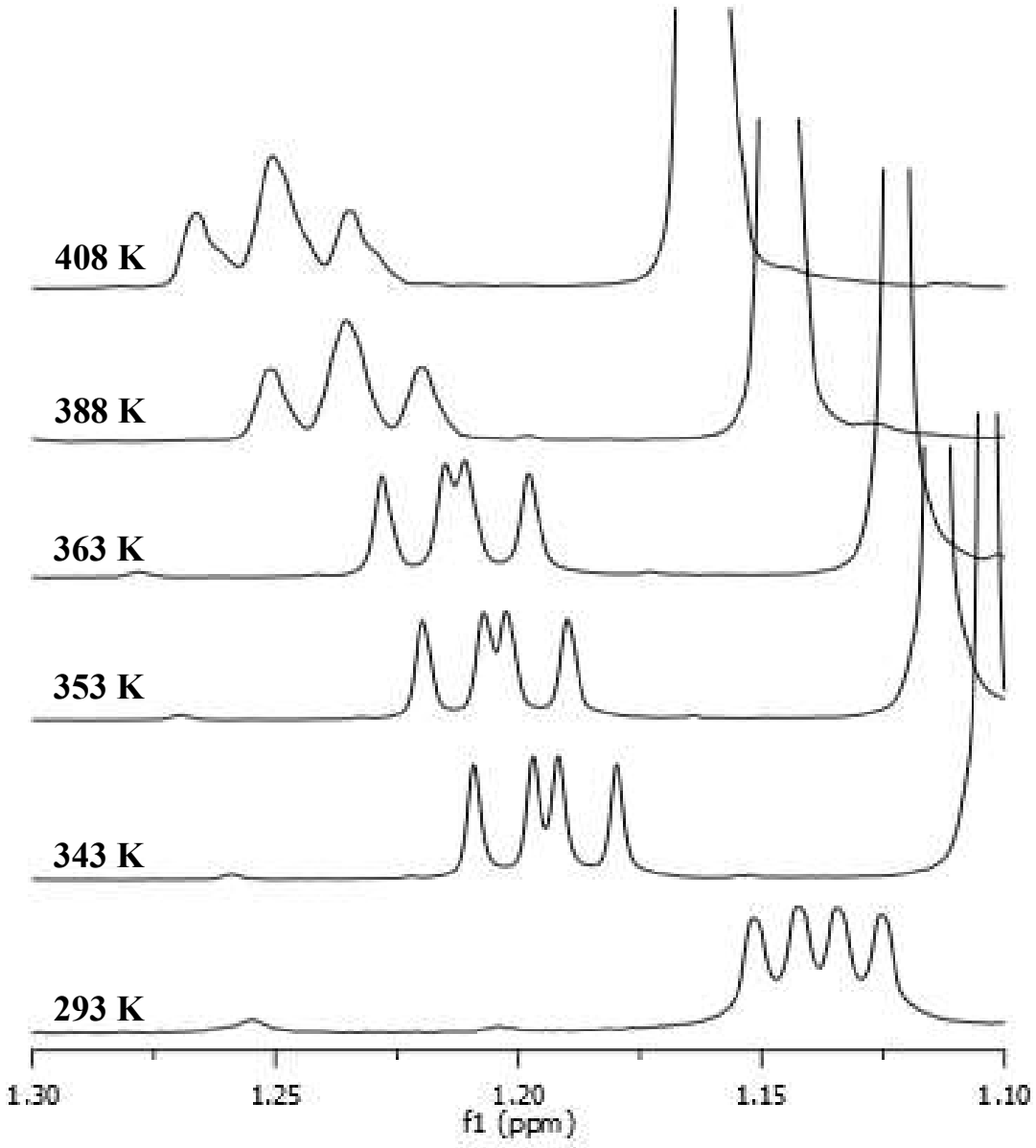

Figure 58: ^{1}H Variable-Temperature NMR spectra of isopropyl anthracene **115**.

As in the case of **113**, the doublets from the diastereotopic methyl groups were clearly resolved at 293 K and still observed at 408 K. Therefore, it was not possible to determine the barrier for interconversion since the coalescence of the two groups was not observed. It was

noted that there was an overlapping of doublets (388-408 K) in the spectrum of **115**. This change is temperature dependent as noted by the merging of the internal "middle" signals with increasing temperatures. There was also a decrease in the coupling constant of 0.8 Hz from 293 K (6.8 Hz) to 408 K (6.0 Hz). At 408 K, the upper limit for the solvent and coalescence was not observed, the barrier of racemization for both **115** and **113** can be estimated to be greater than 24 kcal/mol. Further variable-temperature NMR studies using this approach are not possible in this solvent ($C_2Cl_4D_2$) due to its boiling point, the upper temperature limit of the probe, and insolubility of acenes in higher boiling-point solvents (DMSO-d_6). While this is the case, it may be possible to use other VT NMR experiments including 2D NMR techniques to determine the barriers in these systems.[148]

Extension of the Acene Skeleton

The extension of the acene skeleton has proven to be a difficult task due to factors such as solubility and stability.[118] Additionally, the development of viable synthetic pathways has also been a challenge to this point. However, recently our group was able to develop preliminary schemes which build upon the acene skeleton of **96** and extend it from a pentacene to hexacene **99** (Figure 59).

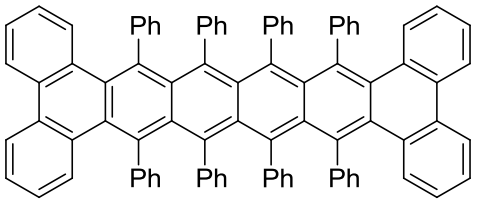

99

Figure 59: Phenanthrene endcapped hexacene **99**.

In a followup to that approach, the pyrene endcapped derivative was attempted. As in the synthesis of **97**, cyclone **117** was obtained from the oxidation and subsequent aldol condensation of pyrene. As a means of extending the skeleton, an intermediate was required which would allow for extension of the benzene bridge while retaining the dienophile required to complete subsequent Diels-Alder reactions to add the corresponding end cap. Naphthazarin (**125**) was identified and synthesized from the procedure by Toribara (Figure 60).[149, 150]

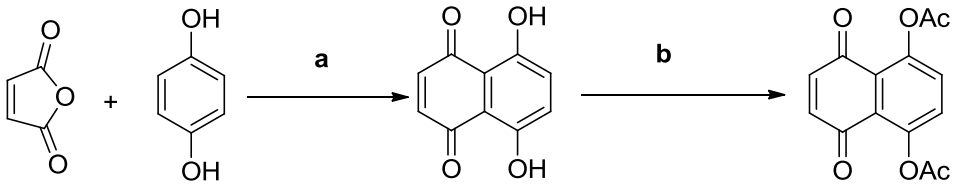

123 **124** **125** **126**

Figure 60: Synthesis of naphthazarin intermediate. Conditions: a) NaCl, $AlCl_3$, HCl, 17.2%; b) acetic anhydride, pyridine, 56.6%.

Naphthazarin (**125**) was then converted to acetate **126** using acetic anhydride and pyridine. The yellow acetate intermediate had the ability to undergo a Diels-Alder reaction while retaining the potential for further reactions to the adjacent end of the compound while extending the backbone. From there, the acetate was heated to 180 ºC for 24 h with cyclone **117** to give quinone **127 (**Figure 61).

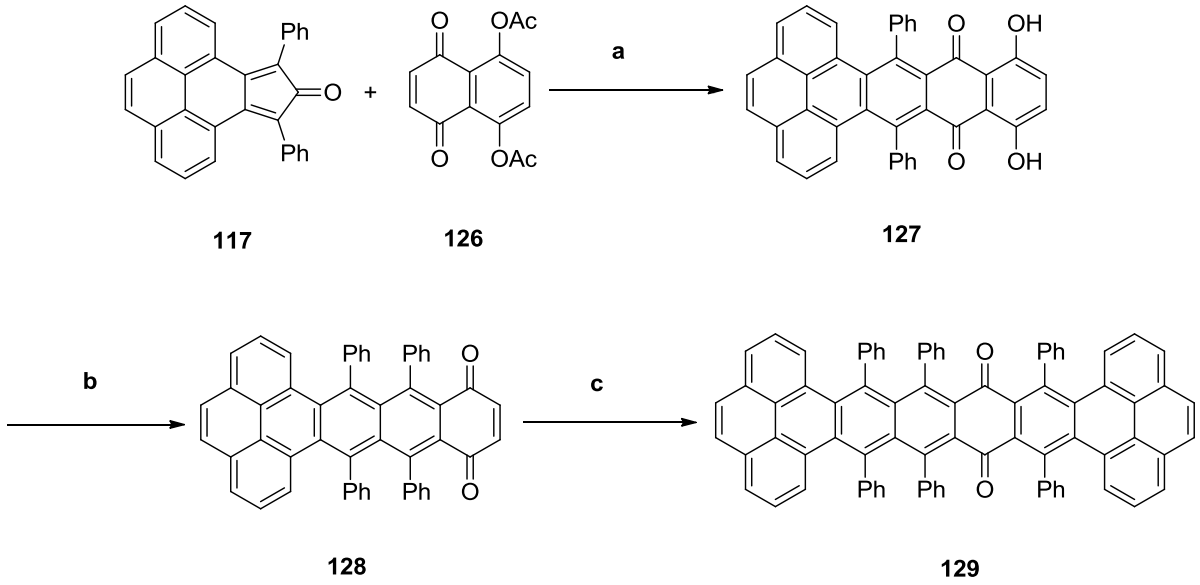

Figure 61: Schematic for the synthesis of pyrene hexacene quinone **129**. Conditions: a) nitrobenzene, 39.5%; b) PhLi, THF, nitrobenzene, 30.6%; c) cyclone **117**, nitrobenzene, 36.0%.

Reduction of quinone **127** using phenyllithium followed by refluxing in nitrobenzene produced the red quinone **128**. A final Diels-Alder reaction with incremental additions of cyclone **117**, followed by heating to 180 ºC in nitrobenzene for 65 h, produced the pyrene

terminal hexacene quinone **129** as a brown solid (36.0% yield). Reduction of quinone **129** was then accomplished by the addition of phenyllithium at rt. (Figure 62).

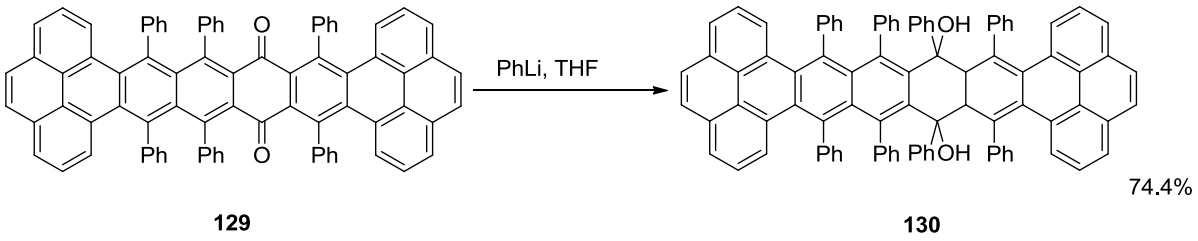

129 **130**

Figure 62: Schematic of preliminary steps for the formation of pyrene hexacene diol **130**.

Acid workup of the reaction gave diol **130** as a brown solid (74.7% crude yield). Quinone **129** and diol **130** were characterized using X-ray crystallographic analysis (Figures 63 and 64, respectively and Table 22).

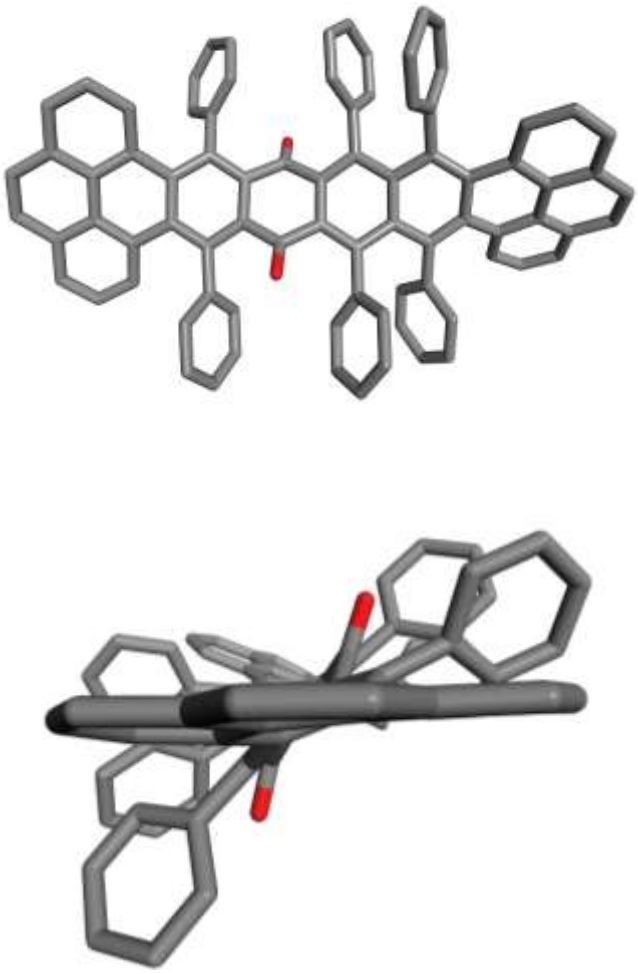

Figure 63: Crystal structure of pyrene hexacene quinone **129**.

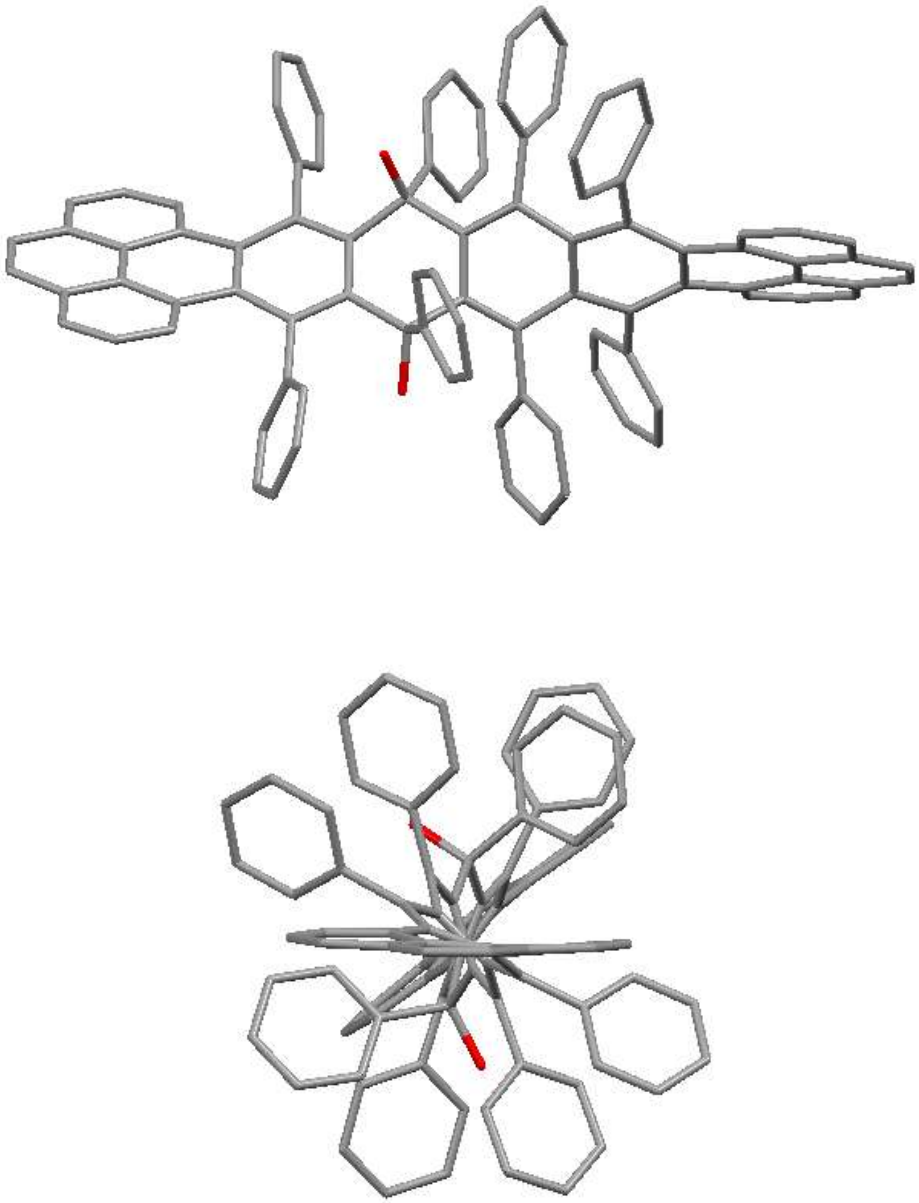

Figure 64: Crystal structures of pyrene hexacene diol **130**.

Table 23: Crystal data for compounds **129** and **130.**

Compound	$C_{82}H_{46}$, C_6H_5Br	$C_{94}H_{58}O_2$, $CHCl_3$
Chemical Formula	$C_{88}H_{51}BrO_2$	$C_{95}H_{59}Cl_3O_2$
Formula weight	1220.19	1338.77
Crystal system	Triclinic	Monoclinic
Space group	*P* -1	$P2_{1/n}$
a, Å	11.1846(5)	12.7289(7)
b, Å	13.1615(5)	26.4201(15)
c, Å	22.2777(9)	20.5383(11)
α, deg.	91.511(1)	90.00
β, deg	104.029(1)	102.9300(10)
γ, deg	111.100(1)	90.00
V, Å^3	2944.8(2)	6731.9(6)
Z	2	4
ρ (calcd.), g cm^{-3}	1.376	1.321
crystal size	0.21 x 0.15 x 0.02	0.26 x 0.14 x 0.05
μ, mm^{-1}	0.754	0.192
T, K	99(2)	100(2)
F(000)	1260.0	2784.0
θ_{max}, deg	30.660	28.700
Reflections		
Total	18126	149839
Unique	3915	17392
observed [I > 2s(l)]	2404	8461
R_{int}	0.1188	0.2019
Parameters	820	938
$R(F)$ (obs data)[a]	0.0651	0.0780
$wR(F^2)$ (obs data)[a]	0.1132	0.1800
R(F) (all data)[a]	0.1439	0.1928
wR(F^2) (all data)[a]	0.1375	0.1461
S (all data)[a]	0.982	1.116

[a] $R(F) = \Sigma||F_o| - |F_c||/\Sigma|F_o|$; $wR(F^2) = [\Sigma w(F_o^2 - F_c^2)^2/\Sigma w(F_o^2)^2]^{1/2}$; *S* = goodness of fit on F^2 = $[\Sigma w(F_o^2 - F_c^2)^2/(n-p)]^{1/2}$, where *n* is the number of reflections and *p* is the number of parameters refined.

Table 24: Atomic coordinates and equivalent isotropic displacement parameters for **129**.

Atom	*x*	*y*	*Z*	U_{eq}
O1	0.20239(16)	0.99603(14)	0.17113(8)	0.0154(4)
O2	0.68337(16)	1.00181(14)	0.25160(8)	0.0159(4)
C1	0.6859(2)	1.0838(2)	0.00574(11)	0.0132(5)
C2	0.7441(2)	1.1078(2)	-0.04323(11)	0.0153(5)
C3	0.7722(2)	1.2090(2)	-0.06422(12)	0.0174(5)
C4	0.7671(3)	1.3965(2)	-0.05781(14)	0.0244(6)
C5	0.7378(3)	1.4733(2)	-0.03055(14)	0.0257(7)
C6	0.6409(3)	1.5294(2)	0.04736(14)	0.0232(6)
C7	0.5746(3)	1.5040(2)	0.09288(13)	0.0232(6)
C8	0.5301(3)	1.3978(2)	0.10805(13)	0.0189(6)
C9	0.4178(2)	1.16153(19)	0.12955(11)	0.0119(5)
C10	0.3192(2)	1.01784(19)	0.19726(11)	0.0127(5)
C11	0.2925(2)	0.95778(19)	0.30129(11)	0.0118(5)
C12	0.2769(2)	0.88607(19)	0.40495(11)	0.0123(5)
C13	0.2829(3)	0.8890(2)	0.54427(12)	0.0199(6)
C14	0.2790(3)	0.8843(2)	0.60626(12)	0.0230(6)
C15	0.2522(3)	0.7873(2)	0.63077(13)	0.0231(6)
C16	0.1900(3)	0.5871(2)	0.61786(13)	0.0253(6)
C17	0.1517(3)	0.4918(2)	0.58081(13)	0.0260(7)
C18	0.1131(3)	0.3931(2)	0.47767(14)	0.0228(6)
C19	0.1206(3)	0.3952(2)	0.41704(13)	0.0221(6)
C20	0.1760(3)	0.4944(2)	0.39449(13)	0.0191(6)
C21	0.3482(2)	0.7155(2)	0.36403(11)	0.0135(5)
C22	0.4717(2)	0.84844(19)	0.29880(11)	0.0118(5)
C23	0.5672(2)	0.98685(19)	0.22834(11)	0.0118(5)
C24	0.6042(2)	1.06160(19)	0.12888(11)	0.0112(5)
C25	0.7385(2)	1.2891(2)	-0.03764(12)	0.0167(5)
C26	0.6705(3)	1.4499(2)	0.01782(13)	0.0197(6)
C27	0.5554(2)	1.3150(2)	0.07948(12)	0.0144(5)
C28	0.5197(2)	1.20478(19)	0.09854(11)	0.0124(5)
C29	0.4258(2)	1.07970(19)	0.16735(11)	0.0125(5)
C30	0.3585(2)	0.96980(19)	0.25523(11)	0.0116(5)
C31	0.3150(2)	0.88768(19)	0.34771(11)	0.0123(5)
C32	0.2697(2)	0.7977(2)	0.43927(11)	0.0141(5)
C33	0.2585(2)	0.7952(2)	0.50438(12)	0.0145(5)
C34	0.2273(3)	0.6910(2)	0.59367(13)	0.0217(6)
C35	0.1552(3)	0.4911(2)	0.51673(13)	0.0210(6)

Table continued

Table 24 Continued

Atom	*x*	*y*	*Z*	U_{eq}
C37	0.2035(3)	0.5936(2)	0.49291(12)	0.0166(5)
C38	0.2213(2)	0.5946(2)	0.43198(12)	0.0162(5)
C39	0.2806(2)	0.7024(2)	0.41025(11)	0.0138(5)
C40	0.3792(2)	0.81609(19)	0.33659(11)	0.0123(5)
C41	0.4623(2)	0.9288(2)	0.26006(11)	0.0124(5)
C42	0.5315(2)	1.04228(19)	0.17304(11)	0.0125(5)
C43	0.5931(2)	1.14045(19)	0.08804(11)	0.0114(5)
C44	0.6539(2)	1.16171(19)	0.03543(11)	0.0116(5)
C45	0.6750(2)	1.2639(2)	0.01144(12)	0.0148(5)
C46	0.6331(2)	1.3433(2)	0.03594(12)	0.0147(5)
C47	0.3006(2)	1.19470(19)	0.11586(12)	0.0140(5)
C48	0.2290(3)	1.1835(2)	0.05361(12)	0.0170(5)
C49	0.1163(3)	1.2092(2)	0.03777(13)	0.0211(6)
C50	0.0750(3)	1.2489(2)	0.08411(14)	0.0217(6)
C51	0.1454(3)	1.2609(2)	0.14600(13)	0.0203(6)
C52	0.2570(2)	1.2337(2)	0.16158(13)	0.0176(5)
C53	0.1967(2)	1.0138(2)	0.29948(11)	0.0132(5)
C54	0.0611(2)	0.9528(2)	0.28882(12)	0.0159(5)
C55	-0.0276(3)	1.0050(2)	0.28645(12)	0.0191(6)
C56	0.0178(3)	1.1179(2)	0.29435(12)	0.0202(6)
C57	0.1526(3)	1.1797(2)	0.30457(12)	0.0199(6)
C58	0.2414(3)	1.1278(2)	0.30698(12)	0.0162(5)
C59	0.2678(2)	0.9896(2)	0.42866(11)	0.0130(5)
C60	0.1494(3)	0.9967(2)	0.43481(12)	0.0188(6)
C61	0.1494(3)	1.0968(2)	0.45661(12)	0.0237(6)
C62	0.2661(3)	1.1891(2)	0.47319(12)	0.0239(6)
C63	0.3836(3)	1.1830(2)	0.46755(12)	0.0218(6)
C64	0.3834(3)	1.0837(2)	0.44464(12)	0.0175(5)
C65	0.3827(3)	0.6259(2)	0.34012(12)	0.0178(5)
C66	0.4635(3)	0.5820(2)	0.37992(15)	0.0246(6)
C67	0.4954(3)	0.4988(2)	0.35762(18)	0.0362(8)
C68	0.4447(3)	0.4571(2)	0.29501(18)	0.0395(9)
C69	0.3641(3)	0.4987(2)	0.25480(16)	0.0350(8)
C70	0.3341(3)	0.5834(2)	0.27727(13)	0.0230(6)
C71	0.5815(2)	0.8078(2)	0.30563(12)	0.0143(5)
C72	0.6687(2)	0.8216(2)	0.36431(12)	0.0180(6)

Table continued

Table 24 continued

Atom	*x*	*y*	*Z*	U_{eq}
C74	0.7918(3)	0.7364(2)	0.32192(14)	0.0237(6)
C75	0.7063(3)	0.7225(2)	0.26306(14)	0.0237(6)
C76	0.6016(3)	0.7579(2)	0.25496(13)	0.0178(5)
C77	0.6872(2)	0.99597(19)	0.12579(11)	0.0118(5)
C78	0.6238(3)	0.8826(2)	0.11100(12)	0.0184(6)
C79	0.6968(3)	0.8190(2)	0.10574(13)	0.0266(7)
C80	0.8337(3)	0.8679(3)	0.11573(13)	0.0274(7)
C81	0.8975(3)	0.9802(2)	0.13062(12)	0.0219(6)
C82	0.8243(2)	1.0442(2)	0.13580(11)	0.0159(5)
C83	0.9350(3)	0.4755(2)	0.20770(13)	0.0199(6)
C84	0.9313(3)	0.5071(2)	0.14869(13)	0.0255(6)
C85	0.9785(3)	0.6180(2)	0.14269(14)	0.0294(7)
C86	1.0310(3)	0.6964(2)	0.19474(13)	0.0226(6)
C87	1.0337(3)	0.6627(2)	0.25291(13)	0.0218(6)
C88	0.9847(3)	0.5525(2)	0.26004(13)	0.0201(6)

Table 25: Atomic coordinates and equivalent isotropic displacement parameters for **130**.

Atom	*x*	*y*	*Z*	U_{eq}
O1	0.3574(2)	0.70525(8)	0.4379(11)	0.0249(5)
O2	0.1940(2)	0.66293(8)	0.64126(10)	0.0211(5)
C1	0.0125(3)	0.96397(12)	0.5928(2)	0.0283(8)
C2	-0.0185(3)	1.01227(13)	0.6075(2)	0.0355(9)
C3	-0.1155(3)	1.03165(14)	0.5719(2)	0.0408(10)
C3A	-0.1792(3)	1.00485(13)	0.5196(2)	0.0365(9)
C4	-0.2792(3)	1.0246(2)	0.4810(2)	0.0516(12)
C5	-0.3383(3)	0.9992(2)	0.4290(2)	0.0509(12)
C5A	-0.3028(3)	0.5173(14)	0.4078(2)	0.0332(8)
C6	-0.3620(3)	0.92622(14)	0.3518(2)	0.0368(9)
C7	-0.3255(3)	0.88102(14)	0.3323(2)	0.0314(8)
C8	-0.2279(3)	0.86098(13)	0.3667(2)	0.0270(8)
C8A	-0.1633(2)	0.88556(12)	0.4213(2)	0.0217(7)
C8B	-0.0595(2)	0.86506(11)	0.4589(2)	0.0198(7)
C9	0.0023(2)	0.82913(11)	0.4342(2)	0.0195(6)
C9A	0.0884(2)	0.80445(11)	0.47886(15)	0.0176(6)
C10	0.1772(2)	0.77832(11)	0.45955(15)	0.0180(6)
C10A	0.2374(2)	0.74486(11)	0.50333(15)	0.0166(6)
C11	0.3524(2)	0.72831(11)	0.50022(15)	0.0189(6)
C11A	0.3945(2)	0.68408(11)	0.54805(15)	0.0170(6)
C12	0.5028(2)	0.66905(11)	0.56033(14)	0.0175(6)
C12A	0.5325(2)	0.61914(11)	0.58304(15)	0.0184(6)
C12B	0.6459(2)	0.60172(12)	0.6038(2)	0.0200(7)
C13	0.7332(2)	0.63412(12)	0.6242(2)	0.0229(7)
C14	0.8385(3)	0.61669(13)	0.6433(2)	0.0288(8)
C15	0.8611(3)	0.56635(13)	0.6405(2)	0.0307(8)
C15A	0.7771(3)	0.53143(13)	0.6223(2)	0.0285(8)
C16	0.7984(3)	0.47870(14)	0.6189(2)	0.0369(9)
C17	0.7175(3)	0.44464(13)	0.6051(2)	0.0331(8)
C17A	0.6077(3)	0.46019(12)	0.5934(2)	0.0246(7)
C18	0.5251(3)	0.42464(12)	0.5789(2)	0.0248(7)
C19	0.4195(3)	0.44080(12)	0.5631(2)	0.0254(7)
C20	0.3946(3)	0.49170(12)	0.5649(2)	0.0226(7)
C20A	0.4739(2)	0.52891(11)	0.58372(15)	0.0192(7)
C20B	0.4497(2)	0.58352(11)	0.58489(14)	0.0172(6)
C20D	0.6687(2)	0.54868(12)	0.6073(2)	0.0210(7)
C20C	0.5384(2)	0.51256(12)	0.59492(15)	0.0204(7)
C21	0.3450(2)	0.60209(11)	0.58625(14)	0.0166(6)

Table continued

Table 25 continued

Atom	*x*	*y*	*Z*	U_{eq}
C22	0.2097(2)	0.67413(11)	0.57638(15)	0.0176(6)
C22A	0.1997(2)	0.73062(11)	0.56184(15)	0.0169(6)
C23	0.1372(2)	0.76402(11)	0.58830(15)	0.0168(6)
C23A	0.0928(2)	0.80754(11)	0.54793(15)	0.0171(6)
C24	0.0491(2)	0.85137(11)	0.5721(2)	0.0188(6)
C24A	-0.0193(2)	0.88293(11)	0.5263(2)	0.0210(7)
C24B	-0.0509(3)	0.93435(12)	0.5429(2)	0.0252(7)
C24C	-0.1444(3)	0.95639(13)	0.5025(2)	0.0295(8)
C24D	-0.2040(3)	0.93065(12)	0.4443(2)	0.0263(7)
C25	-0.0196(2)	0.81224(12)	0.3629(2)	0.0202(7)
C26	-0.0424(2)	0.76153(12)	0.3486(2)	0.0253(7)
C27	-0.0580(3)	0.74381(13)	0.2836(2)	0.0295(8)
C28	-0.0502(3)	0.77671(14)	0.2321(2)	0.0324(8)
C29	-0.0286(3)	0.82732(14)	0.2459(2)	0.0300(8)
C30	-0.0133(2)	0.84514(13)	0.3107(2)	0.0256(7)
C31	0.2110(2)	0.79875(12)	0.3995(2)	0.0236(7)
C32	0.2059(3)	0.7714(2)	0.3410(2)	0.0340(9)
C33	0.2392(3)	0.7939(2)	0.2882(2)	0.0506(12)
C34	0.2784(3)	0.8429(2)	0.2934(2)	0.0605(15)
C35	0.2839(3)	0.8696(2)	0.3508(2)	0.0488(11)
C36	0.2499(3)	0.84778(14)	0.4036(2)	0.0326(8)
C37	0.4159(2)	0.77850(12)	0.5110(2)	0.0236(7)
C38	0.4712(3)	0.79672(14)	0.4645(2)	0.0329(8)
C39	0.5206(3)	0.8439(2)	0.4731(2)	0.0470(11)
C40	0.5152(3)	0.8733(2)	0.5277(3)	0.0539(13)
C41	0.4602(3)	0.85575(14)	0.5739(2)	0.0438(10)
C42	0.4114(3)	0.80885(12)	0.5659(2)	0.0296(8)
C43	0.5863(2)	0.70419(12)	0.5438(2)	0.0214(7)
C44	0.6265(2)	0.69626(12)	0.4870(2)	0.0258(7)
C45	0.7068(3)	0.72779(14)	0.4732(2)	0.0324(8)
C46	0.7455(3)	0.76739(14)	0.5149(2)	0.0385(10)
C47	0.7060(3)	0.77592(13)	0.5716(2)	0.0331(9)
C48	0.6273(2)	0.74414(12)	0.5858(2)	0.0251(7)
C49	0.2699(2)	0.56799(11)	0.6132(2)	0.0201(7)
C50	0.2993)3)	0.55424(12)	0.6805(2)	0.0248(7)
C51	0.2349(3)	0.52197(13)	0.7080(2)	0.0325(8)

Table continued

Table 25 continued

Atom	*x*	*y*	*Z*	U_{eq}
C52	0.1416(3)	0.50243(13)	0.6685(2)	0.0355(9)
C53	0.1121(3)	0.51499(12)	0.6020(2)	0.0316(8)
C54	0.1748(3)	0.54782(12)	0.5741(2)	0.0251(7)
C55	0.1134(2)	0.65301(11)	0.5242(2)	0.0207(7)
C56	0.0154(3)	0.64399(12)	0.5410(2)	0.0260(7)
C57	-0.0729(3)	0.62755(13)	0.4924(2)	0.0331(8)
C58	-0.0643(3)	0.62059(13)	0.4275(2)	0.0335(8)
C59	0.0324(3)	0.63001(12)	0.4103(2)	0.0279(8)
C60	0.1207(3)	0.64643(12)	0.4582(2)	0.0234(7)
C61	0.0950(2)	0.75454(11)	0.64940(15)	0.0177(6)
C62	0.1604(3)	0.75531(12)	0.7134(2)	0.0246(7)
C63	0.1174(3)	0.74936(13)	0.7690(2)	0.0316(8)
C64	0.0080(3)	0.74206(14)	0.7614(2)	0.0353(9)
C65	-0.0580(3)	0.74097(13)	0.6984(2)	0.0308(8)
C66	-0.0151(2)	0.74734(12)	0.6428(2)	0.0226(7)
C67	0.0854(3)	0.86407(11)	0.6445(2)	0.0218(7)
C68	0.1948(3)	0.87216(12)	0.6712(2)	0.0266(7)
C69	0.2300(3)	0.88695(13)	0.7373(2)	0.0343(9)
C70	0.1573(3)	0.89293(15)	0.7770(2)	0.0405(10)
C71	0.0484(3)	0.88409(14)	0.7516(2)	0.0356(9)
C72	0.0127(3)	0.86968(12)	0.6857(2)	0.0262(7)

Extension of the acene skeleton was completed to produce pyrene hexacene diol **130** in an overall yield of 0.7%. Aromatization of diol **130** should be accomplished through the use of $SnCl_2$, THF, and HCl, but at this point has not been completed.

Conclusion

We have utilized a synthetic pathway, which allows for the introduction of isopropyl substituents to the acene backbone. This addition of a diastereotopic handle could be used in

the determination of the barrier to enantiomerization. The reduction of acene quinones was achieved through in situ formation of an isopropylphenyl lithium adduct. The addition of the isopropyl handle resulted in a 12º decrease in overall twist of the compound in comparison to the parent compound (138º to 126º). The synthesis of the isopropyl containing crowded acenes using organolithium reagents opens the possibility of the addition of alternative substituents.

Preliminary barrier to enantiomerization studies were attempted using Variable Temperature ^{1}H NMR spectroscopy at temperatures up to 408 K. However, even at maximum temperatures, coalescence of the isopropyl peaks was not observed, and a minimum peak separation of 1.6 and 6.0 Hz was obtained for compounds **113** and **115**, respectively. Future investigations utilizing more specialized NMR spectroscopic techniques (e.g., 2D NMR experiments) may allow for the determination of the barrier to enantiomerization, but the current data suggests the barriers for these systems are higher than 24 kcal/mol.

Additional synthetic pathways were examined for the synthesis of additional endcaps (corannulene), central units (pyrene), and backbone extension (pyrene hexacene). The corannulene capped acene and pyrene central unit targets were not successful at this time using currently known procedures. While both targets remain of high interest, additional reaction conditions must be developed to pursue the targets. Alternatively, pyrene hexacene diol **130** was synthesized in eight steps with a 0.7% overall yield. Future attempts at aromatization may be possible using $SnCl_2$. Additionally, the development of the phenylisopropyl derivative should be accessible utilizing this synthesis.

Experimental Section

General procedures. Proton NMR spectra were recorded on a Varian AC MHz spectrometer operating at 400 MHz. Carbon NMR spectra were recorded on a Varian AC 400 spectrometer operating at 100 MHz. Unless otherwise stated, all commercial chemicals and solvents were used as supplied.

Dibenzo[*ghi,mno*]fluoranthene-1,2-dione (108). Compound **108** was synthesized from a procedure adapted from Preda.[146] An aliquot of 4M H_2SO_4 (11 mL) was added to a solution of corannulene (313 mg, 1.25 mmol) and acetonitrile (60 mL) in a 250-mL three-neck round bottom flask under argon. Ammonium cerium sulfate (4.19 g, 6.62 mmol) was dissolved in 4M H_2SO_4 (52 mL), and added to the corannulene solution, and heated to 70 ºC for 20 h. The orange solution was poured into water (300 mL), extracted using CH_2Cl_2 (2 x 250 mL), dried over Na_2SO_4, and concentrated to an orange solid that was collected via vacuum filtration. The solid was subjected to column chromatography (silica gel; solvent: hexanes, followed by 50% CH_2Cl_2–hexanes, CH_2Cl_2), and an orange band was collected (R_f 0.37 TLC, silica gel; solvent: CH_2Cl_2). The solvents were removed under reduced pressure to give **108** as a yellow-orange solid (197 mg, 0.703 mmol, 35.0%): mp 316-320 ºC; ^{1}H NMR (400 MHz, $CDCl_3$) δ 7.71–7.75 (t, J = 6.0 Hz, 3H), 7.78 (d, J = 2.8 Hz, 2H), 7.80–7.84 (t, J = 8.8 Hz, 3H) ppm; ^{13}C NMR (100 MHz, $CDCl_3$) δ 124.5, 127.4, 128.1, 128.9, 130.1, 130.7, 134.5, 134.8, 139.9, 142.1, 179.4 ppm. HRMS calcd for $C_{20}H_8O_2$ 280.05, found 280.0524.

Pyrene-4,5-dione (107). Compound **107** was synthesized from an adapted procedure by Hu et al.[141] Pyrene (4.12 g, 20.4 mmol), CH_2Cl_2 (100 mL), and CH_3CN (100 mL) were combined in a 500-mL screw-capped Erlenmeyer flask and stirred until pyrene was completely dissolved. $NaIO_4$ (20.2 g, 94.7 mmol), H_2O (100 mL), and $RuCl_3 \cdot H_2O$ (0.40 g,

1.95 mmol) were added sequentially to the pyrene solution and stirred at rt for 21 h. Water (600 mL) was added, and the aqueous suspension was extracted using CH_2Cl_2 (4 x 200 mL). The organic phases were combined, washed with H_2O (2 x 200 mL), dried over Na_2SO_4, and filtered. The solvent was removed under reduced pressure. The precipitate was collected via vacuum filtration and rinsed with methanol. The orange solid was subjected to column chromatography (silica gel; solvent: CH_2Cl_2), and an orange band was collected (R_f 0.40 TLC, silica gel; solvent: CH_2Cl_2). The solvent was removed under reduced pressure to give **107** as an orange solid, which was used in the next step without any further purification (1.70 g, 7.32 mmol, 36.0%). An analytical sample was obtained by recrystallizing a small amount of **107** from $CHCl_3$–MeOH: mp 299–302 ºC; ^{1}H NMR (400 MHz, $CDCl_3$) δ 7.74–7.78 (d, J = 8.0 Hz, 2H), 7.86 (s, 2H), 8.17–8.20 (dd, J = 12.0, 8.0 Hz, 2H), 8.49–8.51 (dd, J = 12.0, 8.0 Hz, 2H) ppm; ^{13}C NMR (100 MHz, $CDCl_3$) δ 127.2, 128.0, 128.3, 130.0, 130.1, 131.9, 135.7, 180.3 ppm.

2,7-di-*tert*-butylpyrene (110). Compound **110** was synthesized according to adapted procedures by Suzuki and Yamato.[151, 152] $AlCl_3$ (17.2 g, 129 mmol) was added to a solution of pyrene (16.3 g, 80.8 mmol) in *t*-butylchloride (400 mL) at 0 ºC. The red solution was then allowed to warm to rt while stirring for 3 h. Water (300 mL) was added, and the suspension was extracted using CH_2Cl_2 (2 x 250 mL). The organic phases were combined, washed with H_2O (2 x 150 mL), dried with Na_2SO_4, and filtered. The solvent was removed under reduced pressure. The precipitate was collected via vacuum filtration and rinsed with methanol to give **110** as a white solid (20.1 g, 63.9 mmol, 79.3%), which was used without any further purification. mp 208-210 ºC (lit[152] 209-211 ºC); ^{1}H NMR (400 MHz, $CDCl_3$) δ 1.58 (s, 18H), 8.04 (s, 4H), 8.18 (s, 4H) ppm.

2,7-di-tert-butylpyrene-4,5,9,10-tetraone (111). Compound **111** was synthesized from an adapted procedure by Hu et al.[141] *t*-Butylpyrene (3.20 g, 10.2 mmol), CH_2Cl_2 (40 mL), and CH_3CN (40 mL) were combined in a 500-mL screw-capped Erlenmeyer flask and stirred until the *t*-butylpyrene was completely dissolved. $NaIO_4$ (17.6 g, 82.3 mmol), H_2O (50 mL), and $RuCl_3 \cdot H_2O$ (0.25 g, 1.22 mmol) were added sequentially to the pyrene solution and stirred at 40 ºC for 21 h. Water (200 mL) was added, and the aqueous suspension was extracted using CH_2Cl_2 (3 x 250 mL). The organic phases were combined and washed with H_2O (2 x 200 mL), dried over Na_2SO_4, and filtered. The solvent was removed under reduced pressure. The precipitate was collected via vacuum filtration and rinsed with methanol to give **111** as an orange-red solid which was used in the next step without any further purification (641 mg, 1.71 mmol, 16.8%). mp >400 ºC (lit[141] >350 ºC);^{1}H NMR (400 MHz, $CDCl_3$) δ 1.56 (s, 18H), 8.48 (s, 4H) ppm.

9,11-diphenyl-10H-cyclopenta[*e*]pyren-10-one (117). Compound **117** was synthesized according to an adapted procedure by Pascal et al.[126] Quinone **107** (3.85 g, 16.6 mmol), 1,3-diphenylacetone (3.63 g, 17.3 mmol), and ethanol (400 mL) were combined in a 500-mL beaker and stirred. NaOH (1.10 g, 27.5 mmol) was dissolved in H_2O (5 mL), added dropwise to the suspension, and stirred at rt for 15 min. The solution was then heated to a gentle reflux, at which point the beaker was immediately placed into an ice bath. The precipitate was collected via vacuum filtration and rinsed with ethanol. Recrystallization from $CHCl_3$–MeOH gave **117** as a brown solid, which was used in the next step without any further purification (3.96 g, 9.74 mmol, 58.8%). mp >400 ºC; ^{1}H NMR ($CDCl_3$, 400 MHz) δ 7.23–7.27 (t, J = 8.0 Hz, 2H), 7.39–7.50 (m, 10 H), 7.66 (s, 2 H), 7.24–7.75 (dd, J = 8.0, 1.2 Hz, 2H), 7.86–7.88 (dd, J = 7.6, 1.2 Hz, 2H) ppm; ^{13}C NMR ($CDCl_3$, 100.5 MHz) δ 123.6,

126.9, 127.0, 127.1, 127.3, 127.7, 128.1, 128.7, 130.0, 131.2, 132.3, 132.6, 147.9, 200.4 ppm.

9,14-Diphenyldibenzo[*de*,*qr*]tetracene-10,13-dione (118). Pyrenecyclone **117** (280 mg, 0.688 mmol), *p*-benzoquinone (612 mg, 5.66 mmol), and nitrobenzene (5 mL) were heated to reflux for 1 h in a screw-capped vial. Methanol (40 mL) was added to the reaction contents and the precipitate was collected via vacuum filtration. The red-orange solid was subjected to column chromatography (silica gel; solvent: toluene, followed by 20% CH_2Cl_2–toluene). A red band was collected (R_f 0.50 TLC, silica gel; solvent: 10% ethyl acetate–toluene). The solvent was removed under reduced pressure to give **118** as a red solid, which was used in the next step without any further purification (193 mg, 0.398 mmol, 58.0%). An analytical sample was obtained by recrystallizing a small amount of **118** from $CHCl_3$–MeOH: mp >400 ºC; ^{1}H NMR (400 MHz, $CDCl_3$) δ 6.86 (s, 2H), 7.29–7.31 (m, 4H), 7.38–7.50 (m, 8H), 7.74–7.76 (dd, J = 8.0, 0.8 Hz, 2H), 7.94 (s, 2H), 7.97–7.99 (dd, J = 7.6, 0.8 Hz, 2H) ppm; ^{13}C NMR (100 MHz, $CDCl_3$) δ 124.6, 126.0, 126.9, 127.0, 127.7, 128.6, 129.1, 130.5, 130.6, 130.7, 137.0, 139.0, 140.6, 141.6, 187.1 ppm.

9,11,20,22-tetraphenyltetrabenzo[c₁d₁,de,no,st]heptacene-10,21-dione (114). Quinone **118** (660 mg, 1.36 mmol), pyrenecyclone **117** (612 mg, 1.51 mmol), and nitrobenzene (6 mL) were heated to reflux for 24 h in a screw-capped vial. Acetone (40 mL) was added to the reaction contents. The precipitate was collected via vacuum filtration and rinsed with CH_2Cl_2 to give **114** as a greenish solid, which was used in the next step without any further purification (686 mg, 0.797 mmol, 58.5%): mp >400 ºC. HRMS calcd for $C_{66}H_{36}O_2$ 860.27, found 860.2709.

10,21-bis(4-isopropylphenyl)-9,11,20,22-tetraphenyl-10,21-dihydrotetrabenzo[c₁d₁,de,no,st]heptacene-10,21-diol (119). *n*-Butyllithium (2.5 M in hexanes, 0.5 mL, 1.3 mmol) was added to a solution of 1-bromo-4-isopropylbenzene (0.2 mL, 0.8 mmol) and THF (5 mL) at -78 ºC, and the reaction was stirred for 40 min. The isopropyl adduct was then added to a suspension of **114** (205 mg, 0.238 mmol) in THF (5 mL) and stirred at rt for 24 h. The reaction was quenched by the addition of water (10 mL), acidified with acetic acid (0.5 mL), poured into water (30 mL), and extracted with ethyl acetate (2 x 40 mL). The organic phases combined and dried under Na_2SO_4. The solvents were removed under reduced pressure. The precipitate was collected via vacuum filtration and rinsed with methanol to give **119** as a yellow solid, which was used in the next step without any further purification (121 mg, 0.110 mmol, 46.2%).

10,21-bis(4-isopropylphenyl)-9,11,20,22-tetraphenyltetrabenzo[*c₁d₁,de,no,st*]heptacene (113). Diol **119** (77 mg, 0.070 mmol), $SnCl_2$•2 H_20 (1.34 g, 5.94 mmol), HCl (0.5 mL), and THF (5 mL) were heated to 70 ºC for 1 h in a screw-capped vial. Methanol (40 mL) was added, and the precipitate was collected via vacuum filtration. The red-orange solid was subjected to column chromatography (silica gel; solvent: hexanes; 50% toluene–hexanes). A red band was collected R_f 0.50 TLC (silica gel; solvent: 10% ethyl acetate–toluene). The solvent was removed under reduced pressure to give **113** as a red-orange solid (29.4 mg, 0.028 mmol, 39.5%). An analytical sample was obtained by recrystallizing a small amount of **113** from $CHCl_3$–MeOH: mp >400 ºC; ^{1}H NMR (400 MHz, $CDCl_3$) δ 0.97–1.00 (dd, J = 6.8, 3.2 Hz, 12H), 2.42–2.29 (septet, J = 6.8 Hz, 2H), 6.19–6.21 (d, J = 8.4 Hz, 4H), 6.50–6.52 (d, J = 8.0 Hz, 4H), 6.54–6.60 (m, 8H), 6.80–6.84 (t, J = 6.8 Hz, 8H), 6.86–6.87 (d, J = 7.6 Hz, 4H), 6.95–6.99 (t, J = 7.6 Hz, 4H), 7.06–7.10 (t, J = 7.6

Hz, 4H), 7.69–7.71 (d, J = 6.8 Hz, 4H), 7.79 (s, 4H) ppm; ^{13}C NMR (100 MHz, $CDCl_3$) δ 23.6, 23.7, 33.8, 124.3, 124.6, 125.3, 126.0, 126.1, 126.6, 127.5, 127.8, 127.9, 128.3, 130.6, 130.9, 132.8, 133.1, 133.3, 134.1, 135.0, 1356, 137.7, 141.6, 145.3 ppm. HRMS calcd for $C_{84}H_{58}$ 1066.4539, found 1066.4517. Crystals suitable for X-ray analysis were obtained from $CHCl_3$-MeOH.

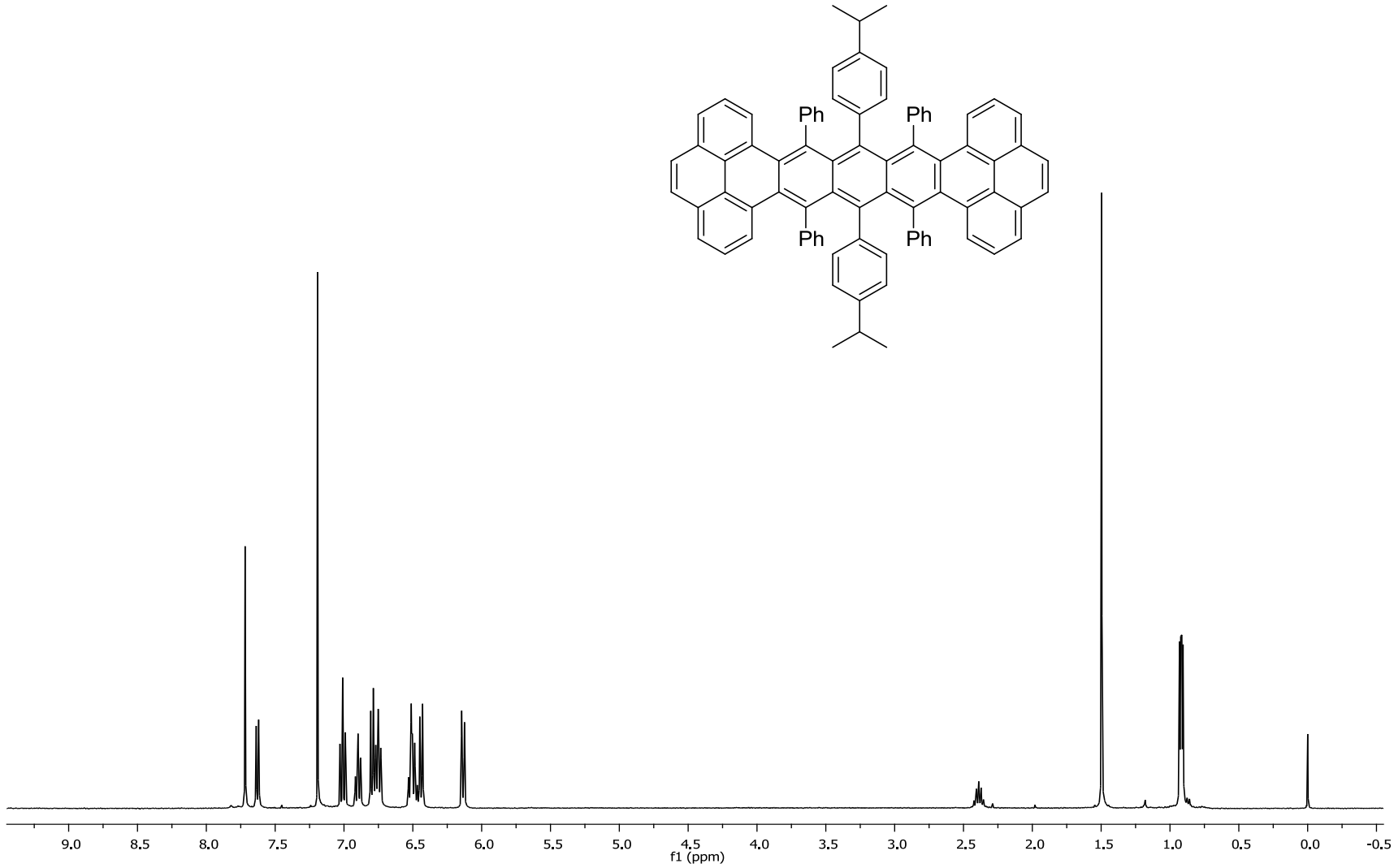
Ph
Ph
Ph
Ph
9.0
8.5
8.0
7.5
7.0
6.5
6.0
5.5
5.0
4.5
4.0
3.5
3.0
2.5
2.0
1.5
1.0
0.5
0.0
-0.5
f1 (ppm)

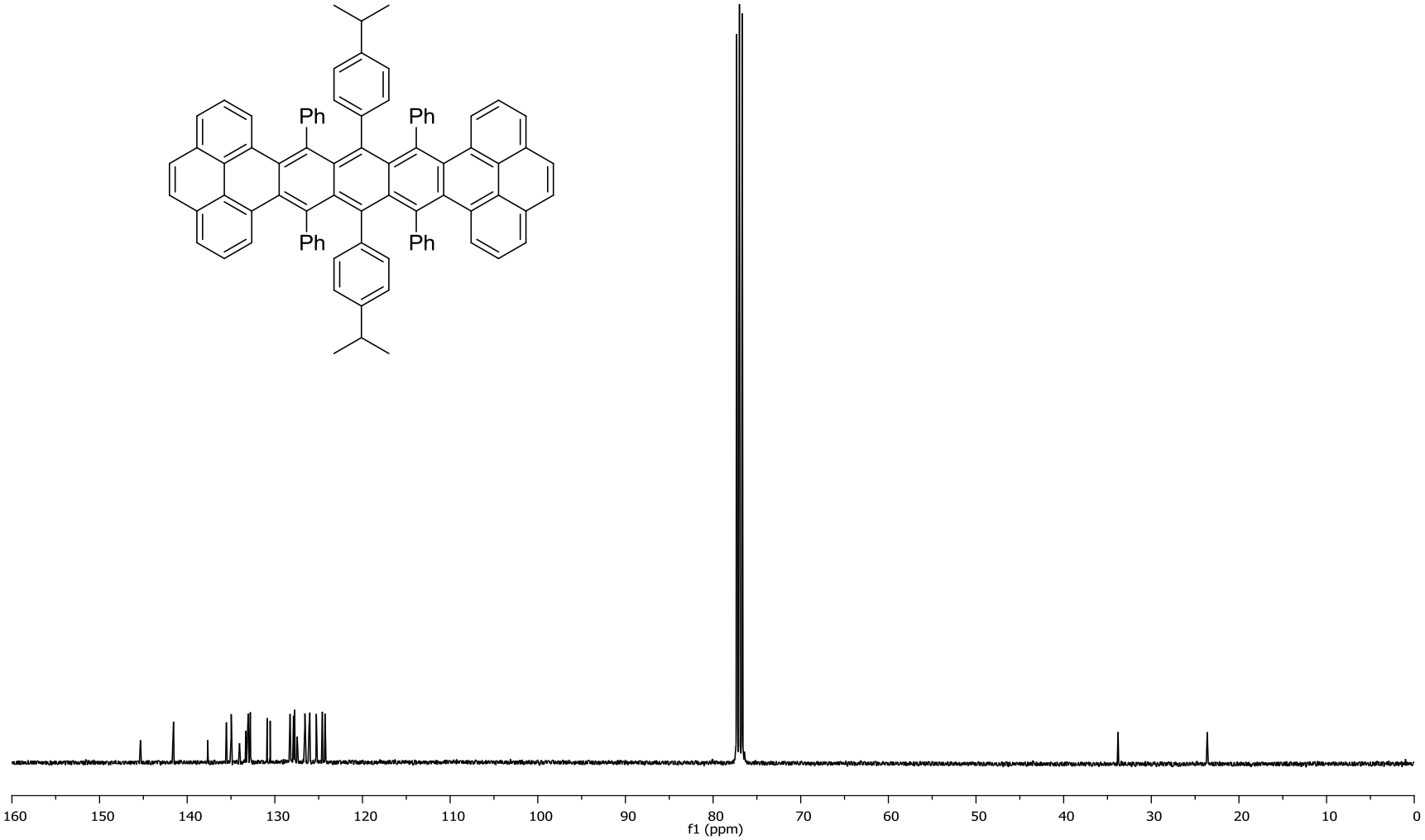
Ph
Ph
Ph
Ph
160
150
140
130
120
110
100
90
80
70
60
50
40
30
20
10
0
f1 (ppm)

Acenaphthene isopropyl anthracene (115). *n*-Butyllithium (2.5 M in hexanes, 1.2 mL, 3.0 mmol) was added to a solution of 1-bromo-4-isopropylbenzene (0.5 mL, 3.2 mmol) and THF (7 mL) at -78 ºC and stirred for 40 min. The isopropyl adduct was then added to a refluxing solution of **116** (205 mg, 0.178 mmol) in benzene (15 mL) and reflux was continued for 1 h. The solution was then cooled to rt and stirred for 24 h. The reaction was quenched by the addition of water (10 mL), acidified with acetic acid (0.5 mL), poured into water (30 mL), and extracted with ethyl acetate (2 x 40 mL). The organic phases were combined and dried with Na_2SO_4. The solvents were removed under reduced pressure. The precipitate was collected via vacuum filtration and rinsed with methanol to give **121** as a brown-green solid, which was used in the next step without any further purification (88.6 mg, 0.063 mmol, 35.7% crude yield). Diol **121** (88.6 mg, 0.063 mmol), $SnCl_2$•2 H_20 (1.56 g, 6.91 mmol), HCl (0.5 mL), and THF (4 mL) were heated to 70 ºC for 1 h in a screw-capped vial. Methanol (40 mL) was added, and the precipitate was collected via vacuum filtration. The green solid was subjected to column chromatography (silica gel; solvent: 10% CH_2Cl_2–hexanes). The solvent was removed under reduced pressure to give **115** as a dark green solid (5.6 mg, 0.004 mmol, 2.3%). An analytical sample was obtained by recrystallizing a small amount of **115** from $CHCl_3$–MeOH: ^{1}H NMR (400 MHz, $CDCl_3$) δ 1.04 (s, 36H), 1.08–1.12 (dd, J = 7.2, 8.4 Hz, 12H), 1.64 (s, 36H), 2.70–2.74 (p, J = 7.2 Hz, 2H), 6.75 (s, 4H), 7.04–7.06 (d, J = 8.4 Hz, 4H), 7.53 (s, 4H), 7.78 (s, 4H), 8.01–8.03 (d, J = 8.4 Hz, 4H), 8.89 (s, 4H) ppm; ^{13}C NMR (100 MHz, $CDCl_3$) δ 22.5, 23.8, 31.8, 31.9, 33.0, 35.4, 35.7, 121.7, 122.1, 122.6, 125.0, 127.6, 128.1, 128.8, 130.9, 133.6, 134.9, 136.7, 136.8, 138.0, 139.3, 148.1, 150.6, 151.5 ppm.

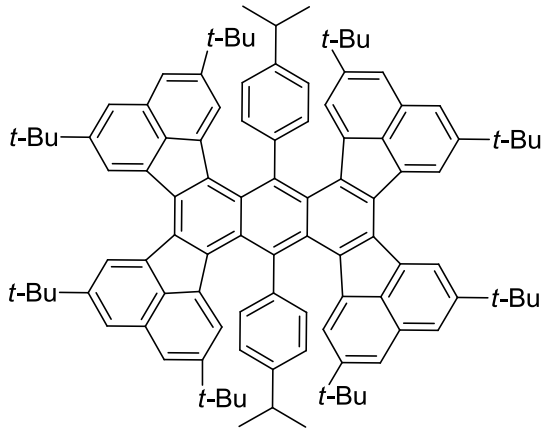
t-Bu
t-Bu
t-Bu
t-Bu
t-Bu
t-Bu
t-Bu
t-Bu

10.5
10.0
9.5
9.0
8.5
8.0
7.5
7.0
6.5
6.0
5.5
5.0
4.5
4.0
3.5
3.0
2.5
2.0
1.5
1.0
0.5
0.0
-0.5
-1.0
f1 (ppm)

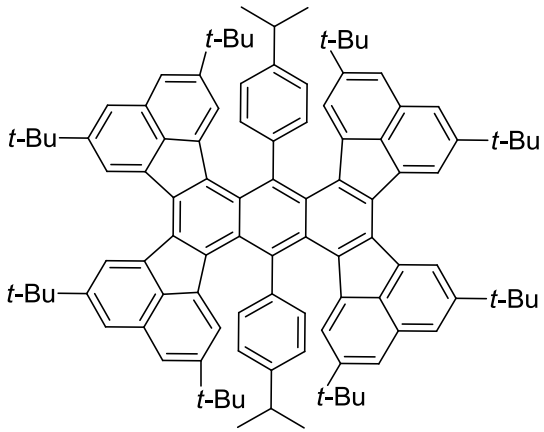
t-Bu
t-Bu
t-Bu
t-Bu
t-Bu
t-Bu
t-Bu
t-Bu

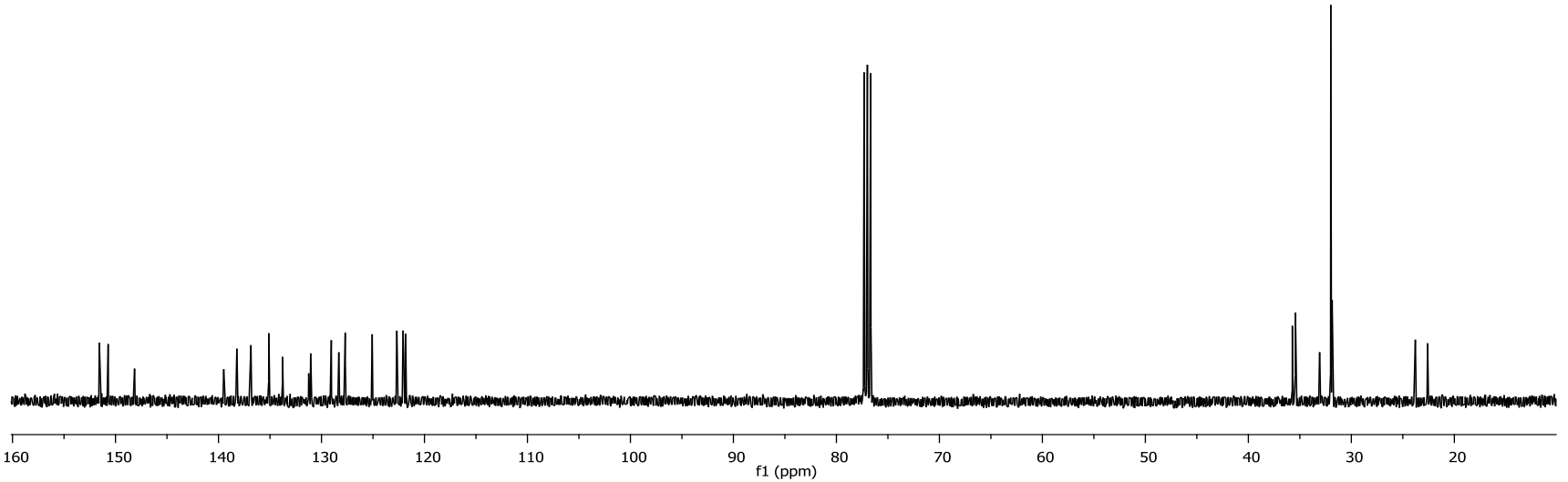
160
150
140
130
120
110
100
90
80
70
60
50
40
30
20
f1 (ppm)

5,8-dihydroxynaphthalene-1,4-dione (naphthazarin, 125). Compound **125** was synthesized from an adapted procedure by Toribara et al.[149, 150] Aluminum chloride (100 g) and NaCl (20 g) were heated to a melt on a hotplate at 190 ºC. Maleic anhydride (10.2 g, 104 mmol) and hydroquinone (11.3 g, 103 mmol) were added, and the solution was stirred at 240 ºC for 1 h. Water was carefully added (~350 mL), and the contents were heated to a boil until the mixture appeared homogenous. Concentrated HCl (120 mL) was added, and the black solution stirred at rt overnight (16 h). The precipitate was collected via vacuum filtration, dried, and boiled in toluene (200 mL) for 2 h. The precipitate was removed via vacuum filtration, and the filtrate was concentrated under reduced pressure. The resulting solid was stirred in hexanes (300 mL) for 1 h and collected via vacuum filtration to give **125** as a metallic brown solid (3.35 g, 17.6 mmol, 17.2%), which was used without any further purification: mp 234-235 ºC; ^{1}H NMR (400 MHz, $CDCl_3$) δ 7.15 (s, 4 H), 12.42 (s, 2 H) ppm; ^{13}C NMR (100 MHz, $CDCl_3$) δ 111.8, 134.6, 172.8 ppm.

5,8-dioxo-5,8-dihydronaphthalene-1,4-diyl diacetate (126). Naphthazarin **125** (6.02 g, 31.7 mmol), acetic anhydride (84 mL), and pyridine (0.5 mL) were heated to 90 ºC on a hotplate for 2 h and then stirred at rt for an additional 1 h. Water (0.5 mL) was added, and the reaction mixture was allowed to stir overnight (14 h). The precipitate was collected via vacuum filtration and washed with ethanol to give **126** as a yellow solid, which was used without any further purification (4.92 g, 17.9 mmol, 56.6%). An analytical sample was obtained by recrystallizing a small amount of **126** from $CHCl_3$–MeOH: mp 191-192 ºC; ^{1}H NMR (400 MHz, $CDCl_3$) δ 2.44 (s, 6 H), 6.80 (s, 2 H), 7.40 (s, 2 H) ppm; ^{13}C NMR (100 MHz, $CDCl_3$) δ 21.0, 124.3, 131.0, 138.5, 147.5, 169.3, 183.1 ppm.

11,14-dihydroxy-9,16-diphenyldibenzo[*de,uv*]pentacene-10,15-dione (127).

Pyrenecyclone **117** (1.03 g, 2.53 mmol), acetate **126** (687 mg, 2.51 mmol), and nitrobenzene (4 mL) were heated to 180 ºC for 24 h in a screw-capped vial. The reaction contents were cooled to rt and CH_2Cl_2 (40 mL) was added, and the reaction was stirred for 21 h at rt. The solvents were removed under reduced pressure, methanol (150 mL) was added, and the precipitate was collected via vacuum filtration to give **127** as a red solid, which was used in the next step without any further purification (561 mg, 0.990 mmol, 39.5%). An analytical sample was obtained by recrystallizing a small amount of **127** from $CHCl_3$–MeOH: mp >350 ˚C; ^{1}H NMR (400 MHz, $CDCl_3$) δ 7.34–7.51 (m, 14H), 7.64–7.66 (d, J = 8.4 Hz, 2H), 7.96 (s, 2H), 7.99–8.01 (d, J = 8 Hz, 2H), 12.26 (s, 2H) ppm; ^{13}C NMR (100 MHz, $CDCl_3$) δ 114.2, 124.7, 126.1, 127.1, 127.2, 127.9, 128.3, 128.4, 128.9, 129.2, 130.7, 130.8, 131.2, 138.2, 141.2, 142.0, 156.3, 188.8 ppm; HRMS calcd for $C_{40}H_{22}O_4$ 566.1518, found 566.1389.

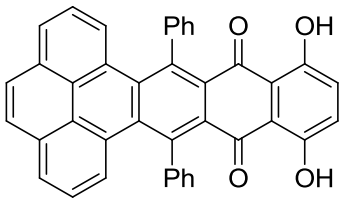
Ph
O
OH
Ph
O
OH

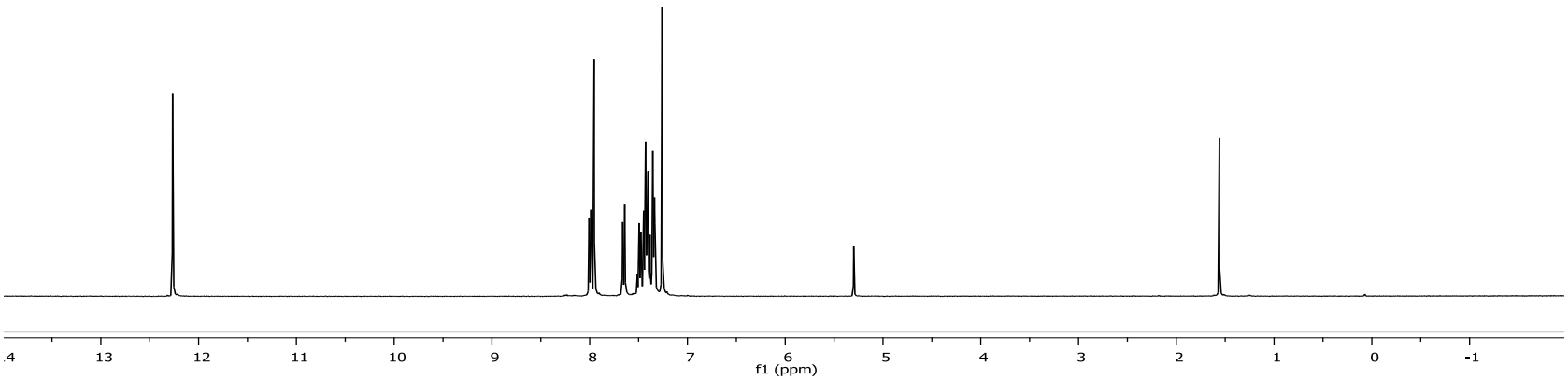
.4
13
12
11
10
9
8
7
6
5
4
3
2
1
0
-1
f1 (ppm)

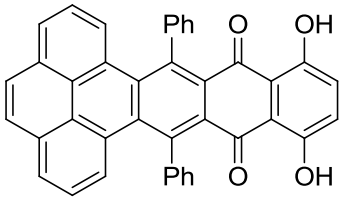
Ph
O
OH
Ph
O
OH

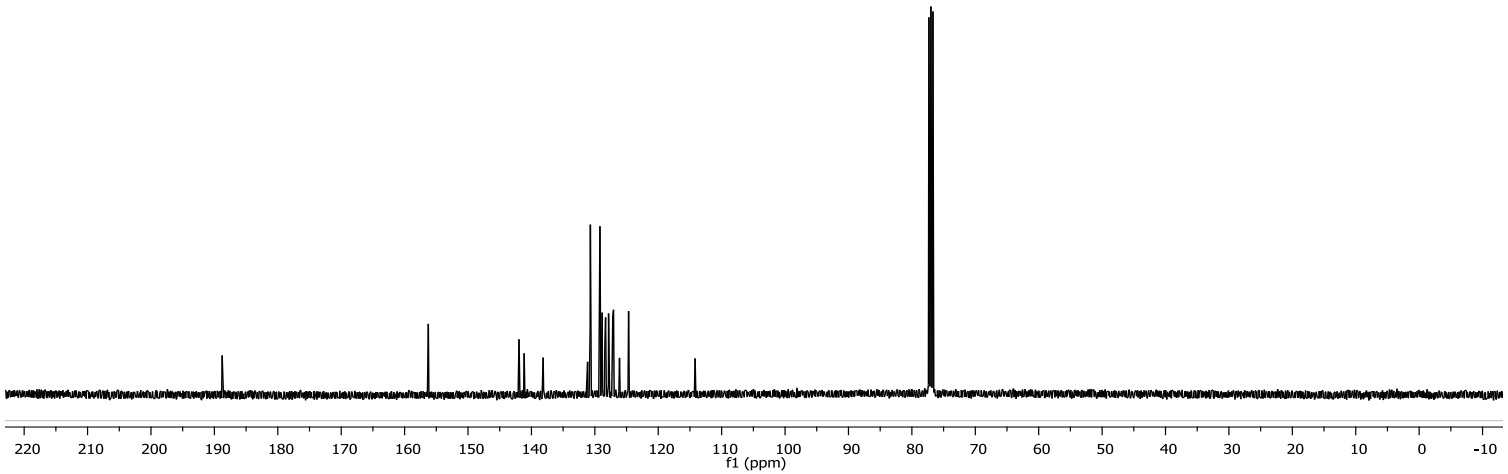
220
210
200
190
180
170
160
150
140
130
120
110
100
90
80
70
60
50
40
30
20
10
0
-10
f1 (ppm)

9,10,15,16-tetraphenyldibenzo[de,uv]pentacene-11,14-dione (128). Phenyllithium (2M in dibutyl ether, 4 mL, 8 mmol) was added to a suspension of quinone **127** (394 mg, 0.695 mmol) in dry THF (10 mL), and the contents were stirred for 24 h at rt under argon. The reaction was quenched by the addition of water (10 mL), acidified with acetic acid (0.5 mL), poured into water (30 mL), and steam distilled to remove the organic solvents. The precipitate was collected via vacuum filtration and washed with ethanol to give a light brown solid. Recrystallization from $CHCl_3$–MeOH gave a brown solid, which was refluxed in nitrobenzene (1 mL) in a screw-capped vial for 1 h. Methanol (15 mL) was added, the solution was allowed to sit for 16 h, and the precipitate was collected via vacuum filtration. The brown solid was subjected to column chromatography (silica gel; solvent: CH_2Cl_2). The solvent was removed under reduced pressure to give **128** as a red solid, which was used in the next step without any further purification (146 mg, 0.213 mmol, 30.6%). mp > 350 ˚C; ^{1}H NMR (400 MHz, $CDCl_3$) δ 6.85–6.87 (d, J = 7.6 Hz, 2H), 6.99–7.02 (dt, J = 6.8, 2 Hz, 2H), 7.16–7.21 (m, 4H), 7.29–7.33 (m, 2H), 7.41–7.47 (m, 4H), 7.58–7.68 (m, 6H), 7.74 (s, 2H), 7.78–7.84 (m, 4H), 8.30–8.32 (m, 4H); ^{13}C NMR (100 MHz, $CDCl_3$) δ 124.5, 126.0, 126.2, 126.5, 126.8, 127.1, 127.2, 127.3, 128.1, 128.2, 129.0, 129.2, 129.3, 130.6, 131.0, 131.9, 132.4, 133.3, 137.2, 139.6, 139.7, 141.1, 142.9, 187.0 ppm.

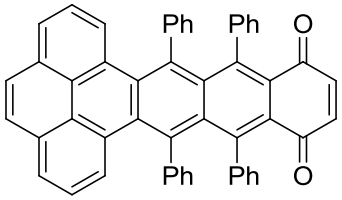
Ph
Ph
O
Ph
Ph
O

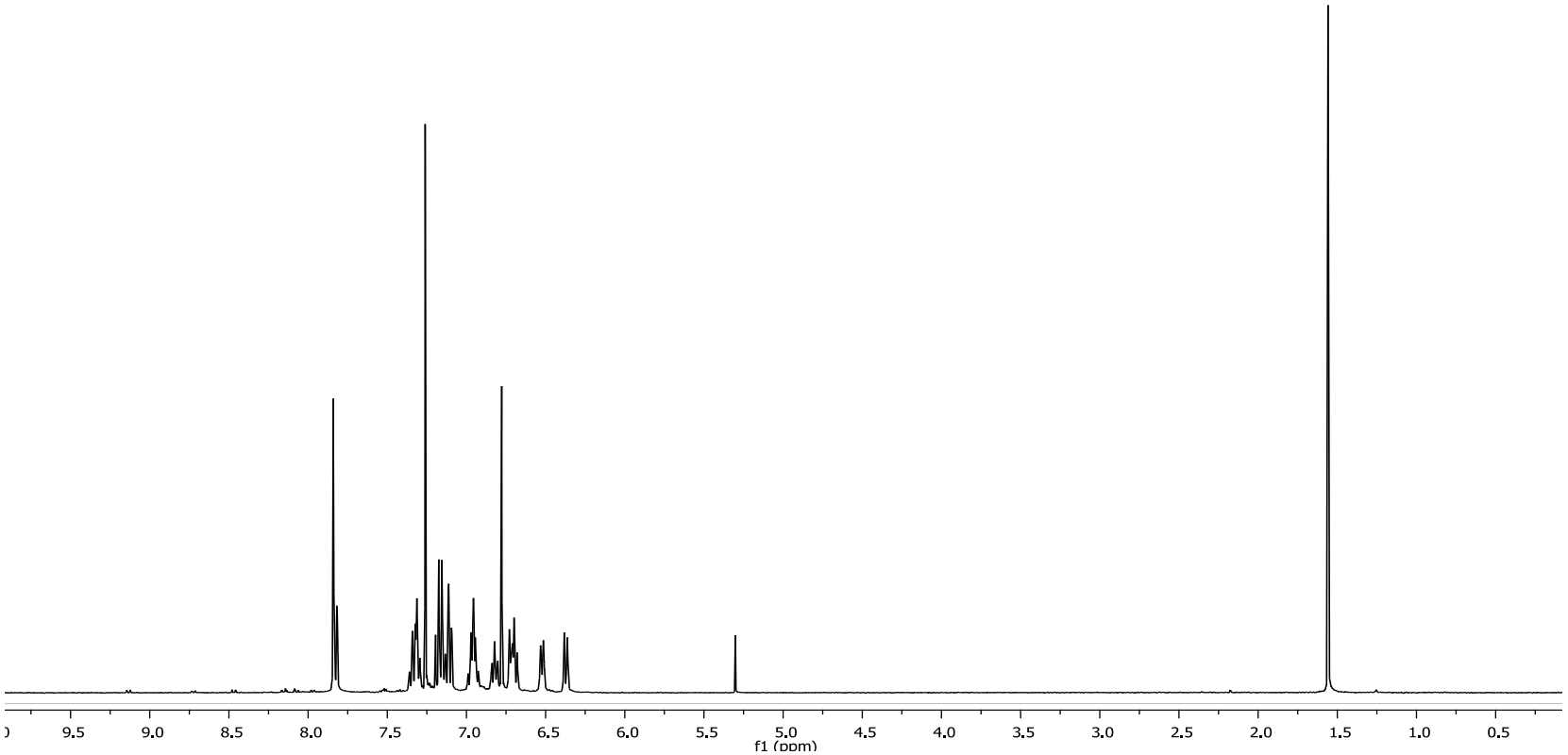
9.5
9.0
8.5
8.0
7.5
7.0
6.5
6.0
5.5
5.0
4.5
4.0
3.5
3.0
2.5
2.0
1.5
1.0
0.5
f1 (ppm)

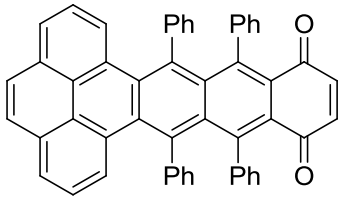
Ph
Ph
O
Ph
Ph
O

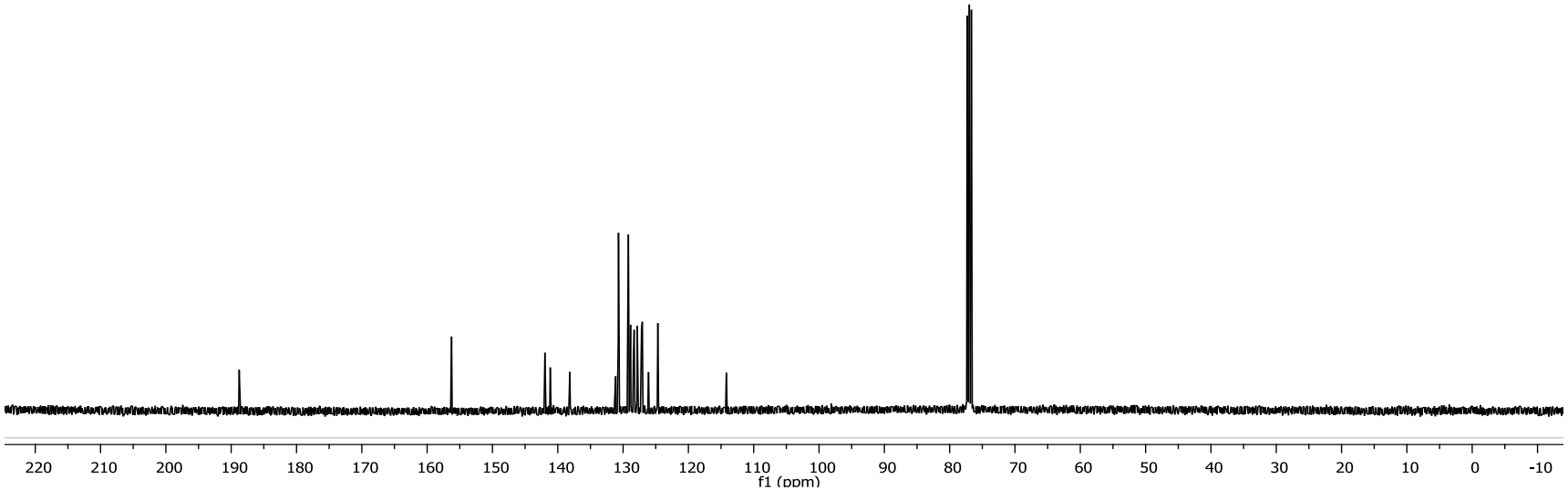
220
210
200
190
180
170
160
150
140
130
120
110
100
90
80
70
60
50
40
30
20
10
0
-10
f1 (ppm)

9,11,12,21,22,24-hexaphenyl-tetrabenzo[de,g₁h₁,pq,uv] octacene-10,23-dione (129). Quinone **128** (1.03 g, 1.50 mmol), cyclone **117** (693 mg, 1.70 mmol), and nitrobenzene (4 mL) were heated to 180 ºC in a screw-capped vial. After 30 and 60 min, additional cyclone **117** (372 mg and 101 mg, respectively) was added, and the solution heated for an additional 65 h. Methanol (30 mL) was added, and the reaction contents were heated for 1 h. Acetone (10 mL) was added, and the suspension was allowed to stand for 72 h. The precipitate was collected via vacuum filtration, and the resulting red solid was subjected to column chromatography (silica gel; solvent: toluene). A yellow band was collected (R_f 0.3 TLC, silica gel; solvent: toluene). The solvent was removed under reduced pressure to give **129** as a red solid which was used in the next step without any further purification (574 mg, 0.540 mmol, 36.0%). An analytical sample was obtained by recrystallizing a small amount of **129** from $CHCl_3$–MeOH: mp >350 ˚C; HRMS calcd for $C_{82}H_{46}O_2$ 1062.3498, found 1062.3467. Crystals suitable for X-ray analysis were obtained from $CHCl_3$-MeOH.

9,10,11,12,21,22,23,24-octaphenyl-9a,10,23,23a-tetrahydrotetrabenzo[de,g₁h₁,pq,uv]octacene-10,23-diol (130). Phenyllithium (2.0 M in diphenyl ether, 2 mL, 4 mmol) was added to a suspension of **129** (94.3 mg, 0.088 mmol) in THF (5 mL) and stirred at rt for 24 h. The reaction was quenched by the addition of water (10 mL), acidified with acetic acid (0.5 mL), poured into water (30 mL), and extracted with ethyl acetate (2 x 40 mL). The organic phases combined, dried under Na_2SO_4, and the solvents were removed under reduced pressure. The precipitate was collected via vacuum filtration and rinsed with methanol to give **130** as a yellow solid (86.5 mg, 0.071 mmol,

74.4% crude); HRMS calcd for $C_{94}H_{58}O_2$ 1218.44, found 1218.4401. Crystals suitable for X-ray analysis were obtained from $CHCl_3$-MeOH.

Variable Temperature NMR Measurements on Compounds 113 and 115. Compounds **113** and **115** (~2 mg) were dissolved in 1,1,2,2-tetrachloroethane-d_2 (1 mL), and 400 MHz ^{1}H NMR spectra were recorded. The sample was allowed to equilibrate at each of the chosen temperatures for 15 min prior to the collection of the spectrum. Temperatures were measured by the use of a thermocouple inside the NMR spectrometer probe.

X-ray Crystallography. Samples of compounds **113**, **129**, and **130** were heated to a gentle reflux for less than a min in a loosely capped screw-capped vial. The vial was then placed in the dark and allowed to sit for >1 week. Crystals suitable for X-ray analysis formed upon the slow evaporation of solvent ($CHCl_3$–MeOH).

References

(1) Groen, N.; van de Peppel, J.; Yuan, H.; van Leeuwen, J.P.T.M.; van Blitterswijk, C.A.; de Boer, J. *Biomaterials* **2013**, *34*, 5552-5561.

(2) Vani, K.; Thomas, S.; Prabhawathi, V.; Boobalan, T.; Sawant, S.N.; Doble, M. *Colloids Surf., B* **2013**, *108*, 191-198.

(3) Qi, C.; Zhu, Y.J.; Lu, B.Q. et al. *Chem. Eur. J.* **2013**, *19*, 5332-5341.

(4) Wang, M.O.; Etheridge, J.M.; Thompson, J.A.; Vorwald, C.E.; Dean, D.; Fisher, J.P. *Biomacromolecules* **2013**, *14*, 1321-1329.

(5) Borzacchiello, A.; Ambrosio, L.; Nicolais, L.; Harper, E.J.; Tanner, K.E.; Bonfield, W. *J. Mater. Sci- Mater. M.* **1998**, *9,*12, 835-838.

(6) Liu-Snyder, P.; Webster, T.J. *Nanosci.* **2008**, *4,* 1, 111-118.

(7) Mahomed, N.N.; Barrett, J.; Katz, J.N.; Baron, J.A.; Wright, J.; Losina, E. *J. Bone Joint Surg. Am.* **2005**, *87,* 6, 1222-1228.

(8) Mendenhall, S. *Orthopedic Network News* **2006**, *17*, 3.

(9) Lewis, G.*J. Biomed. Mater. Res. B Appl. Biomater.* **2008**, *84B,* 2, 301-319.

(10) Puska, M.A.; Närthi, T.O.; Aho, A.J.; Yli-Urpo, A.; Vallittu, P.K. *J. Mater. Sci-Mater. M.* **2004**, *15,* 9, 1037-1043.

(11) Mitzner, E.; Pelt, P.A.H.M.; Mueller, C.; Strohwig, A.; Mueller, W.D. *Mat. Res.* **2009**, *12,* 4, 447-454.

(12) Gomoll, A.H.; Fitz, W.; Scott, R.D.; Thornhill, T.S.; Bellare, A. *Acta Orthop.* **2008**, *79* (3), 421-427.

(13) Demian, H.W.; McDermott, K. *Biomaterials* **1998**, *19* (17), 1607-1618.

(14) Stańczyk, M.; van Rietbergen, B. *J. Biomech.* **2004**, *37,* 12, 1803-1810.

(15) Vallo, C.I.; Schroeder, W.F. *J. Biomed. Mater. Res. B Appl. Biomater.* **2005**, *74B,* 2, 676-685.

(16) Shinzato, S.; Kobayashi, M.; Mousa, W.F. et al. *J. Biomed. Mater. Res.* **2000**, *53,* 1, 51-61.

(17) Lewis, G. *J. Biomed. Mater. Res. B Appl. Biomater.* **2006**, *76B,* 2, 456-468.

(18) Gbureck, U.; Barralet, J.E.; Hofmann, M.P.; Thuli, R. *J. Dent. Res.* **2004**, *83,* 5, 425-428.

(19) Barralet, J.E.; Lilley, K.J.; Grover, L.M.; Farrar, D.F.; Ansell, C.; Gbureck, U. *J. Mater. Sci-Mater. M* **2004**, *15,*4, 407-411.

(20) Mickiewicz, R.A.; Mayes, A.M.; Knaack, D. *J. Biomed. Mater. Res.* **2002**, *61* 4, 581-592.

(21) Deramond, H.; Wright, N.T.; Belkoff, S.M. *Bone* **1999**, *25,* 2, 17S-21S.

(22) DiCicco, M.; Duong, T.; Chu, A.; Jansen, S.A. *J. Biomed. Mater. Res. B Appl. Biomater.* **2003**, *65B,* 1, 137-149.

(23) DiCicco, M.; Compton, R.; Jansen-Varnum, S.A. *J. Mater. Res. B Appl. Biomater.* **2005**, *72B,* 1, 146-155.

(24) Erbe, E.; Clineff, T.; Gualtieri, G. *Eur. Spine J.* **2001**, *10,* 0, S147-S152.

(25) Al-Hiyasat, A.S.; Darmani, H. *J. Biomed. Mater. Res. A* **2006**, *78A,* 1, 66-72.

(26) Söderholm, K.J.; Mariotti, A. *J. Am. Dent. Assoc.* **1999**, *130,* 2, 201-209.

(27) Buchbinder, R.; Osborne, R.H.; Ebeling, P.R. et al. *Engl. J. Med.* **2009**, *361,* 6, 557-568.

(28) Kallmes, D.F.; Comstock, B.A.; Heagerty, P.J. et al. *Engl. J. Med.* **2009**, *361,* 6, 569-579.

(29) Eick, J.D.; Barragan-Adjemian, C.; Rosser, J. et al. *J. Biomed. Mater. Res. B Appl. Biomater.* **2012**, *100,* 3, 850-861.

(30) Guggenberger, R.; Weinmann, W. *Am. J. Dent.* **2000**, *13(Spec No)*, 82D-84D.

(31) Weinmann, W.; Thalacker, C.; Guggenberger, R. *Dent. Mater.* **2005**, *21*, 68-74.

(32) Eick, J.D.; Smith, R.E.; Pinzino, C.S.; Kostoryz, E.L. *J. Dent.* **2006**, *34*, 405-410.

(33) Braga, R.R.; Ferracane, J.L. *Crit. Ev. Oral Biol. Med.* **2004**, *15*, 176-184.

(34) Kostoryz, E.L.; Wetmore, L.A.; Brockmann, W.G.; Yourtee, D.M.; Eick, J.D. *J. Biomed. Mater. Res. A* **2004**, *68*, 660-667.

(35) Schweikl, H.; Schmalz, G.; Weinmann, W. *J. Dent. Res.* **2004**, *83*, 17-21.

(36) Schweikl, H.; Schmalz, G.; Weinmann, W. *Mut. Res. Gen. Toxicol. Environ. Mut.* **2000**, *521*, 19-27.

(37) Palin, W.M.; Fleming, G.J.; Nathwani, H.; Burke, F.J.; Randall, R.C. *Dent. Mater.* **2005**, *21*, 324-335.

(38) Alster, D.; Feilzer, A.J.; de Gee, A.J.; Davidson, C.L. *Dent. Mater.* **1997**, *13*, 146-150.

(39) Holder, A.J.; Kilway, K.V.; Code, J.E. et al. *Macromol. Theo. Sim.* **2005**, *14*, 117-124.

(40) Eick, J.D.; Kotha, S.P.; Chappelow, C.C. et al. *Dent. Mater.* **2007**, *8*, 1011-1017.

(41) Crivello, J.V.; Bi, D. *J Polym. Sci. Part A: Polym Chem.* **1994**, *32*, 683-697.

(42) Crivello, J.V.; Lee, J.L. *J Polym Sci, Part A: Poly Chem.* **1990**, *28*, 479-503.

(43) Sommer, L.H.; Pietrusza, E.W.; Whitmore, F.C. *J. Am. Chem. Soc.* **1947**, *69,* 1, 188.

(44) Field, L.D.; Ward, A.J. *J. Organomet. Chem.* **2003**, *681*, 91-97.

(45) Speier, J.L. *Adv. Organomet. Chem.* **1979**, *17*, 407-447.

(46) Marciniec, B. *Adv. Silicon Sci.* **2009**, *1*, 3-51.

(47) Horino, Y.; Livinghouse, T. *Organometallics* **2004**, *23*, 12-14.

(48) Reiner, K.; Högerl, M.P.; Gigler, P.; Kühn, F.E. *ACS Catal.* **2012**, *2*, 613-621.

(49) Sunada, Y.; Fujimura, Y.; Nagashima, H. *Organometallics* **2008**, *27*, 3502-3513.

(50) Chalk, A.J.; Harrod, J.F. *J. Am. Chem. Soc.* **1965**, *87*, 16-21.

(51) Putzien, S.; Nuyken, O.; Kühn, F.E. *Prog. Polym. Sci.* **2010**, *35*, 687-713.

(52) Sasaki, S.; Sumimoto, M.; Fukuhara, M.; Sugimoto, M.; Fujimoto, H.; Matsuzaki, S. *Organometallics* **2002**, *21*, 3788-3802.

(53) Marciniec, B. *Coord. Chem. Rev.* **2005**, *249*, 2374-2390.

(54) Chung, L.W.; Wu, Y.D.; Trost, B.M.; Ball, Z.T. *J. Am. Chem. Soc.* **2003,** *125*, 11578-11582.

(55) Schroeder, M.A.; Wrighton, M.S. , *J. Organomet. Chem.* **1977**, *128,* 3, 345-358.

(56) Takeuchi, R.; Yasue, H. *Organometallics* **1996**, *15*, 2098-2102.

(57) Gigler, P.; Bechlars, B.; Herrmann, W.A.; Kühn, F.E. *J. Am. Chem. Soc.* **2011**, *133,* 1589-1596.

(58) Schneider, N.; Finger, M.; Haferkemper, C.; Bellemin-Laponnaz, S.; Hofmann, Gade, L.H. *Angew. Chem. Int. Ed.* **2009**, *48*, 1609-1613.

(59) Schneider, N.; Finger, M.; Haferkemper, C.; Bellemin-Laponnaz, Hofmann, P.; Gade, L.H. *Chem.-Eur. J.* **2009**, *15*, 11515-11529.

(60) Itami, K.; Mitsudo, K.; Nishino, A.; Yoshida, J. *J. Org. Chem.* **2002**, *67*, 2645-2652.

(61) Roy, A. K. *Adv. Organomet. Chem.* **2007**, *55*, 1-59.

(62) Brook, M. A. Silicon in Organic, Organometallic, and Polymer Chemistry; John Wiley & Sons: New York, **2000**, 404-417.

(63) Stein, J.; Lewis, L.N.; Gao, Y.; Scott, R.A. , *J. Am. Chem. Soc.* **1999**, *121*, 3693-3703.

(64) Tondreau, A.M.; Atienza, C.C.H.; Darmon, J.M.et al. *Organometallics* **2012**, *31*, 4886-4893.

(65) Markó, I.E.; Stérin, S.; Buisine, O. et al. *Adv. Synth. Catal.* **2004**, *346*, 1429-1434.

(66) Buisine, O.; Bethon-Gelloz, G.; Brière, J.P. et al. *Chem. Commun.* **2005**, 3856-3858.

(67) Buch, F.; Brettar, J.; Harder, S. *Angew. Chem. Int. Ed.* **2006**, *45,* 2741-2745.

(68) Hopf, A.; Dötz, K.H. *J. Mol. Cat. A: Chem.* **2000**, *164*, 191-194.

(69) Tondreau, A.M.; Atienza, C.C.H.; Weller, K.J. et al. *Science* **2012**, *335*, 567-570.

(70) Li, J.; Peng, J.; Bai, Y.; Zhang, G.; Lai, G.; Li, X. *J. Organomet. Chem.* **2010**, *695*, 431-436.

(71) Li, J.; Peng, J.; Wang, D.; Bai, Y.; Jiang, J.; Lai, G. *J. Organomet. Chem.* **2011**, *696*, 263-268.

(72) Tsuchiya, Y.; Uchimura, H.; Kobayashi, K.; Nishiyama, H. *Synlett* **2004**, *12*, 2099-2102.

(73) Steffanut, P.; Osborn, J.A.; DeCian, A.; Fisher, J. *Chem.- Eur. J.* **1998,** *4,* 2008-2017.

(74) Lamoreaux, H. F. *U.S. Patent 3,220,972* **1965**.

(75) Lewis, L.N.; Sumpter, C.A. *J. Mol. Catal. A* **1996**, *104*, 293-297.

(76) Ye, H.; Zhang, X.S.; Li, Y.J.; Wang, T. *J. Polym. Res.* **2012**, *19*, 19.

(77) Nielsen, L.; Skrydstrup, T. *J. Am. Chem. Soc.* **2008**, *130*, 13145-13151.

(78) Christ, M.L.; Sabo-Etienne, S.; Chaudret, B. *Organomettalics* **1995**, *14*, 1082-1084.

(79) Crivello, J.V.; Löhden, G. *Macromolecules* **1995**, *28*, 8057-8064.

(80) Crivello, J.V.; Löhden, G. *Chem. Mater.* **1996**, *8*, 209-218.

(81) Kim, W.G.; Ahn, H.K.; Lee, H.W.; Kim, S.H.; Crivello, J.V. *Opt. Materials* **2002**, *21*, 343-347.

(82) Aoki, S. *U.S. Patent 6,255,428* **2001**.

(83) Bartholomew, C.H. *App. Catal. A* **2012**, *212,* 17-60.

(84) Mondal, R.; Tonshoff, C.; Khon, D.; Neckers, D.C.; Bettinger, H.F. *J. Am. Chem. Soc.* **2009**, *131*, 14281-14289.

(85) Anthony, J.E. *Chem. Rev.* **2006**, *106*, 5028-5048.

(86) Kuninobu, Y.; Seiki, T.; Kanamaru, S.; Nishina, Y.; Takai, K. *Org. Lett.* **2010**, *12*, 5287-5289.

(87) Qu, H.; Cui, W.; Li, J.; Shao, J.; Chi, C. *Org. Lett.* **2011**, *13*, 924-927.

(88) Fukutani, T.; Hirano, K.; Satoh, T.; Miura, M. *J. Org. Chem.* **2011**, *76*, 2867-2874.

(89) Kitamura, C.; Naito, T.; Yoneda, A.; Kawase, T.; Komatsu, T. *Chem. Lett.* **2010**, *39*, 771-773.

(90) Ostroverkhova, O.; Cooke, D.G.; Hegmann, F.A.; Tykwinski, R.R.; Parkin, S.R.; Anthony, J.E. *Appl. Phys. Lett.* **2006**, *89*, 19113.

(91) Anthony, J.E. *Angew. Chem. Int. Ed.* **2008**, *47*, 452-483.

(92) Kaur, I.; Jazdzyk, M.; Stein, N.N.; Prusevich, P.; Miller, G.P. *J. Am. Chem. Soc.* **2010**, *132*, 1261-1263.

(93) Zhang, Q.; Divayana, Y.; Xiao, J. et al. *Chem.-Eur. J.* **2010**, *16*, 7422-7426.

(94) Fogel, Y.; Zhi, L.; Rouhanipour, A.; Andrienko, D.; Räder, H.J.; Müllen, K. *Macromolecules* **2009**, *42*, 6878-6884.

(95) Dimitrakopoulos, C.D.; Malenfant, P.R.L. *Adv. Mater.* **2002**, *14*, 99-117.

(96) Mei, J.; Diao, Y.; Appleton, A.L.; Fang, L.; Bao, Z. *J. Am. Chem. Soc.* **2013**, *135*, 6724-6746.

(97) Pilevarshahri, R.; Rungger, I.; Archer, T.; Sanvito, S.; Shahtahmasebi, N. *Condensed Matter* **2011**, 1-13.

(98) Rieger, R.; Müllen, K. *J. Phys. Org. Chem.* **2010**, *23*, 315-325.

(99) Boggiano, B.; Clar, E.; *J. Chem. Soc.* **1957**, 2681.

(100) Mondal, R.; Shah, B.K.; Neckers, D.C. *J. Am. Chem. Soc.* **2006**, *128*, 9612-9613.

(101) Bailey, W.J.; Liao, C. *J. Am. Chem. Soc.* **1955**, *77*, 992.

(102) Goodings, E.P.; Mitchard, D.A.; Owen, G. *J. Chem. Soc. Perkin Trans.1* **1972**, *1*, 1310.

(103) Li, S.; Jia, Z.; Nakajima, K.; Kanno, K.; Takahashi, T. *J. Org. Chem.* **2011**, *76*, 9983-9987.

(104) Watanabe, M.; Chang, Y.J.; Liu, S.W. et al. *Nat. Chem.* **2012**, *4*, 574-578.

(105) Simons, J.P. *Trans. Faraday Soc.* **1960**, *56*, 391-397.

(106) Arora, A. Organic Chemistry: Aromatic, Alcohols, Aldehydes, & Acids; Discovery Publishing House: New Delhi, **2006**.

(107) Ferrari, J.L.; Hunsberger, I.M.; Gutowsky, H.S. *J. Am. Chem. Soc.* **1965**, *87*, 1247-1255.

(108) Reddy, A.R.; Bendikov, M. *Chem. Comm.* **2006**, 1179-1181.

(109) Berg, O.; Chronister, E.L.; Yamashita, T.; Scott, G.W.; Sweet, R.M.; Calabrese, J. *J. Phys. Chem. A* **1999**, *103*, 2451-2459.

(110) Swartz, C.R.; Parkin, S.R.; Bullock, J.E.; Anthony, J.E.; Mayer, A.C.; Malliaras, G.G. *Org. Lett.* **2005**, *7*, 3163-3166.

(111) Bendikov, M.; Wudl, F.; Perepichka, D.F. *Chem. Rev.* **2004**, *104*, 4891-4945.

(112) Dodge, J.A.; Bain, J.D.; Chamberlin, A.R. *J. Org. Chem.* **1990**, *55*, 4190-4198.

(113) Ono, K.; Totani, H.; Hiei, T. et al. *Tetrahedron* **2007**, *63*, 9699-9704.

(114) Maulding, D.R.; Roberts, B.G. *J. Org. Chem.* **1969**, *34*, 1734-1736.

(115) Paraskar, A.S.; Reddy, A.R.; Patra, A. et al. *Chem.-Eur. J.* **2008**, *14*, 10639-10647.

(116) Briseno, A.L.; Miao, Q.; Ling, M.M. et al. *J. Am. Chem. Soc.* **2006**, *128*, 15576-15577.

(117) Rainbolt, J.E.; Miller, G.P. *J. Org. Chem.* **2007**, *72*, 3020-3030.

(118) Pascal, R.A.Jr. *Chem. Rev.* **2006**, *106*, 4809-4819.

(119) Qiao, X.; Padula, M.A.; Ho, D.M.; Vegelaar, N.J.; Schutt, C.E.; Pascal, R.A. Jr. *J. Am. Chem. Soc.* **1996**, *118*, 741-745.

(120) Tong, L.; Ho, D.M.; Vogelaar, N.J.; Schutt, C.E.; Pascal, R.A. Jr. *J. Am. Chem. Soc.* **1997**, *119*, 7291-7302.

(121) Balasubramaniyan, V. *Chem Rev.* **1966**, *66*, 567-641.

(122) Duong, H.M.; Bendikov, M.; Steiger, D. et al. *Org. Lett.* **2003**, *5*, 4433-4436.

(123) Xiao, J.; Duong, H.M.; Liu, Y. et al. *Angew. Chem. Int. Ed.* **2012**, *51*, 6094-6098.

(124) Lu, J.; Ho, D.M.; Vogelaar, N.J. et al. *J. Am. Chem. Soc.* **2006**, *128*, 17043-17050.

(125) Lu, J.; Ho, D.M.; Vogelaar, N.J.; Kraml, C.M.; Pascal, R.A. Jr. *J. Am. Chem. Soc.* **2004**, *126*, 11168-11169.

(126) Pascal, R.A. Jr.; McMillan, W.D.; Van Engen, D.; Eason, R.G. *J. Am. Chem. Soc.* **1987**, *109*, 4660-4665.

(127) Watson, J.A. Jr.; Pascal, R.A. Jr.; Ho, D.M.; Kilway, K.V. *Tetrahedron Lett.* **2000**, *41*, 5005-5008.

(128) Smyth, N.; Van Engen, D.; Pascal, R.A. Jr. *J. Org. Chem.* **1990**, *55*, 1937-1940.

(129) Anger, E.; Srebro, M.; Vanthuyne, N. et al. *J. Am. Chem. Soc.* **2012**, *134*, 15628-15631.

(130) Shen, Y.; Chen, C.-F. *Chem Rev.* **2012**, *112*, 1463.

(131) Cahn, R.S.; Ingold, S.C.; Prelog, V. *Angew. Chem. Int. Ed. Engl.* **1966**, *5*, 385-415.

(132) Janke, R.H.; Haufe, G.; Würthwein, E.U.; Borkent, J.H. *J. Am. Chem. Soc.* **1996**, *118*, 6031-6035.

(133) Pascal, R.A. Jr.; Qin, Q. *Tetrahedron* **2008**, *64*, 8630-8637.

(134) Bragg, R.A.; Clayden, J.; Morris, G.A.; Pink, J.H. *Chem.-Eur. J.* **2002**, *8,* 6, 1279-1289.

(135) Hilton, C.L.; Crowfoot, J.M.; Rempala, P.; King, B.T. *J. Am. Chem. Soc.* **2008**, *130*, 13392-13300.

(136) Wang, X.; Rheingold, A.L.; DiPasquale, A.G.; Mallory, F.B.; Mallory, C.W.; Beckmann, P.A. *J. Chem. Phys.* **2008**, *128*, 124502.

(137) Beckmann, P.A.; Roe, B.A. *J. Phys.: Condens. Matter* **1996**, *8*, 7991-7999.

(138) Nikitin, K.; Fleming, C.; Muller-Bunz, H.; Ortin, Y.; McGlinchey, M.J. *Eur. J. Org. Chem.* **2010**, 5203-5216.

(139) Gutowsky, H.S.; Holm, C.H. *J. Chem. Phys.* **1956**, *25*, 1228-1234.

(140) Kilway, K.V.; Clevenger, R.G.; Marquez, G.B.; Weiler, R.A.; Silva, M.A. *Abstract of Papers GENERAL 234, 42nd Midwest Regional Meeting of American Chemical Society, Kansas City, MO, November 7-10* **2007**.

(141) Hu, J.; Zhang, D.; Harris, F.W. *J. Org. Chem.* **2005**, *70*, 707-708.

(142) Sygula, A.; Sygula, R.; Rabideau, P.W. *Org. Lett.* **2006**, *8*, 5909-5911.

(143) Seiders, T.J.; Baldridge, K.K.; Elliott, E.L.; Grube, G.H.; Siegel, J.S. *J. Am. Chem. Soc.* **1999**, *121*, 7439-7440.

(144) Sygula, A.; Rabideau, P.W. *J. Am. Chem. Soc.* **1999,,***121*, 7800-7803.

(145) Seiders, T.J.; Elliott, E.L.; Grube, G.H.; Siegel, J.S. *J. Am. Chem. Soc.* **1999**, *121*, 7804-7813.

(146) Preda, D.V. *Ph.D. Dissertation, Boston College, Boston, MA* **2001**.

(147) Yamato, T.; Fujimoto, M.; Miyazawa, A.; Matsuo, K. *J. Chem. Soc., Perkin Trans. 1* **1997**, *1*, 1201-1207.

(148) Perrin, C L.; Dwyer, T.J. *Chem. Rev.* **1990**, *90*, 935-967.

(149) Toribara, T.Y.; Underwood, A.L. *Anal. Chem.* **1949**, *21*, 1352-1356.

(150) Zahn, K.; Ochwat, P. *Liebigs Ann.Chem.* **1928**, *462*, 72-97.

(151) Suzuki, K.; Yamada, N.; Ueno, K. *U.S. Patent 7,622,201* **2009**.

(152) Yamato, T.; Miyazawa, A.; Tashiro, M. *Chem. Ber.* **1993,** *126*, 2505-2511.

VITA

Bradley David Miller was born on August 1, 1984 in LeMars, Iowa. He received a Bachelor of Science degree from the University of Nebraska at Kearney in 2007. Shortly after, he entered the University of Missouri – Kansas City as an Interdisciplinary Ph.D. student while working as a Graduate Teaching Assistant. In the spring of 2008, Bradley joined the lab group of Dr. Kathleen V. Kilway where he worked as a Graduate Research Assistant from May of 2008 until July 2013. During this time he focused his research on the synthesis of silorane monomers and twisted polycyclic aromatic hydrocarbons.

In his time at UMKC, he was selected as the first graduate student from the Department of Chemistry for the Preparing Future Faculty (PFF) Fellowship through the School of Graduate Studies. Through the PFF Fellowship, Bradley was awarded a Graduate Certificate in College Teaching/Academic Career Preparation. Additionally, he was chosen for the GTA Superior Teaching Award through the School of Graduate Studies in 2008-2009. He presented his research at several meetings, including the Midwest Regional Meeting of the American Chemical Society, the International Association for Dental Research, and the Gordon Research Conference on Physical Organic Chemistry. His favorite hobbies include following the Kansas City Royals and running in organized races where he has completed two half-marathons.

Publications:

Eick, J.D.; Barragan-Adjemian, C.; Rosser, J.; Melander, J.R.; Dusevich, V.; Weiler, R.A.; **Miller, B.D.**; Kilway, K.V.; Dallas, M.R.; Bi, L.; Nalvarte, E.L.; Bonewald, L.F. *J. Biomed. Mater. Res. Part B,* **2012,** *100B*, 850-861.

Melander, J.R.; Weiler, R.A.; **Miller, B.D.**; Schuman, T.P.; Kilway, K.V.; Day, D.E.; Velez, M.; Eick, J.D. *J. Biomed. Mater. Res. Part B*, **2012**, *100B*, 163-169.

Presentations:

Miller, B.D.; Clevenger, R.G.; Kilway, K.V., "Extended Twisted Molecular Ribbons: An Approach to Highly Twisted Acenes," 2011 Gordon Research Conference on Physical Organic Chemistry, Holderness, NH, June 26-July 1, 2011.

Miller, B.D.; Weiler, R.A.; Melander, J.R.; Nalvarte, E.N.; Kilway, K.V.;Bonewald, L.V.; Eick, J.D., "Biocompatibility of a Chemically Initiated Silorane Resin," 89th General Session & Exhibition of the IADR, San Diego, CA, March 16-19, 2011.

Miller, B.D.; Burneson, J.B.; Weiler, R.A.; Eick, J.D.; Kilway, K.V., "Synthesis of Silicon Containing Monomers," 87th General Session & Exhibition of the International Association for Dental Research Conference, Miami, FL, April 1-4, 2009.

Miller, B.D.; Burneson, J.B.; Weiler, R.A.; Kilway, K.V., "Synthesis and Optimization of Siloranes," Abstract of Papers GENERAL 265, 43rd Midwest Regional Meeting of the American Chemical Society, Kearney, NE, October 8-11, 2008.